HISTOLOGICAL, ULTRASTRUCTURAL, AND BIOCHEMICAL STUDIES ON THE HEPATOPANCREAS OF THE SHRIMP *Metapenaeus ensis*

by

Ka-ming LEUNG

A thesis submitted as partial fulfillment of

the requirement for the degree of

Master of Philosophy

May, 1991

Division of Biology

Graduate School

The Chinese University of Hong Kong

ABSTRACT

This research examined the hepatopancreas of shrimp Metapenaeus ensis with emphasis on post-embryonic development of the organ and its changes during the digestive cycle and starvation. The hepatopancreas in M. ensis was an elaborate diverticulum of the midgut, consisting of numerous blind-ended tubules. The hepatopancreas was enclosed in a perforated connective tissue sheath. Four types of cells, E-, F-, R-, and B-cells, were present on the tubular epithelium. The nucleus of E-cells was large relative to the cell size. F-cells consisted of extensive rough endoplasmic reticulum and numerous ribosomes giving the cell fibrillar or foamy appearance. R-cells had supranuclear vacuole and lipid droplets in their cytoplasm. B-cells were easily recognizable by the large vacuole. The tubules of the hepatopancreas were invested by a network of myoepithelial cells situated outside the basal lamina of the tubular epithelium.

The hepatopancreas of M. ensis developed from one pair of gut caeca which first appeared in nauplius IV. Two pairs of hepatopancreatic rudiments, anterior and posterior pairs, were emerged at the anterior end of the tubular midgut in protozoea I. From protozoea to postlarva, the anterior pair of hepatopancreatic rudiments had little changes but regressed by postlarva 6. The posterior pair of hepatopancreatic rudiments developed branches and ramified into numerous blind-ended tubules and transformed into the adult form. The ultrastrucutre of different cell types found in the hepatopancreatic

rudiments were similar to those found in the adult hepatopancreas.

The ultrastructure and digestive enzyme activities of the hepatopancreas was studied during the digestive cycle of M. ensis which lasted for about 24 h. F-cells showed transformation to B-cells upon feeding. The process of transformation involved pinocytosis, resulting in numerous pinocytotic vesicles. The vesicles enlarged and fused together to form the large digestive vacuole which characterized the B-cells. Rough endoplasmic reticulum in R-cells developed extensively after food intake and regressed at the middle of the digestive cycle while the smooth endoplasmic reticulum proliferated in the basal region of R-cells. Lipid droplets in R-cells increased in size and number during the cycle.

Starvation affected the histological structure, ultrastructure, biochemical composition and digestive enzyme activities of the hepatopancreas. The number of B-cells decreased significantly after starvation. Ultrastructure of F- and B-cells had little changes. Enormous mitochondria were developed in F-cells during starvation. The lipid droplets in R-cells became smaller and decreased in number. Residual bodies of lysozomes, dilated mitochondria and constricted smooth endoplasmic reticulum were found in R-cells after starvation. The hepatosomatic index, lipid and carbohydrate concentrations of the hepatopancreas decreased upon starvation. The activities of amylase and protease also declined. After the shrimp was refed for 2 days, the number of B-cells, lipid and carbohydrate concentration, and the activities of amylase and

protease appeared to increase to the levels found in daily-fed shrimp. At the same time, the ultrastructure of the cells was similar to that of the daily-fed shrimp.

ACKNOWLEDGEMENTS

I would like to offer my sincere appreciation to my supervisors, Dr. K.H. Chu and Dr. V.E.C. Ooi, for their patient guidance and support and to Dr. D.L. Mykles to be my external examiner. Special thank is given to my examiner, Dr. W.W.K. Cheung, for his counsel and assistance in reading the thesis, Dr. N.Y.S. Woo and Dr. C.K. Wong for their encouragement.

I am also indebted to Mr. W.K. Chu, Mr. K.C. Chung and Mr. Y.C. Tam for their assistance in purchasing the spawners and shrimp samples and in rearing the shrimp larvae. Thanks are also given to Ms F.Y. Ho for her technical advice in electron microscopy and histology and also thanks to Mr. C.F. Mok for sharing his invaluable experience in microphotography and histological techniques.

Thanks to the Department of Anatomy for they allowed me to use its transmission and scanning electron microscopes during the break down of the electron microscopes of my department and the Technical Services Unit for their hard work in repairing the electron microscopes.

Help from Mr. K.C. Au, Mr. M.K. Cheung, and Mr. K. Ngan, colleagues of the Marine Science Laboratory, during the study is also greatly appreciated.

LIST OF CONTENTS

LIST OF FIGURES

LIST OF ABBREVIATIONS

AB	abdomen
AH	anterior hepatopancreatic rudiment
AN	antenna
AU	antennule
B	B-cell
BC	blood capillary
BL	basal lamina
CD	collecting duct
CE	compound eye
CF	connective fibers
CG	cresent-like granules
CM	circular myofibrils
CS	cardiac stomach
CT	connective tissue sheath
CX	cephalothorax
CZ	clear zone
DG	dense granule
DL	dorso-lateral lobe of posterior hepatopancreatic rudiment
DR	dense region
DV	digestive vacuole
E	E-cell
F	F-cell
FB	fibroblast
FG	foregut
FL	fibrous lamina
FS	furcal seta
G	Golgi body
GE	gut epithelium
GF	gland filter
GL	gill
GT	gut
H	heart
HC	haemocoel
HE	haemocyte
HG	hindgut
HP	hepatopancreas
IR	interampullary ridge
S	intercellular space
L	lumen of hepatopancreatic tubule
LC	longitudinal channel
LL	lateral lobe of posterior hepatopancreatic rudiment
LM	longitudinal myofibrils
LP	lipid droplet
LS	lateral ossicle
LY	lysozome
M	mitochondrion

MA	mandible
MF	myofibrils
MG	tubular midgut
MO	mouth
MU	muscle
MV	microvilli
MY	myoepithelial cell
N	nucleus
NO	nucleolus
O	pore
OE	oesophagus
PC	pinocytotic channel
PE	pereiopod
PH	posterior hepatopancreatic rudiment
PL	pleopod
PM	posterior midgut caecum
PS	pyloric stomach
PV	pinocytotic vesicle
R	R-cell
RE	rough endoplasmic reticulum
SA	subapical vacuole
SC	surface enteric coat
SE	smooth endoplasmic reticulum
SN	supranuclear vacuole
T	tubule of hepatopancreas
U	uropod
V	vesicles
VL	ventro-lateral lobe of posterior hepatopancreatic rudiment
YC	yolk cell
YS	yolk sac
Z	Z-line of myofibrils

CHAPTER I

INTRODUCTION

Hepatopancreas is an important organ in decapod crustaceans. It is involved in various metabolic activities such as digestion, absorption, storage of organic reserves and mineral salts, lipid and carbohydrate metabolism, and metabolite mobilization during the moult cycle (Gibson & Barker, 1979).

The hepatopancreas has been studied for more than a century. These studies have been concentrated on two principal areas: (1) physiological and histological investigations on the cytologyical and cellular differentiation of tubules and (2) the range of digestive enzymes present in hepatopancreatic extracts or gastric fluid. Functions of the different cell types in hepatopancreas have been studied in histological investigations. Different routes of cellular differentiation of the tubular cells in the hepatopancreas have been proposed and they are summarized in the review by Gibson & Barker (1979). However, none of these routes has been confirmed to be the exact pathway of differentiation. A great diversity of digestive enzymes has been recorded in crustaceans. The different types of digestive enzymes found in various species have been listed in van Weel (1970), Gibson & Barker (1979), and Dall & Moriarty (1983). The hepatopancreas should be the principal site synthesizing these digestive enzymes.

Although the hepatopancreas has been extensively studied, the development of the hepatopancreas in the larval stages of crustaceans has not drawn much attention. It is of considerable interest to understand how this organ develops from the larval stages into the complicated state in the adult. Since the hepatopancreas involved in digestion, it may respond to the dietary condition. The ultrastructure and digestive enzyme activities may change during the digestive cycle and period of starvation.

Metapenaeus ensis is an appropriate species for this kind of study. In the coastal water of Hong Kong, the spawning season of M. ensis is rather long, lasting from April to October, when gravid females are readily available in local fish market. Since the gravid female can spawn in laboratory conditions, and the larvae can also be reared to adults in the laboratory, studies on the hepatopancreas at various developmental stages are possible.

The objectives of this research are as follows:

1) to study the structure and cytology of the hepatopancreas in M. ensis;
2) to study the post-embryonic development of the alimentary canal in M. ensis with emphasis on the hepatopancreas;
3) to elucidate changes in ultrastructure and digestive enzyme activities in the hepatopancreas during the digestive cycle; and
4) to investigate the effects of starvation on the ultrastructure, digestive enzyme activities and biochemical composition of the hepatopancreas.

CHAPTER II

LITERATURE REVIEW

2.1 Digestive System of Decapod Crustaceans

The structure and functions of the digestive system of decapods have been reviewed by Dall & Moriarty (1983). The following description on the digestive system of decapod crustaceans is mainly based upon the above review and the following studies: Pillai (1960), Dall (1967), Powell (1974), Rigdon & Mensik (1976), Barker & Gibson (1977, 1978), Smith (1978) and Gibson & Barker (1979).

The alimentary canal of decapod crustaceans, as in other arthropods, is divided into three regions: foregut, midgut and hindgut. Both the foregut and hindgut are ectodermal in origin and covered with a cuticular lining whereas the midgut is endodermal and lacks a chitinous cuticle.

2.1.1 Foregut

The foregut consists of an oesophagus and a two-chambered stomach. The oesopahgus is a tube lined with columnar epithelium possessing a chitinous covering. The oesophagus is surrounded by tegumental glands which

secrete mucopolysaccharide to lubricate the passage of food (Dall & Moriarty, 1983).

The stomach is subdivided into anterior cardiac chamber and posterior pyloric chamber, which are separated by the cardio-pyloric valve. The cardiac stomach is a bulbous chamber and reinforced with calcified chitinous ossicles at its posterior end. The ossicles form the gastric mill. Trituration of food is principally conducted in the gastric mill while the mandibles merely tear the food material into fragments (Barker & Gibson, 1977). The pyloric stomach is subdivided into a dorsal and a ventral chamber. The dorsal chamber connects to the midgut and the ventral chamber, possessing the gland filter, leads into the hepatopancreas. Powell's (1974) model of foregut function is applicable to most decapods. Food is triturated and mixed with the fluid from the hepatopancreas at the gastric mill. The fluid contains digestive enzymes so that chemical digestion occurs in the stomach. The food is then passed to the pyloric stomach and filtered by the setae of the gland filter. The smaller particles and fluid able to pass through the gland filter will be directed into the hepatopancreas for further digestion and absorption. Particles which are too large to pass through the gland filter will be manipulated by the gastric mill again or passed to the tubular midgut and eliminated as faecal matter.

2.1.2 Midgut

The midgut is composed of the tubular midgut, the midgut caeca and the hepatopancreas. The tubular midgut is lined with a columnar epithelium which possesses a microvillous border. The tubular midgut of decapods was shown to absorb amino acids (Ahearn, 1974; Brick & Ahearn, 1978) and glucose (Ahearn & Maginniss, 1977; Chu, 1986). But the tubular midgut should not be the principal site of nutrient absorption because of its small surface area as compared to that of the hepatopancreas. The tubular midgut and its caeca may merely serve to increase the absorptive area of the midgut, and functions in the secretion of peritrophic membrane (Forster, 1953; Dall, 1967), and regulation of water and electrolyte concentration (Dall, 1965). Three midgut caeca are typically found in most decapods, but they may be lacking in some species. There are generally three tubular midgut caeca generally found in Brachyura and Anomura. They include a pair of anterior caeca and a single posterior caecum. The anterior midgut caeca are lobular and located near the junction of the foregut and midgut. The anterior midgut caecum in Penaeidea, Thalassinidea and Astacura, is a median, sac-like or bilobed structure and located dorsally at the anterior end of the midgut (Smith, 1978). The posterior caecum is tubular and arises from the tubular midgut just before the hindgut. It marks the end of the midgut and should not be confused as part of the hindgut since the posterior midgut caecum also lacks chitinous cuticle (Smith, 1978; Mykles, 1979). The fluid secreted from the midgut caeca shows little amylolytic and proteolytic activities (Holliday et al.,

1980). The hepatopancreas is a pair of diverticula of the midgut. It serves diverse functions including the secretion of digestive enzymes, absorption of digested food, and storage of organic nutrients and mineral salts. The organ is also involved in the excretion and mobilization of metabolites during the moult cycle (Gibson & Barker, 1979). The structure and functions of the hepatopancreas will be discussed in detail in Section 2.2.

2.1.3 Hindgut

The hindgut possesses a chitinous cuticle on its columnar epithelium. Longitudinal ridges protruding towards the gut lumen giving the lumen a stellate shape. The ridges pull the faecal strand by longitudinal muscular contractions into the hindgut (Smith, 1978; Mykles, 1979). Tegumental glands also surround the hindgut and their mucopolysaccharide secretion is presumed to assist in binding the faecal matter and facilitating its movement (Forster 1953, Hopkin & Nott, 1980). Anal drinking of water was demonstrated in Caridina laevis (Pillai, 1960) and Metapenaeus bennette (Dall, 1967). And the process probably functions to maintain a constant pressure inside the gut and assists defaecation.

2.2 Hepatopancreas in Decapod Crustaceans

The descriptions on the structure and cell types of the decapod hepatopancreas are mainly based on the following studies: Bunt (1968), Loizzi (1971), Barker & Gibson (1977, 1978), Gibson & Barker (1979), Hopkin & Nott (1980), Leavitt & Bayer (1982), Dall & Moriarty (1983), Al-Mohanna et al. (1985a), Vogt (1985), Al-Mohanna & Nott (1986, 1987a), and Caceci et al. (1988).

2.2.1 Morphology of Hepatopancreas

The hepatopancreas is a large, paired and elaborate diverticula flanking the stomach and the anterior midgut. It occupies much of the cephalothoracic cavity. The colour of this organ varies from white to green in different species. It may be yellowish-brown, yellowish-green or greenish-brown. The major pigment in the hepatopancreas is β-carotene. The organ is ensheathed by a connective tissue membrane which surrounds the hepatopancreas as a unit. The hepatopancreas arises from the midgut. Each half of the organ is multilobed and each of them is connected to the midgut by a primary duct at the junction of the pyloric stomach and the tubular midgut. The primary duct branches into secondary ductules which ramify into an extensive system of blind-ended tubules.

2.2.2. Cell Types in Hepatopancreas

There are usually four types of cells on the epithelium of the tubules in the hepatopancreas. The names of the cell types originally proposed by Jacobs (1928) are Embryonalzellen, Fibrillenzellen, Blasenzellen and Restzellen. Now they are commonly known as E- (embryonic) cell, F- (fibrillar) cell, B- (blister) cell and R- (resorptive/absorptive) cell, respectively.

a) E-cells (Embryonic Cells)

E-cell is the smallest cell type found on the tubular epithelium. It has a large centrally located nucleus. The cytoplasm possesses abundant free ribosomes and smooth endoplasmic reticulum, but few mitochondria. E-cells are located at the distal tip of tubules and form a mitotic centre. They undergo mitotic division and differentiate into F- and R-cells.

b) F-cells (Fibrillar Cells)

F-cells consist of abundant free ribosomes and extensive rough endoplasmic reticulum, indicating active protein synthesis. There are several Golgi bodies found in the cytoplasm. The cisternae of the Golgi bodies are always dilated. The apical border of F-cells is lined with microvilli. F-cells

are believed to specialize in the synthesis of digestive enzymes.

c) B-cells (Blister Cells)

B-cells are the largest cell type found on the tubular epithelium. The cell is characterized by a single large vacuole surrounded with a thin rim of cytoplasm. The contents of the vacuole are highly variable. It may contain clumps of particulate matter, or fibers. The apical border of B-cell is lined with microvilli. The cytoplasm in the apical region is dense and filled with numerous pinocytotic vesicles. The nucleus is always compressed by a large vacuole and deflected laterally or basally. B-cells are presumed to be transformed from F-cells. The proposed functions of B-cells include secretion of digestive enzyme, intracellular digestion and packaging wastes in the digestive vacuole.

d) R-cells (Resorptive/Absorptive Cells)

R-cells are the most abundant cell type in the hepatopancreas. The cytoplasm is rich in lysosome-like granules. Lipids and glycogen are the organic reserves stored in the cells. Extensive network of smooth endoplasmic reticulum is found in R-cells. Supernuclear vacuole consisting of stacks of fibers and granules is often found in the cell. Lipolytic activities have been

demonstrated on the brush border of the R-cells. Luminal nutrients are absorbed via contact digestion and molecular transport (Lozzi, 1971) or diffusion (Al-Mohanna & Nott, 1987a). The absorbed nutrients may be digested intracellularly (Barker & Gibson, 1977), and assimilated or detoxified by R-cells (Al-Mohanna & Nott, 1987a).

Some studies showed that five cell types are present on the tubular epithelium. Davis (1966) distinguished a fifth cell type referred as the proximal cells, which are found at the base of the tubules in the hepatopacreas of Procambarus blandingii. Al-Mohanna et al. (1985b) also found a type of cell near the basement membrane of the hepatopancreatic tubules in Penaeus semisulcatus. They named this type of cell 'M-cell (midget cell)'. Its changes during digestive cycle (Al-Mohanna et al., 1985b) and moult cycle (Al-Mohanna & Nott, 1987b) have been studied. Vogt (1985) found a type of small cells present in small amount on the tubular epithelium in the hepatopancreas of Penaeus monodon. The function and origin of these cells are unknown. Basal cells on the tubular epithelium in the hepatopancreas of Callinectus sapidus were reported by Johnson (1980). Whether these cells from different species represent the same type of cell is uncertain.

2.2.3 Myoepithelial Network in Hepatopancreas

The tubules of hepatopancreas are invested by a layer of squamous

myoepithelial cells. They are located outside the basal lamina of the tubular epithelium. Two types of myofibrils, circular and longitudinal myofibrils, are found in the myoepithelial cells. The circular myofibrils surround the tubule at regular intervals along the length of the tubule. The longitudinal myofibrils branch from the circular myofibrils at various angles and connect the circular myofibrils.

The contraction and relaxation of the myofibrils control the dilation and constriction of the tubule and hence the movement of food material in and out of the tubule. The longitudinal myofibrils may maintain the integrity of the tubule during contraction and relaxation of the circular myofibrils and hold them in place. The longitudinal myofibrils may conduct the contraction impulses through consecutive circular myofibrils (Leavitt & Bayer, 1982).

2.3 Digestive Enzymes from the Hepatopancreas

The hepatopancreas is possibly the principal site of digestive enzymes synthesis and secretion. Various digestive enzymes are secreted by the hepatopancreas and the types of digestive enzymes secreted vary among species. In the reviews by van Weel (1970), Gibson & Barker (1979) and Dall & Moriarty (1983), various digestive enzymes found in different species are listed. Three main types of digestive enzymes: proteases, carbohydrases and lipolytic enzymes, are present in most of the species studied. For proteases (proteolytic enzymes), tryptic protease is widely distributed in decapod

crustaceans. Chymotryptic enzymes have been also identified. For carbohydrases, amylases are present in almost every species studied. Cellulase and chitinase are present in low activities in a few species. These two enzymes may come from the symbiotic alimentary micro-organisms. Lipolytic enzymes are generally present in decapods.

2.4 Changes in the Hepatopancreas during Digestive Cycle

The fine structure of the hepatopancreas may undergo changes during the digestive cycle in decapod crustaceans. The digestive cycle starts from intake of food to elimination of undigested materials as faeces. The duration of the digestive cycle varies upon different species. It takes about 12 h in Scylla serrata (Barker & Gibson, 1978) and Homarus gammarus (Barker & Gibson, 1977), 24 h in Penaeus semisulcatus (Al-Mohanna & Nott, 1986) and 48 h in Carcinus maenas (Hopkin & Nott, 1980).

Changes in the ultrastructure of the hepatopancreas have been studied in detail by Hopkin & Nott (1980), Al-Mohanna et al. (1985a), and Al-Mohanna & Nott (1986 & 1987a). The following information concerning the changes of the hepatopancreas during the digestive cycle is based on their studies.

Before feeding, the E-cells at the distal tip of the hepatopancreatic

tubules remain undifferentiated and inactive. During the digestive cycle, the epithelial cells on the hepatopancreatic tubules may be extruded or disintegrated. Feeding can induce mitotic division of the E-cells in order to replace those cells disintegrated or extruded during the digestive cycle.

Digestive enzymes are synthesized in the F-cells and the secretion may be discharged in waves (Barker & Gibson, 1977, 1978). Ultrastructural study on the hepatopancreas of P. semisulcatus by Al-Mohanna et al. (1985a) showed that zymogen granules are synthesized and then exocytosed from the F-cells. Materials in the tubular lumen are absorbed by pinocytosis in the F-cells. The pinocytotic vesicles then fuse together to form digestive bodies which become larger and distend the cell. Intracellular digestion occurs inside the digestive bodies. Eventually the digestive bodies fuse to form a single digestive vacuole characterizing the mature phase of B-cell. The cytoplasm remains as a thin rim surrounding the vacuole and the nucleus is compressed and located laterally or basally. By the end of the digestive cycle, B-cells are extruded from the epithelium. Holocrine secretion of digestive enzymes is supposed to occur during the extrusion of the B-cells. The vacuoles of the B-cells have been found to be intact in the faecal pellets in P. semisulcatus (Al-Mohanna & Nott, 1986) and Carcinus maenas (Hopkin & Nott, 1980). Apocrine secretion from B-cells had been observed in crayfish by Loizzi (1971). The mode of secretion of digestive enzymes by the B-cells may be different for different species.

Early in the digestive cycle, materials from the tubular lumen are supposed to be taken up by the R-cells by diffusion since there is no apical pinocytosis observed (Al-Mohanna & Nott, 1987a). The smooth endoplasmic reticulum proliferates to transfer the soluble metabolites from the site of diffusion. Organic nutrients are stored as lipid droplets or glycogen granules in the cytoplasm. Metals which are found to accumulate in the supranuclear vacuole are presumably detoxified in R-cells since they are stored in an insoluble form.

2.5 Effects of Starvation on Hepatopancreas

Since the hepatopancreas is the principal organ for digestion and absorption of nutrients, it is sensitive to the nutritional status of the animal. Histological studies on hepatopancreas are useful to evaluate the nutritional value of diets for cultured species or the dietary stress in the animal under culture conditions (Pascual et al., 1983; Vogt et al., 1985, 1986). The hepatopancreas will respond to dietary stress with respect to histological structure, biochemical composition and digestive enzyme activities.

2.5.1. Histological and Ultrastructural Changes

The major references for this section are Rosemark et al. (1980), Storch & Anger (1983), Papathanassious & King (1984), and Vogt et al. (1985).

Starvation leads to atrophy of the lobes in the hepatopancreas. The most obvious change in the histological observation on the hepatopancreas is the decrease in the number of B-cells. The ultrastructure of of E- and B-cells do not change upon starvation. Whereas R-cells show greatest changes, F-cells show moderate changes.

The vacuolations in R-cells decrease after starvation, resulting from the decrease in the amount of lipid droplets and glycogen granules. Apical mitochondria become enlarged and have fewer cristae. The rough endoplasmic reticulum has shorter cisternae upon dietary stress. This is the result of hypoactivity since the apical region is involved in absorption. Part of the rough endoplasmic reticulum may transform into multi-layered whorls encircling lipid droplets in the centre. The function of these whorls is unknown.

F-cells showed little change in structure which include rough endoplasmic recticulum with shorter cisternae and fewer but enlarged mitochrondria. The changes are probably related to reduction in protein synthesis and digestive enzyme production.

2.5.2 Changes in Biochemical Composition and Digestive Activities

The hepatopancreas reduces in size during starvation (Cuzon et al., 1980). The organic reserves such as lipid and glycogen are utilized to allow the animal to tolerate starvation. Amylase and trypsin level in the hepatopancreas decrease upon starvation (Cuzon et al., 1980). However, as the hepatopancreas accounts for only 4-10% of the body wet weight (Dall & Moriarty, 1983), the reserve in this organ is limited. Reserves in other body tissues are probably metabolised during prolonged starvation. Barclay et al. (1983) showed that protein and lipids in the abdomen of Penaeus esculentus are the most important energy reserves utilised during starvation.

2.6 Biology of Metapenaeus ensis

Metapenaeus ensis is commonly known as the sand shrimp in Hong Kong. The taxonomy of the species studied in this research is listed below:

Phylum Arthropoda

Superclass Crustacea

Class Malacostraca

Order Decapoda

Suborder Dendrobranchiata

Infraorder Penaeidea

Superfamily Penaeoidea

Family Penaeidae

Genus Metapenaeus (Wood-Masos & Alcock, 1891)

Species ensis (De Haan, 1844)

The distribution of M. ensis ranges from Sri Lanka, Malaysia, South China Sea, Taiwan and southern coast of Japan, New Guinea and Australia (Tseng et al., 1979; Chan, 1984; Yu & Chan, 1986).

The body length of adult M. ensis is commonly 70-140 mm. The rostrum is narrow, straight and uptilted, reaching nearly to the antennular peduncle. It is armed with 4-8 teeth on the dorsal border. There are orbital, antennal, and hepatic spines on the carapace. There are two rostral teeth found on the carapace. The branchio-cardiac groove is long and nearly reaching the hepatic groove. The body colour is grey green to dark green in juvenile, and pale brown yellow in the adult. The body is covered with minute dark brown spots (Fig. 1).

The life history of M. ensis, like other penaeid shrimp, involves several larval stages, including nauplius, protozoea and mysis. The adults spend most of the life cycle in shallow water off the coast in the ocean. During spawning season, the females migrate towards the shore for spawning.

The spawning season of this species in the coastal waters of Hong Kong is rather long, lasting from April to October with peak in August and

September (Chan, 1984). Juveniles are found in the estuaries and brackish water whereas adults are found in oceanic water with depth above 50 m.

Fig. 1. An adult Metapenaeus ensis. AB, abdomen; CX, cephalothorax; PE, pereiopod; PL, pleopod; U, uropod.

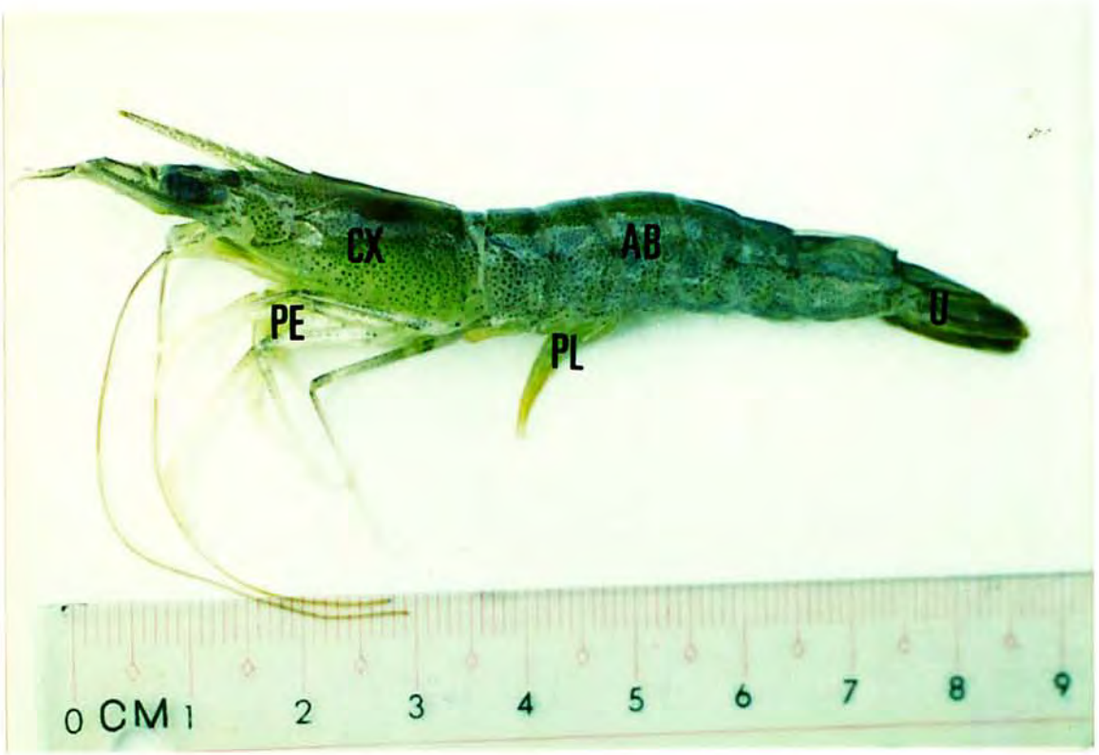

CHAPTER III

HEPATOPANCREAS OF SHRIMP Metapenaeus ensis

3.1 Introduction

The present study is to elucidate the histological and cytological structure of the hepatopancreas in Metapenaeus ensis and to provide basic information for studies on the various effects on the hepatopancreas, such as the cytological changes during digestive cycle or the response to dietary stress.

3.2 Materials and Methods

The hepatopancreas of Metapenaeus ensis was studied with light and electron microscopy. Shrimp were either hatchery-raised or acquired from the fish market at Shatin. The body length (from the tip of the rostrum to the tip of telson) ranged from 6.60 to 7.50 cm and body weight 2.53 to 2.92 g. The shrimp were kept in a water-table. They were fed with chopped green mussel (Perna viridis) at a daily ration about 20% of body weight for 1 week before taken for study. The water temperature was 22 to 25 ^{o}C and salinity 30 to 33 ppt. Shrimp at moult stage C or D_0 were used for the study. The

determination of moult stage followed the procedure of Chu et al. (1989), based on the scheme of Drach (1939). The moult stages were determined by placing the animal on a glass slide and examining the endopodite of the uropod using a Leitz inverted microscope. Five individuals each were sacrificed for histological and ultrastructural studies.

3.2.1. Histological Study

The method used in histological study was adopted from Humason (1974). The hepatopancreas of M. ensis was isolated and fixed in cold Bouin's fluid for 24 h. The cold Bouin's fluid would avoid the rapid autolysis of the organ. Dehydration was carried out in an ascending series of ethanol (70%, 80%, 95%, 2 changes for absolute ethanol, 45 min for each change); cleared in xylene and embedded in Paraplast paraffin wax (melting point 56-58 ^{o}C). The specimens were sectioned with American Optical 820 microtome into sections of 5 μm thickness. The sections were stained with Mayer's haematoxylin and eosin (H & E).

3.2.2. Ultrastructural Study

Shrimp were dissected in cold 0.1 M phosphate buffer (pH 7.2). The hepatopancreas was isolated and sliced into small pieces. The samples were

fixed in 1% glutaraldehyde in 0.1 M phosphate buffer, pH 7.2, with a final concentration of 2% paraformaldehyde added. The fixation was carried out at 4 °C for 2 h. The hepatopancreas were post-fixed in 1% osmium tetroxide with the same buffer at 4 °C for 2 h. The samples were then dehydrated in a series of ethanol (50%, 70%, 85%, 95% and two changes for absolute ethanol, 15 min for each change). The tissues were then infiltrated in Spurr's epoxy resin medium at room temperature for 8 hours, and embedded in Spurr's epoxy resin, polymerized at 70 °C in Reichert KT100 incubator for 12 h. The specimens were sectioned with Reichert Om2 ultracut using glass knife. The glass knives were made by LKB KnifeMaker type 801B. The thickness of thin sections was about 60 to 150 nm, as judged by gold-silver reflection. The thin sections were mounted on 200 mesh degreased copper grids. The sections were stained with 2% uranyl acetate in absolute ethanol and lead citrate for 30 min. of each stain. The grids were examined with Zeiss EM9S-2 or Jeol JEM-100 CXII transmission electron microscope.

Some of the specimens were studied with scanning electron microscopy. The fixation and dehydration followed the same procedures as in transmission electron microscopy but they were carried through the critical point drying process after dehydrated in absolute ethanol. The specimens were then coated with gold-palladium alloy and observed with Jeol-35 SEM scanning electron microscope.

3.3 Results

3.3.1 Gross Structure (Fig. 2)

The hepatopancreas of Metapenaeus ensis was a bilobed diverticulum situating in the cephalothoracic region and surrouding the pyloric stomach. The hepatopancreas was wrapped by a connective tissue sheath which was greenish brown to brown in colour. Each lobe of hepatopancreas was connected to the pyloric stomach-intestine junction via a primary duct.

3.3.2 Connective Tissue Sheath (Figs. 3 & 4)

The connective tissue sheath wrapped around the hepatopancreas in Metapenaeus ensis and held the two lobes of the organ together. The sheath was about 20 μm in thickness. The exterior surface of the sheath was rugged but relatively smoother than the interior surface (Figs. 3a & b). The interior surface had more fibers entangled on the surface. The sheath was perforated with many pores of diameter of about 15 μm.

When observed under the transmission electron microscope, the sheath was a foamy layer with many intercellular space (Fig. 4a). The cytoplasm of the sheath cells was filled with many vesicles. The sheath cells were separated by fibrous lamina in between them. The nucleus was peripheral, flattened or

irregular in shape. Groups of cresent-like granules were situated alongside the sheath (Fig. 4b).

3.3.3 Cell Types on the Epithelium of the Hepatopancreatic Tubules (Figs. 5-11)

The hepatopancreas of Metapenaeus ensis was composed of many blind-ended tubules (Fig. 5). The tubules extended and joined with the collecting ducts (Fig. 6). Blood capillaries were observed penetrating into the hepatopancreas. Four types of cells, E-, F-, R-, and B- cells, were found on the tubular epithelium (Fig. 7). E-cells were found at the distal end of the tubule. F-cells and R-cells were located in the medio-distal region. B-cells were mostly found in the medial region. The proximal region was mostly occupied by R-cells. E-cells stained basophilic with haematoxylin and eosin. F-cells stained most intensely. R-cells stained lightly with vacuolated cytoplasm. B-cells were characterized by a single prominent vacuole with a thin layer of dense cytoplasm.

a) E-cells (Fig. 8)

E-cells were the smallest cell type on the tubular epithelium. The cells were columnar in shape with height about 20 μm. The microvilli were found

on the luminal surface of the cells. The nucleus was relatively large. The mitochondria were small and spherical. The golgi body was present. Free ribosomes were scattered in the cytoplasm.

b) F-cells (Fig. 9)

F-cells were also columnar in shape and the height was about 30 μm. The apical border of F-cells was orderly lined with microvilli (Fig. 9a). F-cells had extensive rough endoplasmic reticulum, numerous vesicles, free ribosomes and mitochondria. Several Golgi bodies were found in the cell (Fig. 9b). The cisternae of Golgi body were often dilated. Small lipid droplets might be found in F-cells.

c) R-cells (Fig. 10)

The shape of R-cells was columnar and height of the cell was around 30 to 40 μm. R-cells also had a microvillous border (Fig. 10a). The cytoplasm was less dense than that of the F-cells. Numerous lipid droplets were found in the cytoplasm. A supranuclear vacuole was often present in the cytoplasm of R-cells (Fig. 10b). Its diameter ranged from 4 to 7.5 μm. The vacuole might contain dense granules and fibers. A network of smooth endoplasmic reticulum was located in the basal region (Fig. 10c). The plasma

membrane in the basal region was invaginated to form basal infoldings.

d) B-cells (Fig. 11)

B-cells were the largest cell type in the hepatopancreas. The cell varied from 30 to 60 μm in height and was barrel shaped. The microvillous border was often distorted. The cytoplasm of B-cells was dense and reduced into a thin rim surrounding the vacuole. The vacuole might contain particulate materials and vesicles. The apical region of the B-cells consisted of a microvillous border, subapical vacuoles, pinocytotic vesicles, pinocytotic channels and a dense cytoplasm. The nucleus was flattened and compressed laterally or basally.

3.3.4 Myoepithelial cells around the hepatopancreatic tubules (Fig. 12)

The tubules of hepatopancreas were encompassed with myoepithelial cells. They were squamous cells lined outside the basal lamina of the epithelium of the tubules (Fig. 12a). They were flat and low in height (about 6 to 10 μm). Longitudinal and circular myofibrils were found inside the cytoplasm of the myoepithelial cells. The myofibrils were striated with sacromere length of about 3.0 to 4.5 μm (Fig. 12b). Myofibrils extended from the myoepithelial cells and formed a muscle network surrounding the tubules

(Fig. 12c). Circular myofibrils were extended from the myoepithelial cells and encircled the tubules. Circular myofibrils were around 1.0 to 1.5 μm in diameter and 18 to 20 μm apart. Longitudinal myofibrils were 0.5 to 1.0 μm in diameter and branched from the circular myofibrils at about 7.5 μm interval.

3.4 Discussion

The four types of cells found on the tubular epithelum in the hepatopancreas of Metapenaeus ensis were similar to those described in Orconectes virilis and Procambarus clarkii (Loizzi, 1971). However, the M-cells reported in the hepatopancreas of Penaeus semisulcatus (Al-Mohanna et al., 1985b) was not observed in M. ensis. M-cells were reported to be sparsely distributed in the hepatopancreas, so that it may be difficult to discover.

The F-cells in M. ensis had extensive rough endoplasmic reticulum and several Golgi bodies, implicating that they are active in protein synthesis. F-cells are supposed to be responsible for the synthesis and secretion of digestive enzymes (Gibson & Barker, 1979). Al-Mohanna et al. (1985a) demonstrated that zymogen granules are secreted by F-cells. Discharge of zymogen granules was not observed in M. ensis and was also not reported in Procambarus clarkii (Bunt, 1968) and Penaeus vannamei (Caceci et al., 1988).

Pinocytotic vesicles and channels were observed in the apical region of B-cells in M. ensis, suggesting that B-cells also absorb digested materials from the lumen of the tubules. Digestive enzymes may be secreted from B-cells but the mode of secretion may vary. Apocrine secretion was observed in O. virilis and Procambarus clarkii (Loizzi, 1971), but holocrine secretion was reported in P. semisulcatus (Al-Mohanna & Nott, 1986) and Carcinus maenas (Hopkin & Nott, 1980). B-cells in M. ensis did not show apocrine secretion. On the other hand, holocrine secretion which resembled the mode of secretion in C. maenas and P. semisulcatus was observed. Waste materials might be carried in the digestive vacuole and excreted with the extruded B-cells. The digestive vacuole of the B-cells in P. semisulcatus was shown to contain sulphurous sphercules and being extruded in the faeces (Al-Mohanna & Nott, 1986). Since the ultrastructure and mode of secretion of B-cells in M. ensis were similar to the B-cells in P. semisulcatus, they probably performed similar functions including absorption of food materials through apical pinocytosis for intracellular digestion and excretion of waste materials stored in the digestive vacuole during cell extrusion, as suggested by Al-Mohanna & Nott (1986).

A supranuclear vacuole was often observed in the R-cells of M. ensis. It was also found in the R-cells of P. semisulcatus (Al-Mohanna & Nott, 1987a). Bunt (1968) described the supranuclear vacuole in Procambarus clarkii as a phagosome which was believed to contain undigested material. Al-Mohanna & Nott (1987a) suggested that supranuclear vacuole is the site of

assimilation of absorbed metabolites from the lumen. Wastes of assimilation and metals were stored in the supranuclear vacuole. The supranuclear vacuole in R-cells of M. ensis also showed a similar feature and thus may also be the site of assimilation of absorbed metabolites and storage of wastes as suggested in P. semisulcatus. Basal infoldings in R-cells was observed in M. ensis and also in other species such as O. virilis and Procambarus clarkii (Loizzi, 1971), P. semisulcatus (Al-Mohanna & Nott, 1987a), and P. vannamei (Caceci et al., 1988). The basal infoldings possibly increase the surface area for transferring metabolites to haemolymph.

Since shrimp possess an open circulatory system, the hepatopancreas with its tubules is bathed in the haemolymph. Pores on the connective tissue sheath of the hepatopancreas in M. ensis may be a passage for the outflow of haemolymph from the hepatopancreas. The fibers on the interior surface of the connective tissue sheath may help to bind the sheath to the tubules.

The muscle network surrounding the tubules of the hepatopancreas in M. ensis was found to be striated. Striation of the muscle network was also reported in P. vannamei (Caceci et al., 1988) and in O. virilis and Procambarus clarkii (Loizzi, 1971). The muscle network consists of longitudinal and circular fibers which control dilation and contraction of the tubules. Leavitt et al. (1982) has reported a similar arrangement of the myofibrils in the hepatopancreas of Homarus americanus.

It has been suggested that B-cells are possibly derived from F-cells (Loizzi, 1971; Barker & Gibson, 1977; Hopkin & Nott, 1980; Al-Hohanna et al. 1985a). Since only F- and R-cells were present in the medio-distal region and B-cells in the medial region of the tubules, B-cells must be derived from either one of these two types. B-cells lack any lipid droplets in the cytoplasm and no intermediate forms between R- and B-cells were observed. No basal infoldings of plasma membrane was observed in B-cells which were present in R-cells. On the other hand, both the cytoplasms of F- and B-cells were dense and filled with numerous vesicles. These observations support the hypothesis that B-cells are derived from F-cells.

In the present study, the hepatopancreas of M. ensis is found to be similar to those of other decapod crustaceans in terms of cell types, ultrastructure and muscular network.

Fig. 2. A dissected Metapenaeus ensis showing the alimentary canal. The pyloric stomach is being surrounded by the hepatopancreas (HP). CS, cardiac stomach; HG, hindgut; MG, tubular midgut; OE, oesophagus. Scale bar represents 1 cm.


MG

Fig. 3. Scanning electron micrographs of the connective tissue sheath of the hepatopancreas in Metapenaeus ensis.

(a) Exterior surface. Pores (O) are found on the sheath. HE, haemocyte; O, pore. Scale bar represents 10 μm.

(b) Interior surface of the connective tissue sheath. CF, connective fiber; O, pore. Scale bar represents 10 μm.

a

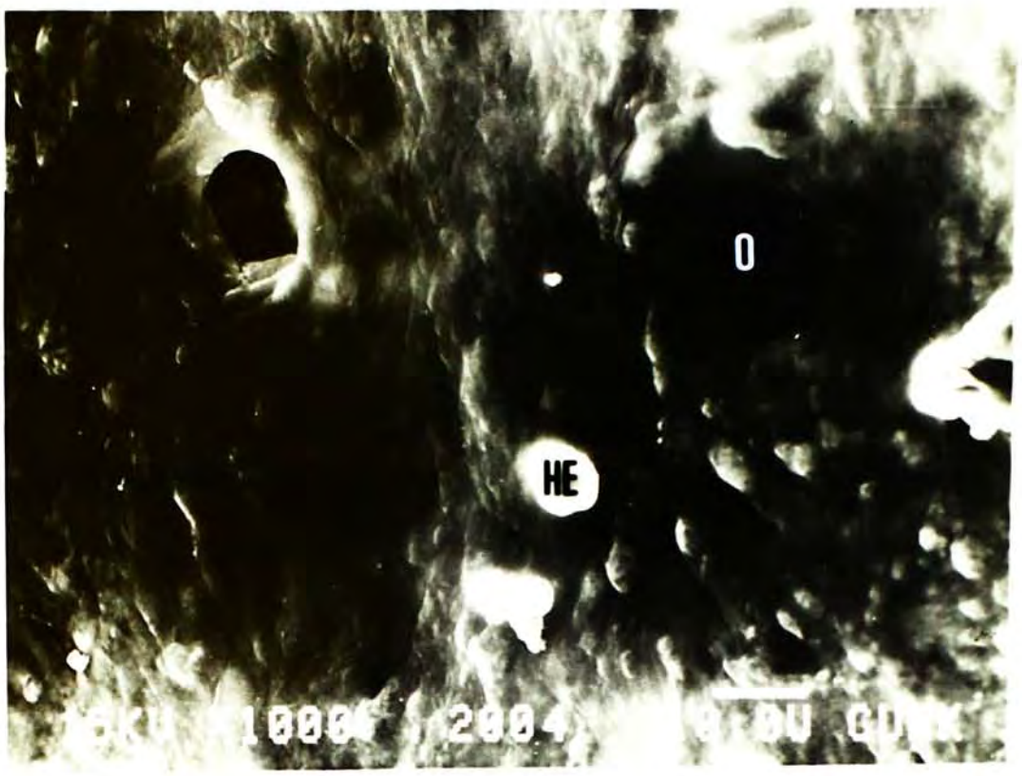

b

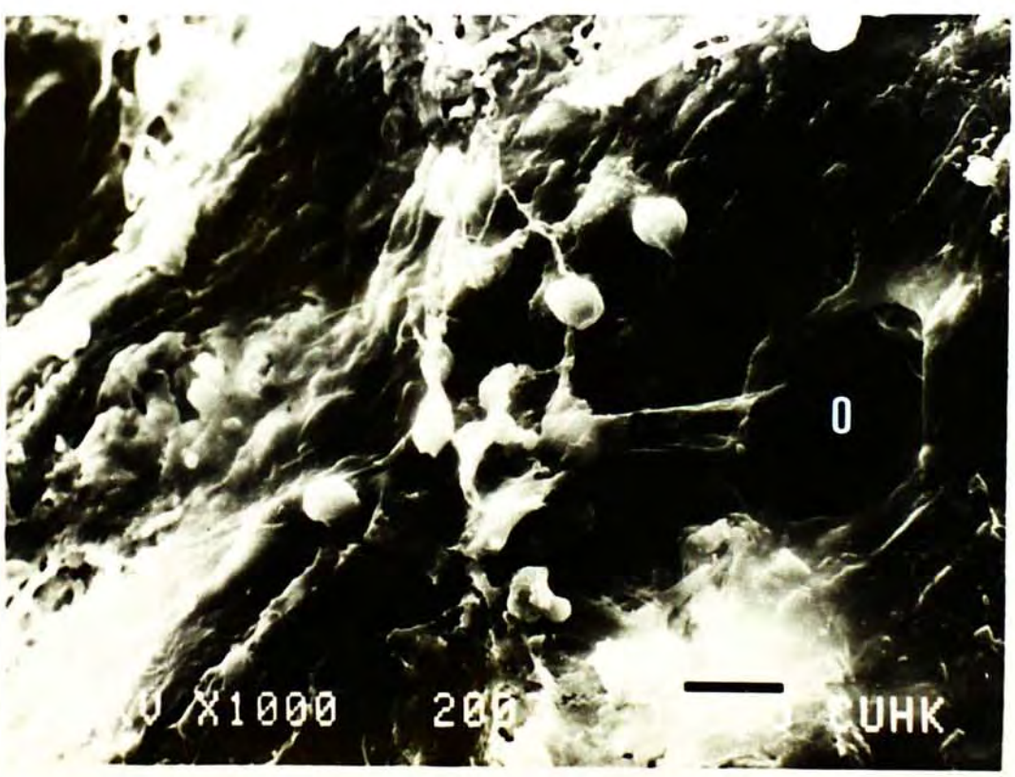

Fig. 4. Transmission electron micrograph of the sections through the connective tissue sheath of the hepatopancreas in Metapenaeus ensis.

(a) Intercellular space (S) and fibrous laminar (FL) are found in the sheath. Groups of cresent-like granules (CG) are located alongside of the sheath. Scale bar represents 5 μm.

(b) Nucleus of the sheath cell. The nucleus (N) is located peripherally. The sheath cells are filled with numerous vesicles (V). CG, cresent-like granules; FL, fibrous laminar. Scale bar represents 1 μm.

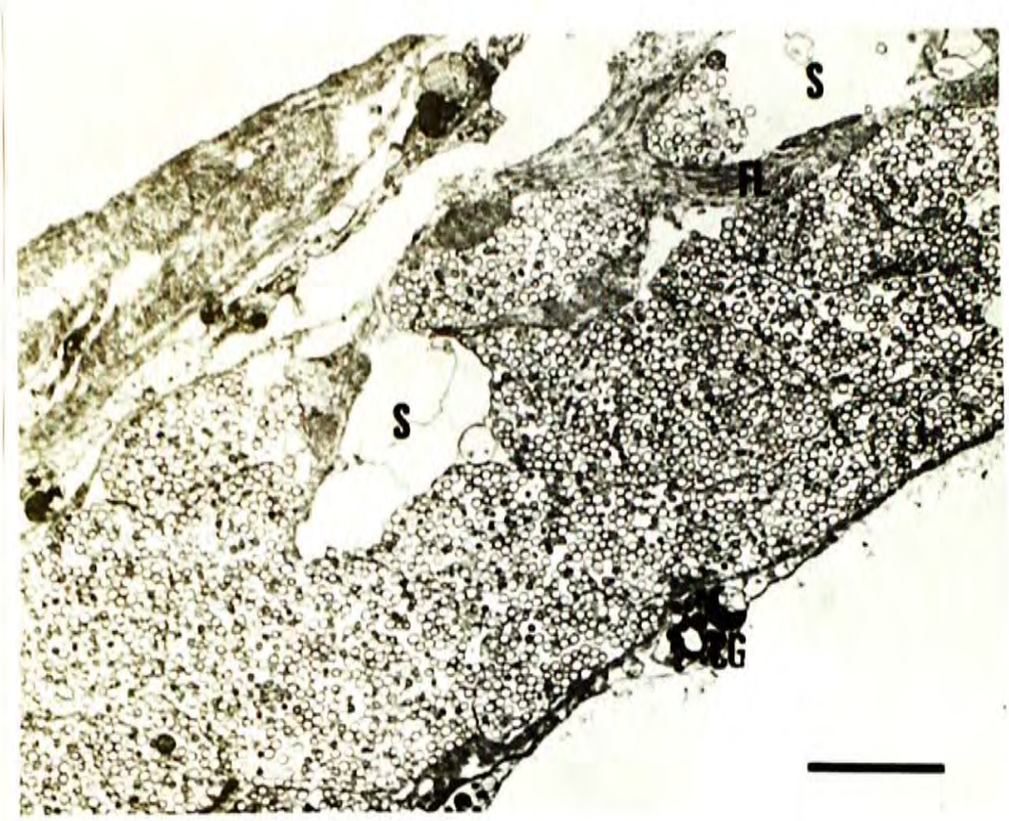

a

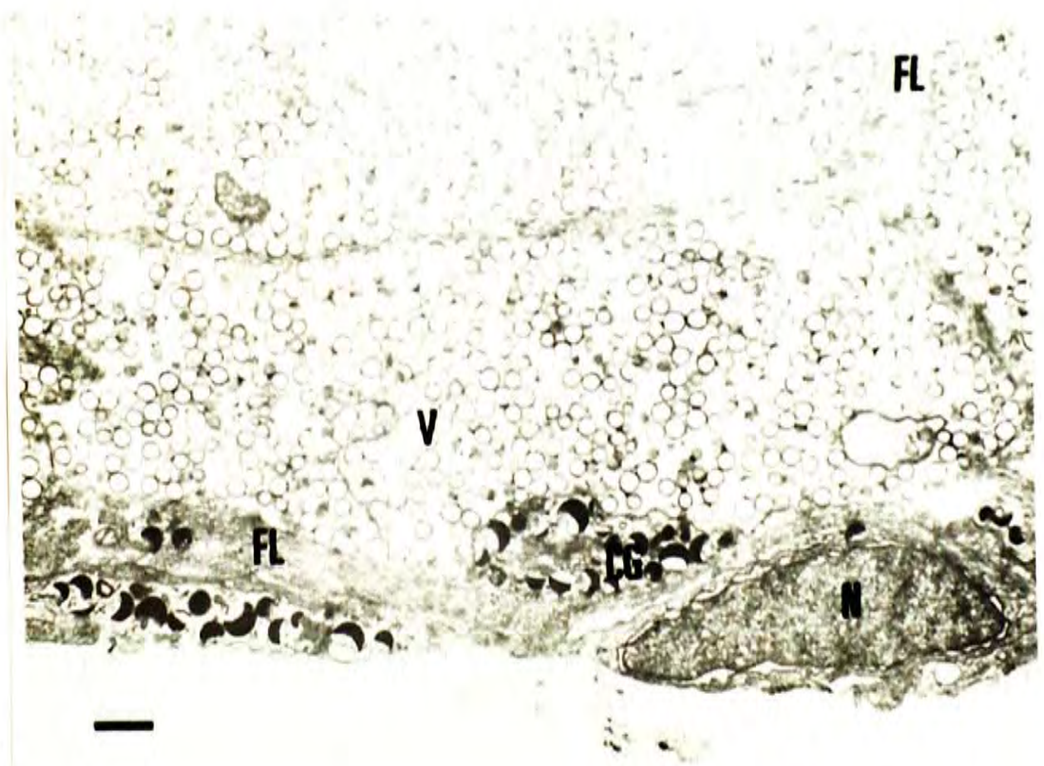

b

Fig. 5. Tubules of hepatopancreas in Metapenaeus ensis. The tubules (T) are blind-ended. Connective fibers (CF) are found among the tubules. CT, connective tissue sheath. Scale bar represents 20 μm. H & E.

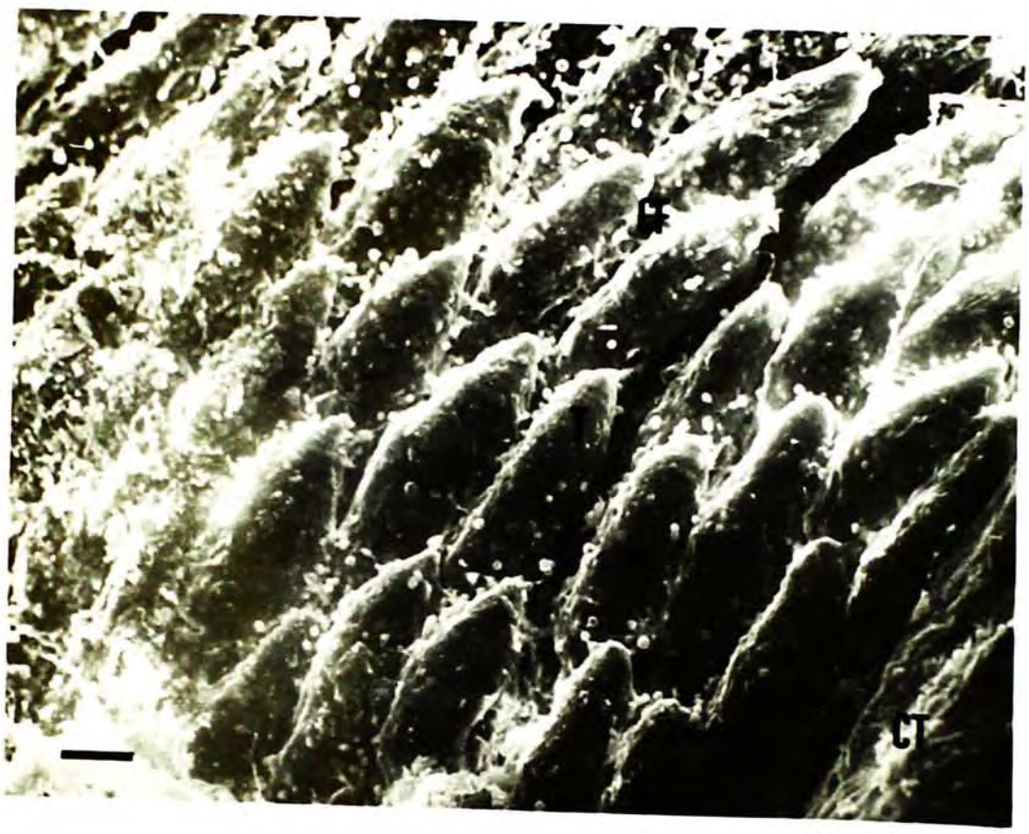

Fig. 6. Section through the hepatopancreas of Metapenaeus ensis. The tubules (T) are open to a collecting duct (CD). Blood capillaries (BC) penetrate into the hepatopancreas to supply haemolymph to the organ. CT, connective tissue sheath. Scale bar represents 50 μm. H & E.

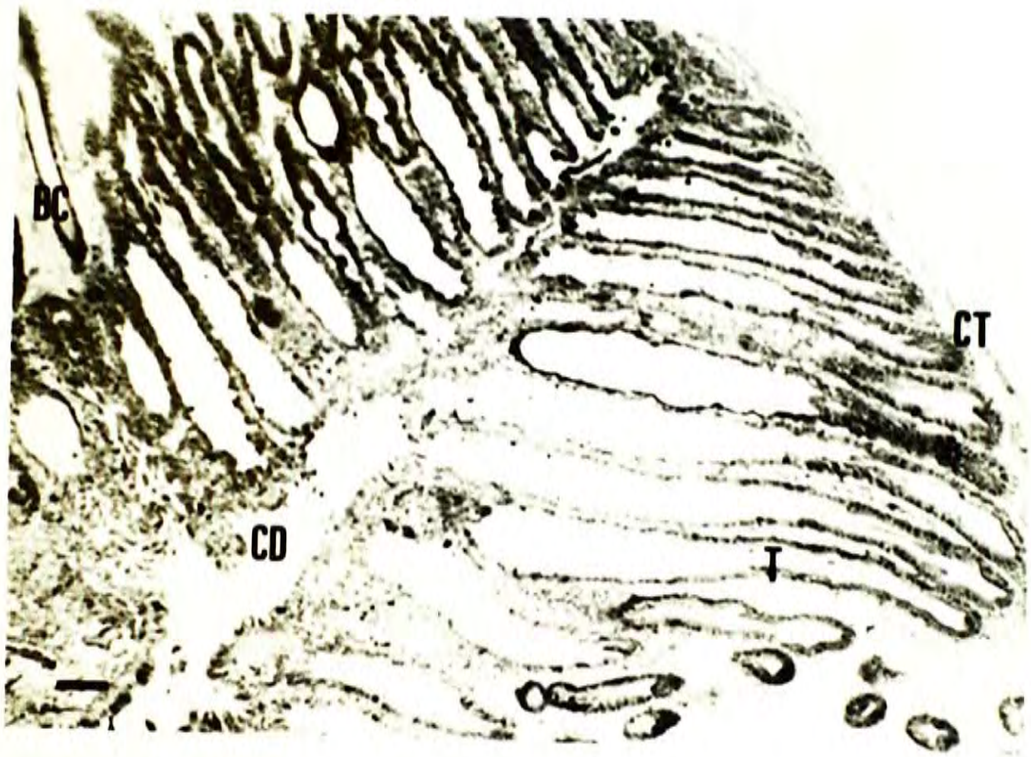
BC
CT
CD
T

Fig. 7. Different cell types found in the hepatopancreas in Metapenaeus ensis. B, B-cell; CT, connective tissue sheath; E, E-cell; F, F-cell; FB, fibroblast; HC, haemocoel; R, R-cell; arrow-head, myoepithelial cell. Scale bar represents 50 μm. H & E.

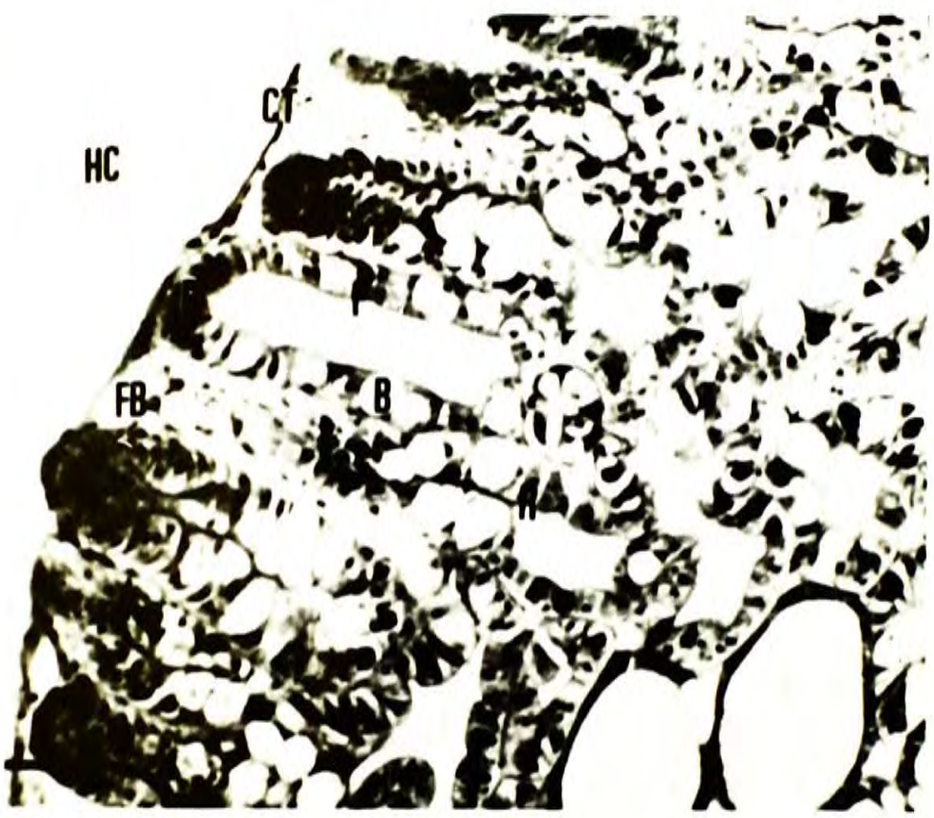
HC
CT
FB
B
A

Fig. 8. Transmission electron micrograph of E-cells in the hepatopancreas of Metapenaeus ensis. The size of the nucleus (N) is relatively large and is basally located. BL, basal lamina; M, mitochondrion; MV, microvilli. Scale bar represents 2 μm.

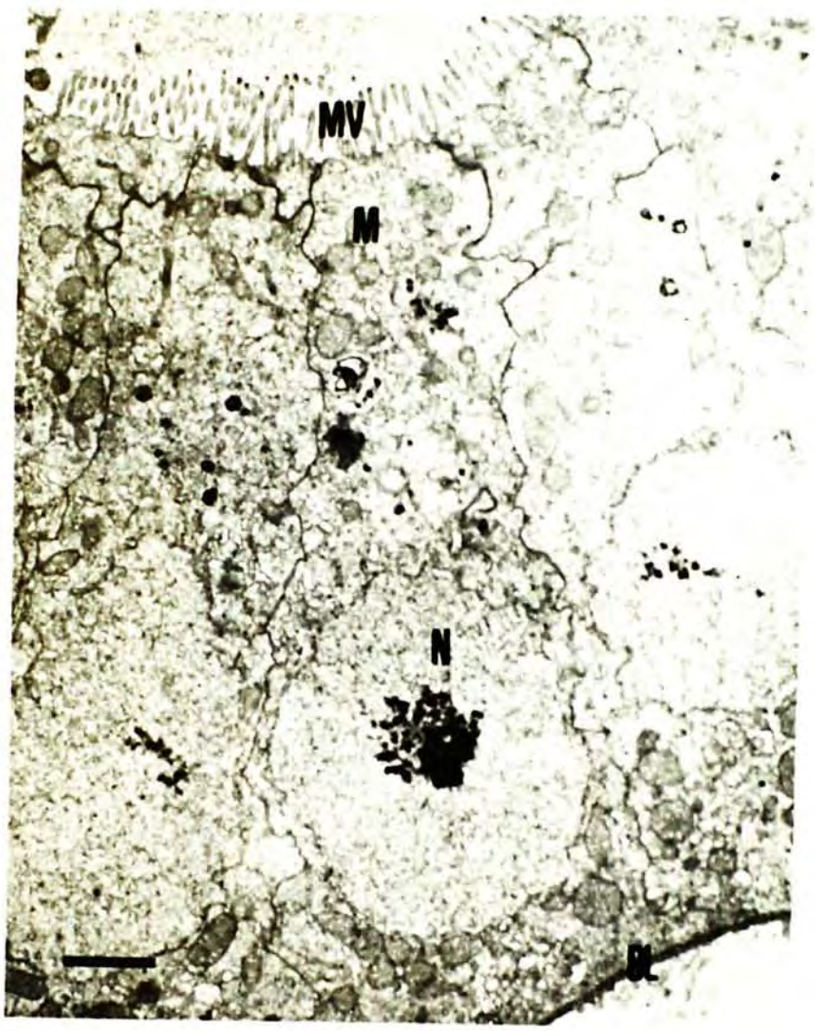
MV
M
N
BL

Fig. 9. Transmission electron micrographs of F-cells in the hepatopancreas of Metapenaeus ensis.

(a) Apical region having numerous vesicles (V). G, Golgi body with dilated cisternae; M, mitochondrion; MV, microvilli. Scale bar represents 1 μm.

(b) Basal region. The cell consists of extensive rough endoplasmic reticulum (RE) and Golgi bodies (G). BL, basal lamina; M, mitochondrion; N, nucleus; NO, nucleolus; R, R-cell. Scale bar represents 2 μm.

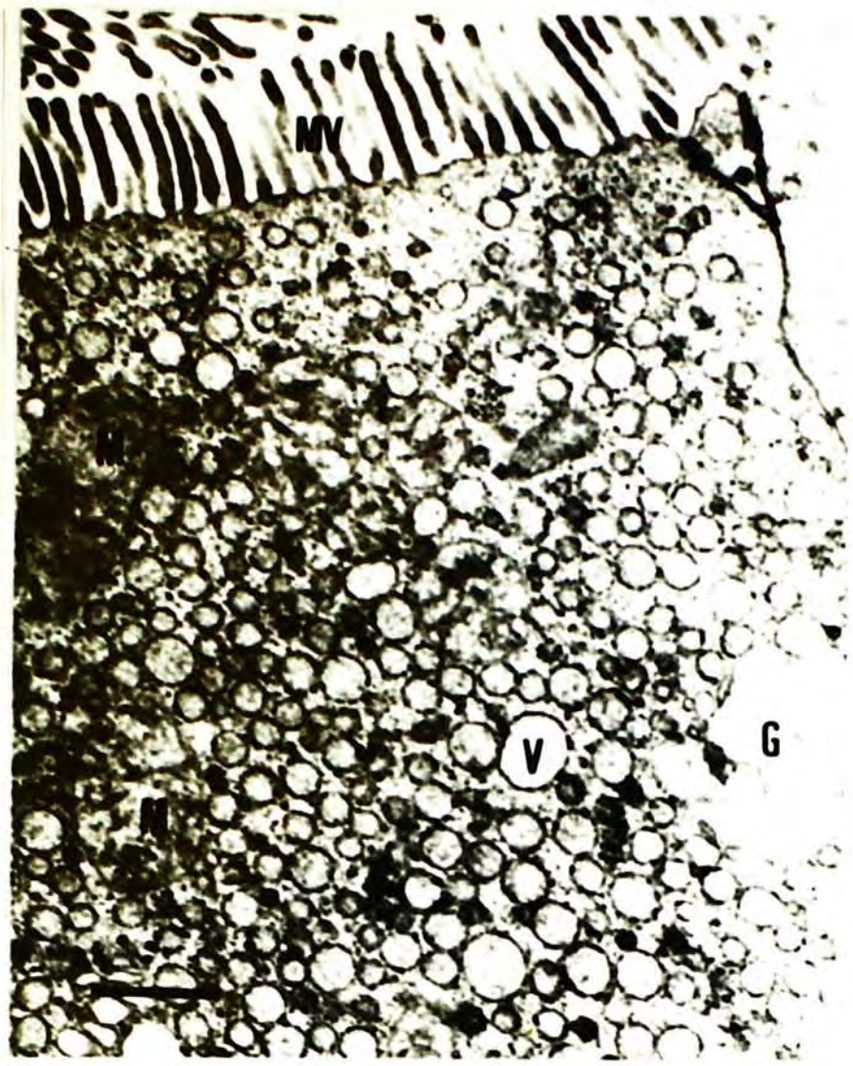

a

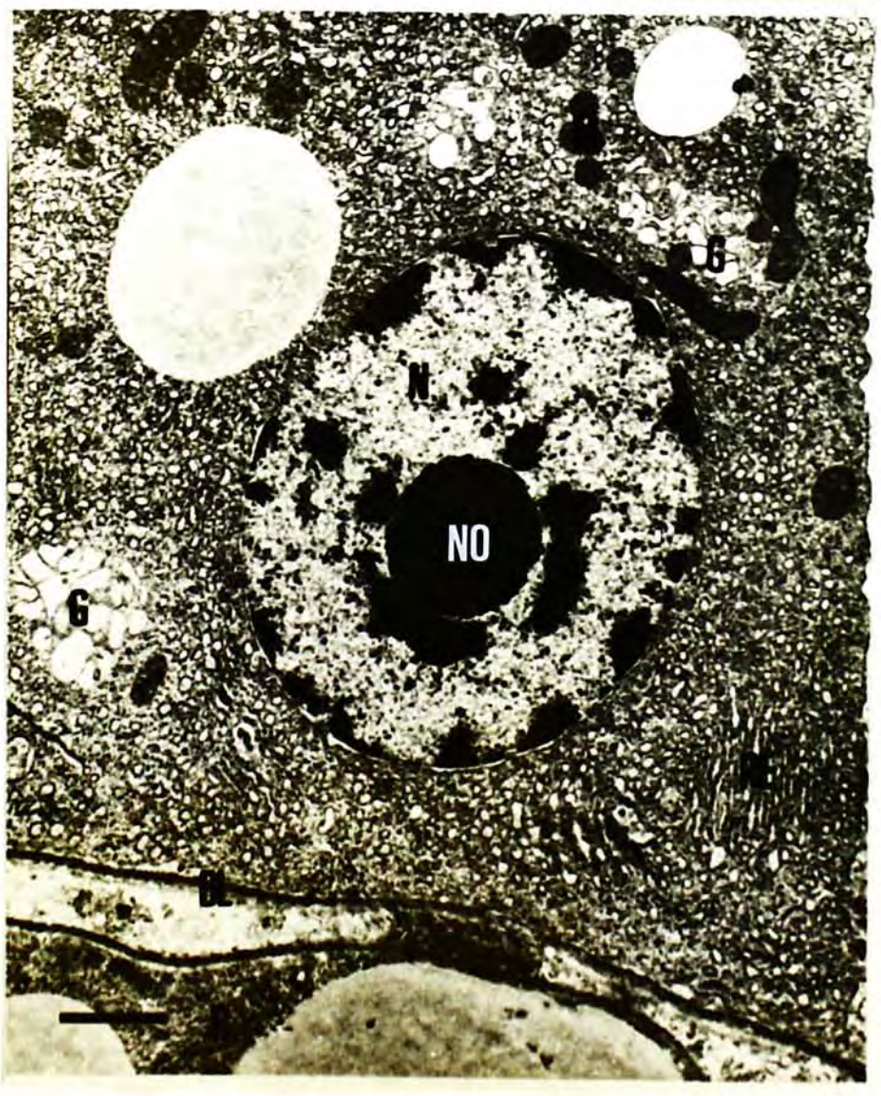

b

Fig. 10. Transmission electron micrographs of R-cells in the hepatopancreas of Metapenaeus ensis.

(a) Lipid droplets (LP) and supranuclear vacuole (SN) are the characteristics of the cell. M, mitochondrion; MV, microvilli; N, nucleus. Scale bar represents 10 μm.

(b) Supranuclear vacuole (SN) of R-cell. Dense granules (arrow-heads) and stacks of fibers (arrow) are found inside the vacuole. M, mitochondrion; MV, microvilli; N, nucleus. Scale bar represents 1 μm.

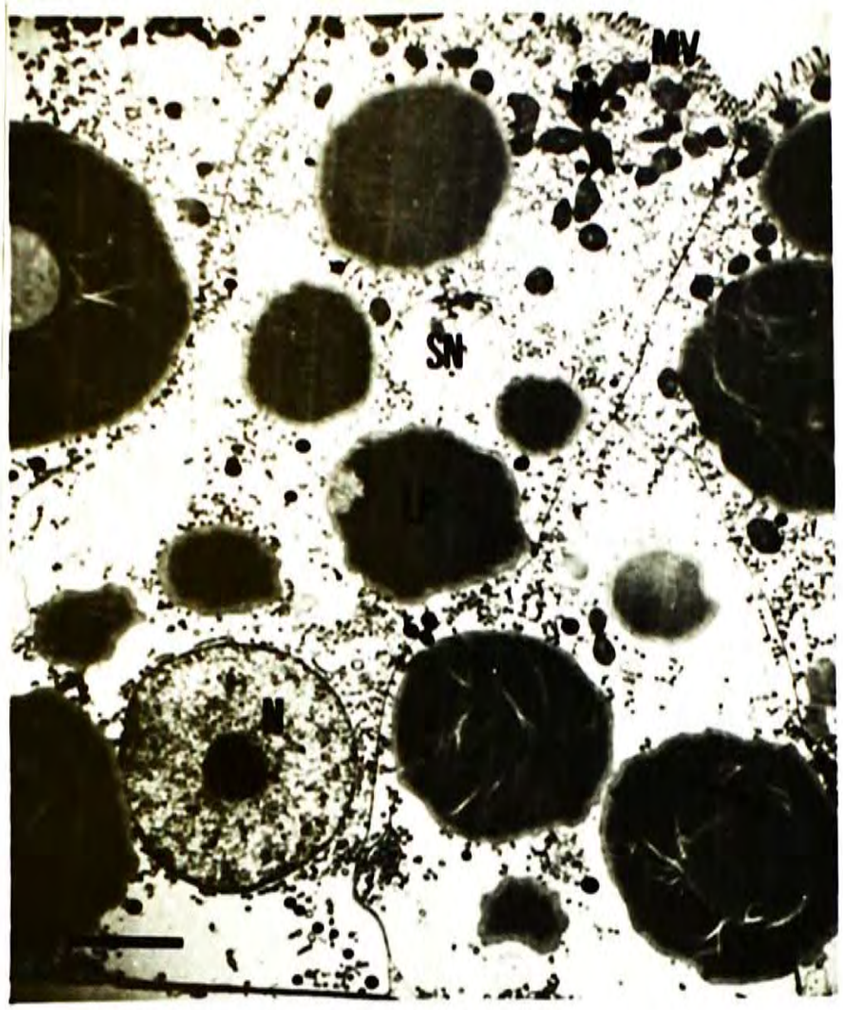

a

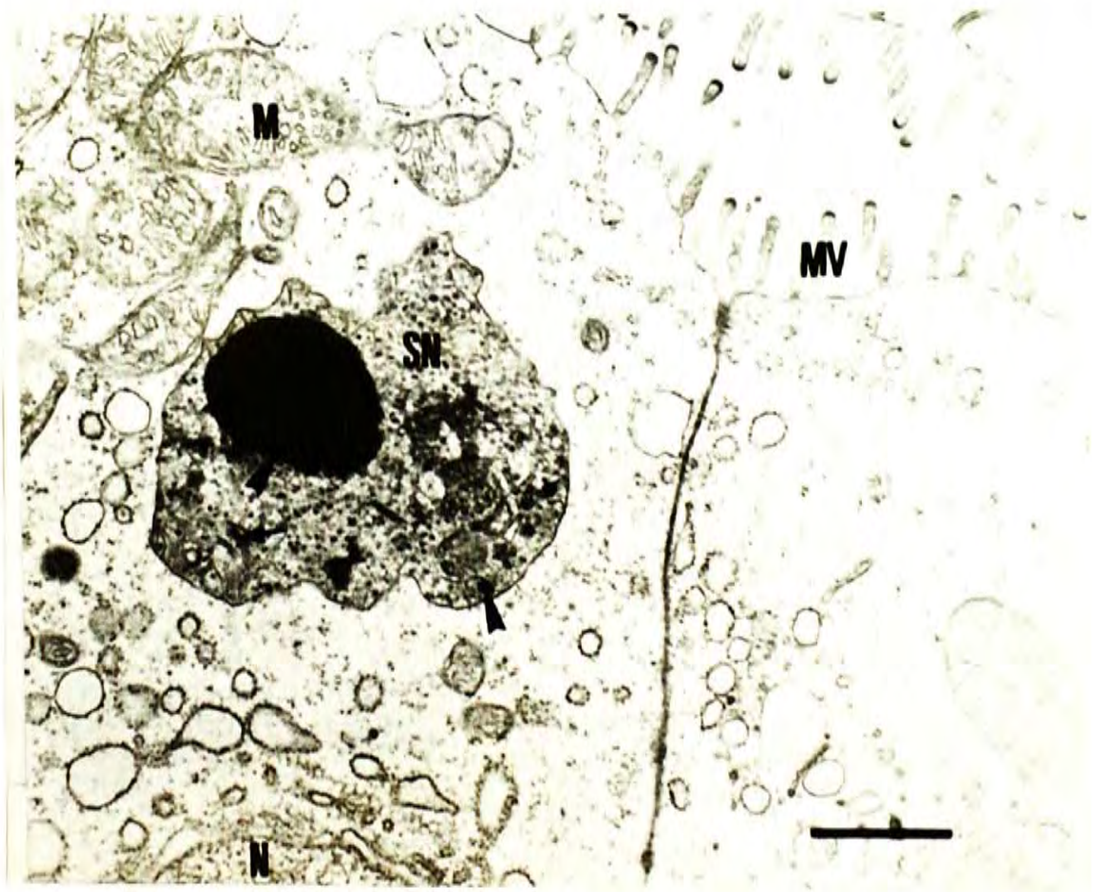

b

Fig. 10 (con't).

(c) Basal region of R-cell showing invagination of the plasma membrane (arrow-heads). BL, basal lamina; LP, lipid droplet; RE, rough endoplasmic reticulum. Scale bar represents 1 μm.

C

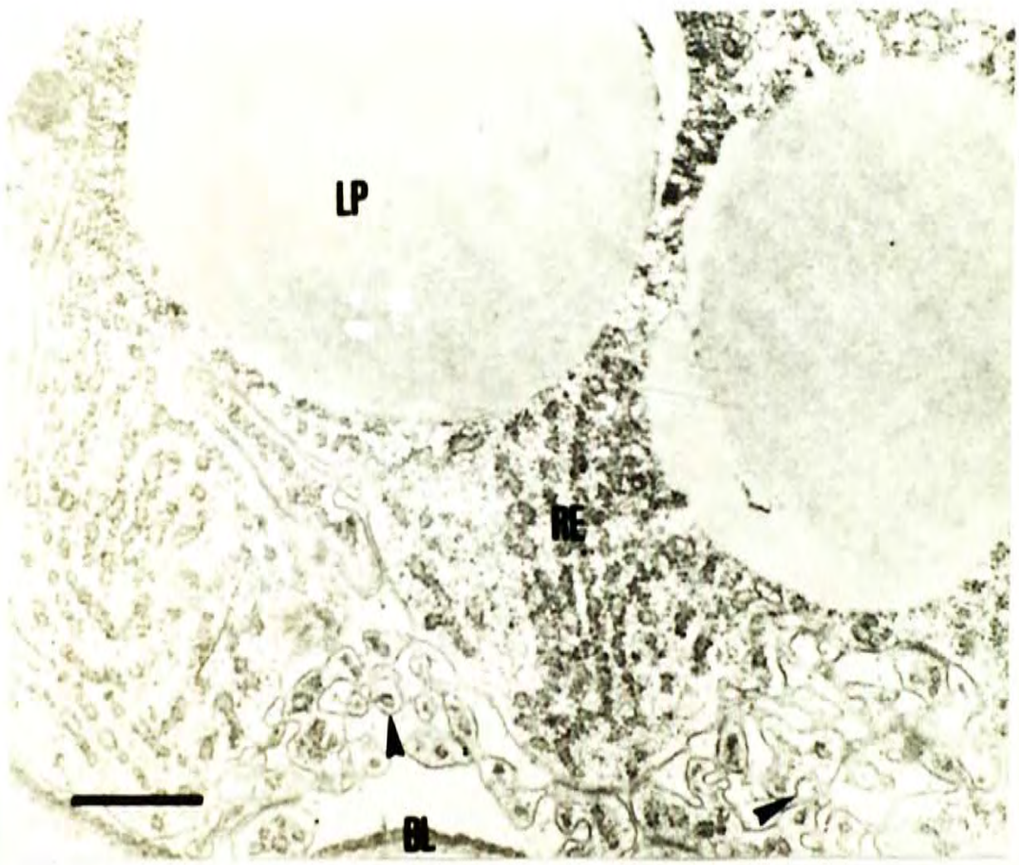

Fig. 11. Electron micrograph of a portion of the hepatopancreas showing a B-cell in Metapenaeus ensis. The B-cell is characterized by the large digestive vacuole (DV). B, B-cell; F, F-cell; MV, microvilli; N, nucleus; R, R-cell; SA, subapical vacuole. Scale bar represents 2 μm.

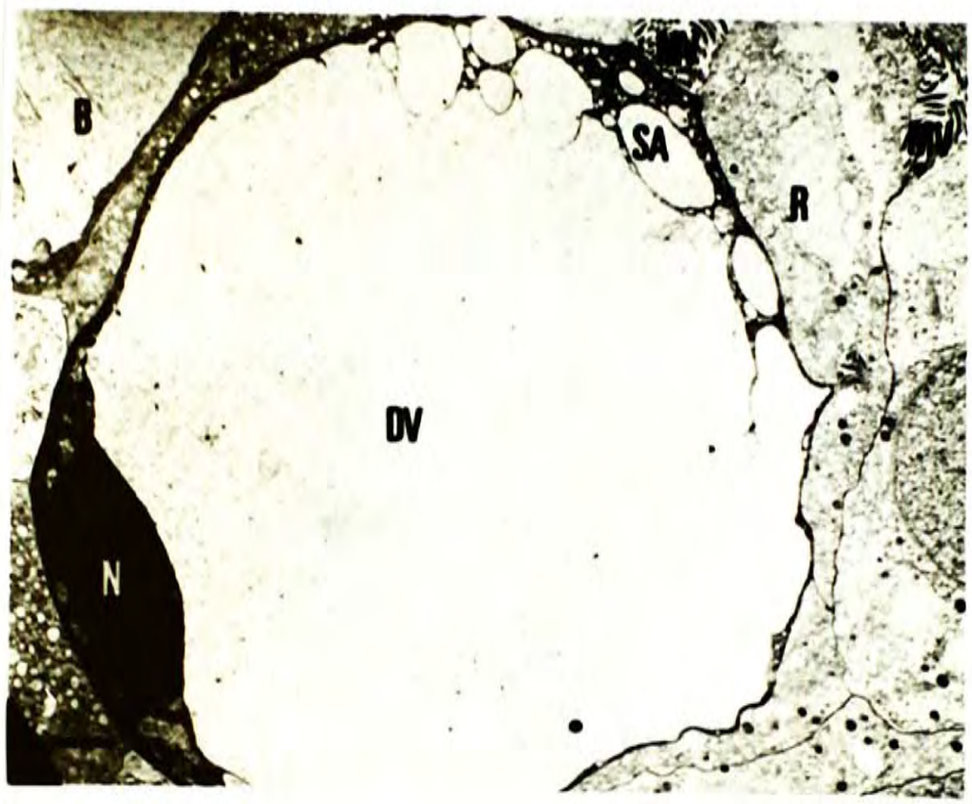
B
SA
R
DV
N

Fig. 12. Electron micrographs of myoepithelial cells in the hepatopancreas of Metapenaeus ensis.

(a) The cell is situated outside the basal lamina (BL) of the tubule. HC, haemocoel; MF, myofibrils; N, nucleus; R, R-cell. Scale bar represents 2 μm.

(b) Striations of the myofibrils in the myoepithelial cell in the hepatopancreas of Metapenaeus ensis. BL, basal lamina; N, nucleus; Z, Z-line of myofibrils. Scale bar represents 2 μm.

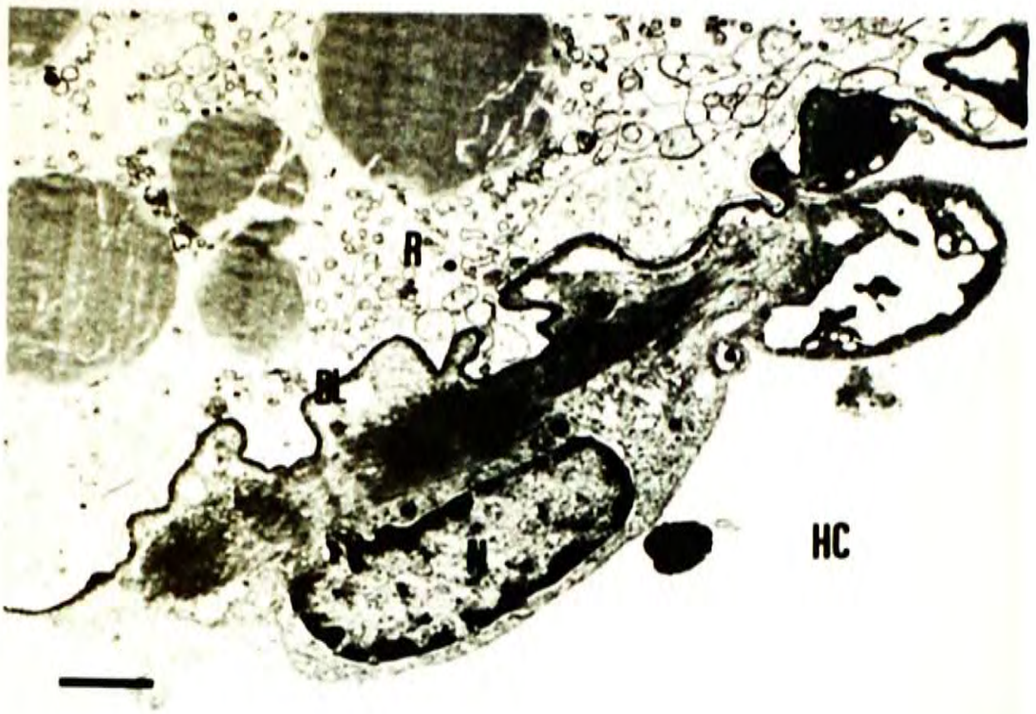

a

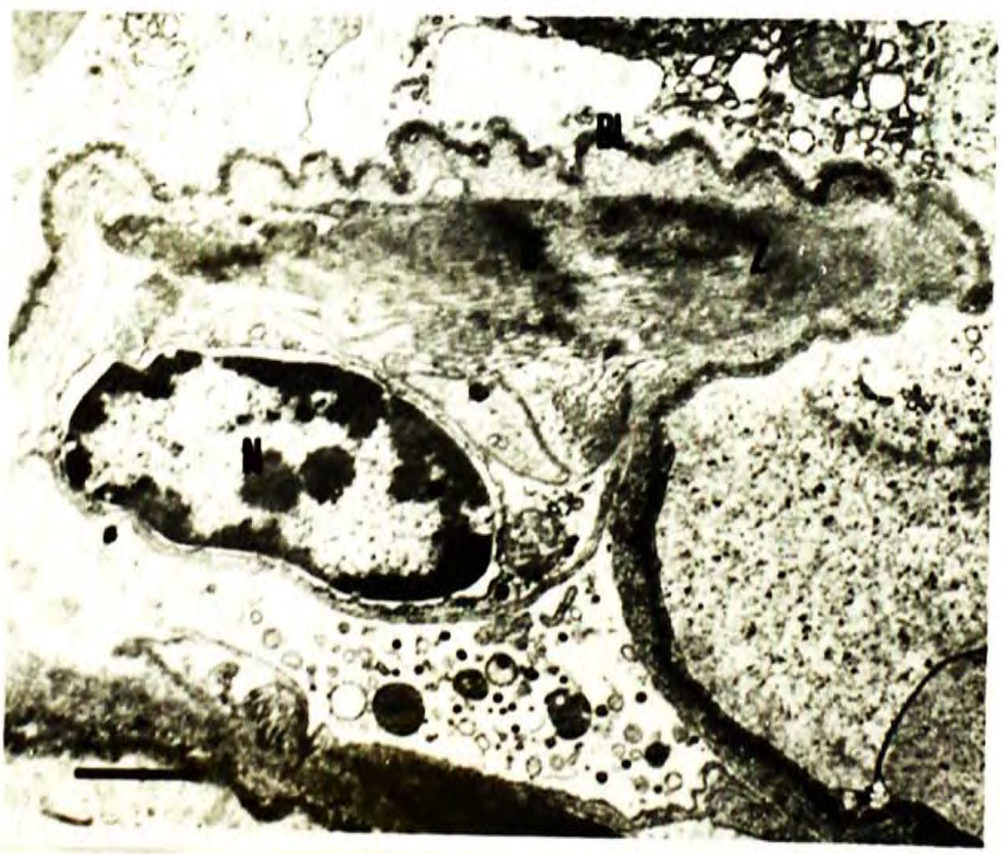

b

Fig. 12 (con't).

(c) Scanning electron micrograph showing myofibrils extending from myoepithelai cell (MY). The tubule is encompassed by the circular myofibrils (CM). Longitudinal myofibrils (LM) branch from the circular myofibrils. Scale bar represents 20 μm.

C

CHAPTER IV

POST-EMBRYONIC DEVELOPMENT OF THE ALIMENTARY CANAL IN SHRIMP Metapenaeus ensis WITH EMPHASIS ON THE HEPATOPANCREAS

4.1 Introduction

The hepatopancreas of decapod crustaceans has been extensively studied. However, little studies deal with the development of this organ during the early life history. Development of the hepatopancreas of the American lobster Homarus americanus was studied by Factor (1981) and Biesiot (1986). The larval development of the lobster is simpler than that of the penaeid shrimp. The lobster larvae are equivalent to the mysid larvae of the penaeid shrimp. Development of the alimentary canal was studied in the penaeid species of Penaeus orientalis (Gao et al., 1986) and P. setiferus (Lovett & Felder, 1989). Kinematics of the larval gut was studied in P. setiferus (Lovett & Felder, 1990). The larval hepatopancreas of the above two penaeid shrimps studied was simple at the early stages and then the organ progressively increases in complexity and develops into the adult hepatopancreas. The morphology of the hepatopancreas these two Penaeus species was described but the cytology of the larval hepatopanceas was not studied.

Metapenaeus ensis has been successfully propagated and reared in the Marine Science Laboratory in the Chinese University of Hong Kong (Tseng et al., 1979). The larval development of M. ensis is typical of the penaeid shrimp. The larval stages are divided into nauplius, protozoea, and mysis (Figs. 13-15). The nauplius is subdivided into six instars (NI-NVI); protozoea, three instars (PZI-PZIII); and mysis, three instars (MI-MIII). After larval development, the animal becomes a postlarva (PL) (Fig. 16). The development of the postlarva are often designated by the number of days since the mysis becomes a postlarva. In the present study, the development and cytology of the alimentary canal with emphasis on the hepatopancreas through the various larval and postlarval stages of M. ensis was studied.

4.2 Materials and Methods

Gravid females of Metapenaeus ensis were acquired from the fish markets at Lei Yu Mun. The shrimp was individually kept in 500 l glass fiber tanks in the laboratory. The tank was covered by a black board to exclude light and disturbance. The seawater was well aerated. The temperature and salinity of seawater were maintained at 30 °C and 33 ppt respectively. Disodium salt of ethylenediaminetetra-acetic acid (EDTA) was added to seawater at a concentration of 10 ppm. Chan (1984) has shown that the addition of EDTA to seawater enhances the hatching rate of shrimp larvae. Metamorphosis would be abnormal and delayed in the absence of EDTA. The

identification of the larval stages of M. ensis was based on Chan (1984). Nauplius is the non-feeding stage and it depends on the yolk material. Protozoeae and myses were fed with laboratory cultured Chaetoceros gracilis. Nauplii of Artemia were added to the the culture tank starting at the second or third mysid stage in the concentration of 3 nauplii/ml. The application of Artemia nauplii also continued through postlarval development.

The post-embryonic development of the alimentary canal in the M. ensis was studied using histological and electron microscopic methods. Samples were taken at stages NI-NVI, PZI-PZIII, MI-MIII, PL1, PL6, PL10, PL20 and PL30 (about 1 cm in length). The shrimp were anaesthetized with a few drops of saturated magnesium sulphate solution before fixation.

The method used in histological study was according to Humason (1974) as described in Chapter III. The animals were fixed in Bouin's fluid for 24 h and dehydrated though ethanol, and then were embedded in paraffin wax with melting point 56-58 ^{o}C. The sections were 5 μm thick and stained with hematoxylin and eosin (H & E).

The method used for electron microscopic study followed that described in Chapter III. The larvae were fixed in 1% glutaraldehyde in 0.1 M phosphate buffer (pH 7.2) with 2% paraformaldehyde added. The samples were post-fixed in 1% osmium tetroxide in the same buffer. Dehydration was carried through ethanol. The samples were embedded in Spurr's epoxy resin.

The sections were stained with uranium acetate and lead citrate. They were examined under a Zeiss EM9S-2 transmssion electron microscope.

4.3 Results

4.3.1 Morphology of the developing alimentary canal (Figs. 17-32)

Bodies of naupius I and II of Metapenaeus ensis were filled with numerous yolk cells (Figs. 17 & 18). The alimentary canal of the animal was not distinguishable until NIII where gut epithelial cells were observable at the rear portion of the gut (Fig. 19). The anterior portion of the alimentary canal was occupied by many yolk cells. The gut epithelial cells were cuboidal with large nucleus and prominent nucleolus.

The gut morphology in NIV was more well defined. The naupliar gut was lined with a layer of cuboidal epithelial cells. The anterior half of the gut was a dilated chamber filled with yolk cells forming the yolk sac (Fig. 20a). A tube ran from the yolk sac to the ventral side of the nauplius forming the foregut (Fig. 20b). A pair of caeca arose from the anterior end of yolk sac (Fig. 20c). Each caecum was circular in shape. This pair of gut caeca became oval in NV (Fig. 21) and NVI (Fig. 22a). The foregut became prominent in NVI (Fig. 22a). The yolk sac was nearly devoid of yolk cells in NVI. The two caeca arose from the lateral side of the yolk sac (Fig. 22b).

The foregut and midgut became distinguishable in protozoeal stage. The foregut of protozoea I was short. The midgut in PZI was a straight tube with two pairs of caeca, namely the anterior and posterior hepatopancreatic rudiments (Fig. 23). The two pairs of rudiments developed from the anterior end of the midgut within the cepthalothoracic region of the animal. The structure and size of the anterior and posterior rudiments were similar. As observed in PZII, the oesophagus joined the ventrally directed mouth to the stomach at almost a right angle (Fig. 24a). The anterior hepatopancreatic rudiments increased in size and the posterior hepatopancreatic rudiments elongated in PZII (Fig. 24b). The stomach was differentiated into cardiac and pyloric chambers in PZIII (Fig. 25a). The cardiac and pyloric stomach were separated by the cardiopyloric valve. The cardiac stomach in PZIII was tubular but no ossicles formed yet. The pyloric stomach was a bulbous chamber with a developing gland filter. The anterior hepatopancreatic rudiments lay dorso-laterally on the foregut and the posterior hepatopancreatic rudiments lay ventro-laterally under the tubular midgut and extended beyond the junction of the foregut and midgut. The interampullary ridge first appeared in PZIII, dividing the ventral chamber of the pyloric stomach into two ventral longitudinal channels (Fig. 25b). The longitudinal channels opened into the tubular midgut at the orifices of the hepatopancreatic rudiments. A proturberance emerged from each of the main lobes of the posterior hepatopancreatic rudiments in PZIII (Fig. 25c).

The foregut in mysis I was similar to that in PZIII, which was divided

into oesophagus, cardiac and pyloric stomach. Anterior midgut caecum emerged as a small bulge from the tubular midgut (Fig. 26a). The anterior hepatopancreatic rudiments increased their size to maximum in MI. The posterior hepatopancreatic rudiments also became larger. Proturberances were observed branching from the main lobes of the posterior hepatopancreatic rudiments (Fig. 26b). The anterior hepatopancreatic rudiments were shown to lie on the dorso-lateral sides of the cardiac stomach (Fig. 26c). Interampullary ridge emerged vertically from the floor of the pyloric stomach and separated the ventral pyloric chamber into two longitudinal channels. Two lateral lobes emerged from the ventro-lateral lobes (main lobes) of the posterior hepatopancreatic rudiments (Fig. 26d). A cross-section through the posterior hepatopancreatic rudiments showed clearly the presence of four lobes representing two lateral lobes and two ventro-lateral lobes surrounding the tubular midgut. The lumina of the lobes tended to be stellate (Fig. 26e). The organization of the foregut in MII was similar to that in MI (Fig. 27a & b). An additional pair of lobes emerged from the dorso-median position of the posterior hepatopancreatic rudiments (Fig. 27b). The posterior hepatopancreatic rudiments appeared to have six lobes in the cross section (Fig. 27c). The organization of the alimentary canal in MIII was similar to those in MII.

The anterior hepatopancreatic rudiments appeared to be smaller in postlarva 1 and the anterior midgut caecum became more prominent (Fig. 28). The anterior hepatopancreatic rudiments regressed in PL6 (Fig. 29a). The

space formerly occupied by the anterior rudiments was occupied by the cardiac stomach whose size had increased. Cardiac plate and median ossicle was observed in the cardiac stomach in PL6. A single tubular posterior midgut caecum was observed in PL6 (Fig. 29b). In PL10, the epithelium of the posterior hepatopancreatic rudiments folded into tubules of short length (Fig. 30a). The hepatopancreas surrounded the posterior part of the pyloric stomach and the anterior end of the tubular midgut. The tubules opened into a collecting duct in the hepatopancreas (Fig. 30b). The collecting duct ran from the anterior to the posterior end of the hepatopancreas (Fig. 30b). Lateral ossicles were developed in the cardiac stomach in PL10 (Fig. 30c). The dorsal lobe of the hepatopancreas in PL20 became greater and the organ almost wrapped around the whole pyloric stomach as in the adult (Fig. 31). Cardiac stomach was greater in PL30 (Fig. 32a). The number of tubules in PL30 appeared to be more (Fig. 32b). The length of the tubules increased. The lateral ossicles in cardiac stomach was enlarged (Fig. 32c). There were more tubules in the hepatopancreas in PL30 and the degree of ramification was less towards the posterior end of the hepatopancreas (Fig. 32d). Most of the tubules were located laterally and ventrally to the pyloric chamber (Fig. 32e).

4.3.2 Ultrastructure of cell types

a) Gut caeca cells in nauplius (Fig. 33)

The gut caeca cells in nauplius were cuboidal in shape. They consisted of a large centrally located nucleus. The nucleolus was large. Microvilli were found on the apical border of the cell. The cytoplasm consisted of extensive rough endoplasmic reticulum and two to three Golgi bodies. Mitochondria were spherical or elongated.

b) Cell types in the hepatopancreas of protozoea, mysis and postlarva

Four types of cells were found in the hepatopancreas in protozoea, mysis and postlarva of Metapenaeus ensis.

i) F-cells (Fig. 34).

The F-cells were similar in protozoea (Fig. 34a), mysis (Fig. 34b) and postlarva (Fig. 34c). The F-cells were cuboidal to columnar in shape. The apical border of the cells was lined with microvilli. The cytoplasm of F-cells was rich in rough endoplasmic reticulum and ribosomes giving the cell dark and fibrillar or foamy appearance. The cell contained several Golgi bodies.

The cisternae of the Golgi boides were generally dilated. The nucleus was round.

ii) B-cells (Fig. 35)

B-cells at different stages of transformation from F-cells could be observed. The B-cells in PZI had microvilli on the apical border (Fig. 35a). Pinocytotic channels and vesicles were observed. Sub-apical vacuoles were found and tended to fuse together. Digestive vacuole was formed. Dense region was found in the digestive vacuole. The nucleus was basal in position and compressed into irregular shape by the digestive vacuole. The cytoplasm was dense. The cell at this stage was columnar with slight dilation. A single large digestive vacuole might be found in the B-cell and the cell was barrel-shaped or tended to be round (Fig. 35b). The cytoplasm was a thin condensed layer. The nucleus was condensed. The B-cells found in MI and PL1 were also characterized by the single large digestive vacuole (Fig. 35c & d). The cells were distended by the digestive vacuole. The vacuole was surrounded by a thin rim of condensed cytoplasm as in PZI. Condensed materials were found in the vacuole. The microvilli were disoriented and lost. Strips of cytoplasm separating the sub-apical vacuoles indicated that the vacuoles are formed by fusion of small vacuoles.

iii) R-cells (Fig. 36)

The R-cell was columnar in shape and lined with microvilli at the apical border (Fig. 36a). Lipid droplets of different size were found in the cell. Numerous mitochondria were accumulated in the apical region of the cell (Fig. 36b). Supranuclear vacuole consisting of stacks of fibers and granular materials was found in R-cells. Rough endoplasmic reticulum was mainly located in the central region of the cell near the nucleus. A network of smooth endoplasmic reticulum developed in the basal region (Fig. 36c).

iv) E-cells (Fig. 37)

The E-cells were cuboidal to short columnar in shape (Fig. 37a). The apical border was lined by microvilli. The nucleus was large relative to the cell size. The cytoplasm contained numerous free ribosomes and endoplasmic reticulum throughout the cell. Some binucleated cells might be found (Fig. 37b).

c) Myoepithelial cells associated with the hepatopancreas in the developmental stages of M. ensis (Fig. 37a)

The myoepithelial cells were squamous. The cells situated outside the

basal lamina of the hepatopancreatic epithelium. The nucleus was flattened. Myofibrils were found inside the cytoplasm.

4.4 Discussion

The naupliar larvae of penaeid shrimp are non-feeding and depend on the yolk for nutrition. In Metapenaeus ensis, the gut epithelium in NIV appeared to encircle a cluster of yolk cells forming the yolk sac. The gut probably functioned in vitellophagsis, since the yolk cells were gradually resorbed inside the yolk sac of the gut. Almost all yolk cells were resorbed by PZI which is first feeding stage. The midgut cells in malacostracans invade the yolk mass and differentiate into a yolky epithelial sac containing a mass of yolk cells during larval development (Anderson, 1982). The midgut cells act as vitellophages and the yolk cells are gradually resorbed. The yolk sac then differentiates into the midgut epithelium and the digestive gland rudiments (hepatopancreas) develop as outpouchings of the sac (Anderson, 1982). M. ensis has similar development as other malacostracans.

The gastric mill was absent in the protozoea and mysis of M. ensis. Mastication of food possibly mainly depended on the mandibles. As the gastric mill of the postlarva was armed with ossicles, mastication of food might then depend on both the gastric mill and the mandibles. The gland filter developed in PZIII and possibly served to filter the triturated food particles.

In a number of crustaceans, the masticatory function of the mandibles shifts to the gastric mill during metamorphosis and the changes coincide with shift in feeding habits and habitat associated with metamorphosis (Factor, 1981). However, the gastric mill in Penaeus setiferus was rudimentary in the early postlarval stages (Lovett & Felder, 1989). Functional gastric mill and gland filter were absent in larvae of P. setiferus as monitored in vivo with video microscopy (Lovett & Felder, 1990). At which stage will the gastric mill and gland filter become functional in the larvae or postlarvae of M. ensis remains to be investigated.

The development of the hepatopancreas in M. ensis was similar to that described in Penaeus orientalis (Gao et al., 1986) and P. setiferus (Lovett & Felder, 1989). Two pairs of caeca were protruded from the anterior end of the midgut in the protozoea of these species. The caeca were named as anterior and lateral midgut caeca in P. setiferus, or distal and proximal liver diverticulum in P. orientalis. The size of the anterior pair of hepatopancreatic rudiments in M. ensis and P. orientalis increased in protozoea and mysis but the rudiments regressed in the postlarvae. The anterior pair of midgut caeca transformed into the anterior midgut caecum in P. setiferus during larval growth. In M. ensis the anterior midgut caecum was developed as a bulge from the tubular midgut. The posterior pair of hepatopancreatic rudiments of the three species enlarged and became the hepatopancreas. The epithelium of the rudiments folded into tubules and ramification of the tubules increased as

larval development advanced. The hepatopancreas eventually encompassed the pyloric stomach and the anterior portion of the tubular midgut as in adult.

The cell types in the hepatopancreas of protozoea, mysis and postlarva in M. ensis are same as those in the adult hepatopancreas. Therefore, they might have the same functions as those in the adult hepatopancreas. Transformation B-cells from F-cells was also observed in the larvae. Gao et al. (1986) described two types of cells in the larval hepatopancreas of P. orientalis under light microscopy. One of which was basophilic and was present in less amount. The other type had vacuoles of different size. These two types of cells were supposed to be the F- and B-cells respectively. The cells were mostly columnar in shape. The hepatopancreas in the larvae of H. americanus is similar to the adult except having fewer and shorter tubules (Factor, 1981; Biesiot, 1986). The four types of cells, E-, R-, F-, and B-cells are present (Biesiot, 1986). H. americanus larvae possesses a more advanced stage of hepatopancreas than that of the penaeid shrimp. This may be related to a simpler larval development in the lobster. Early stages of development of the hepatopancreas may have been bypassed in the eggs.

Myoepithelial cells were scarse in early larval stages of M. ensis. As the number of tubules in the hepatopancreas and the complexity increases, more myoepithelial cells were found to surround the tubules. The contraction and expansion the tubules in the early larval stages might be maintained by

the hydraulic pressure developed in the gut. Larvae of P. setiferus developed hydraulic pressure through antiperistalsis along the midgut trunk, anal drinking, oral drinking, and contractions of the foregut. This hydraulic pressure causes the constricted regions of the midgut and also the contracted hepatopancreatic tubules to expand (Lovett & Felder, 1990). Antiperistalsis along the midgut could also be observed in the larvae of M. ensis. The contraction and expansion may be controlled by the increasing number of myoepithelial cells surrounding the tubules as in the adult.

Fig. 13. Metapenaeus ensis at nauplius V stage. AN, antenna; AU, antennule; MA, mandible; FS, furcal setae. Scale bar represents 0.2 mm.


AU
AN
MA
FS

Fig. 14. Metapenaeus ensis at protozea II stage. AB, abdomen; AN, antenna; AU, antennule; CE, compound eye; CX, cephalothorax. Scale bar represents 0.5 mm.

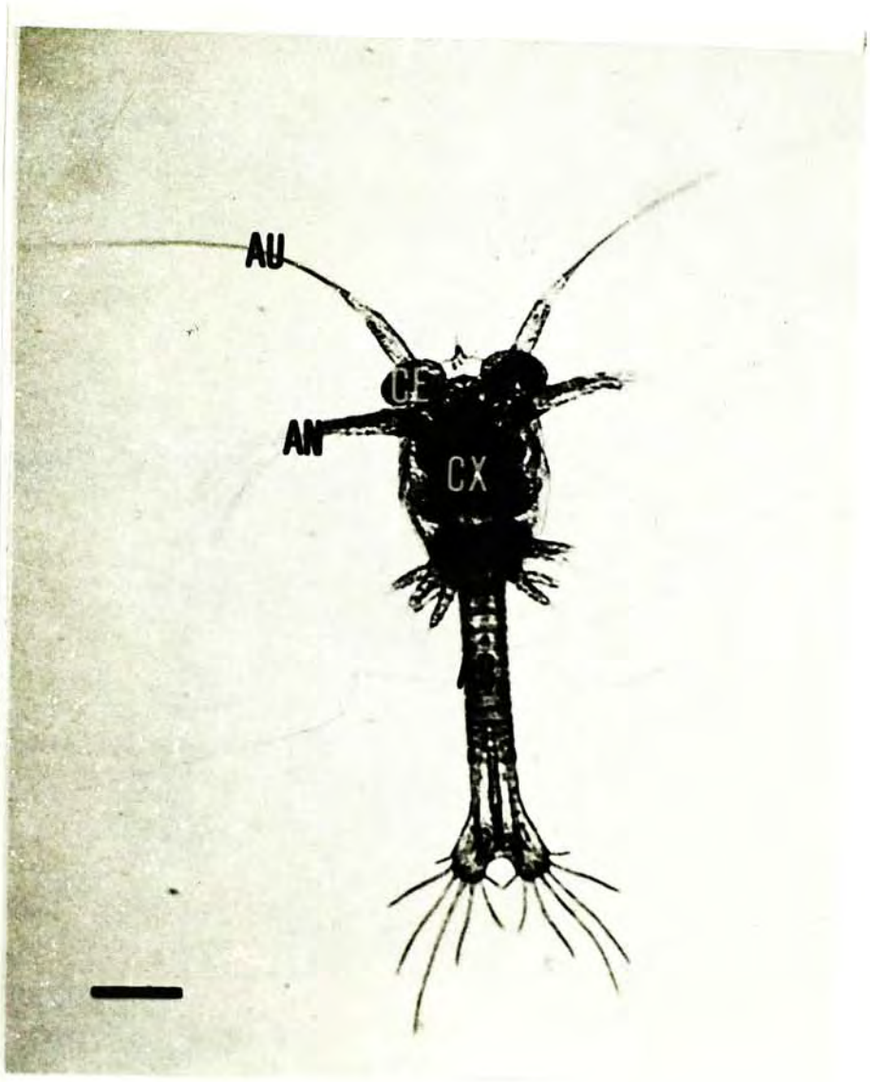
AU
CE
AN
CX

Fig. 15. Metapenaeus ensis at mysis I stage. AB, abdomen; CE, compound eye; CX, cephalothorax; PE, pereiopods. Scale bar represents 0.5 mm.

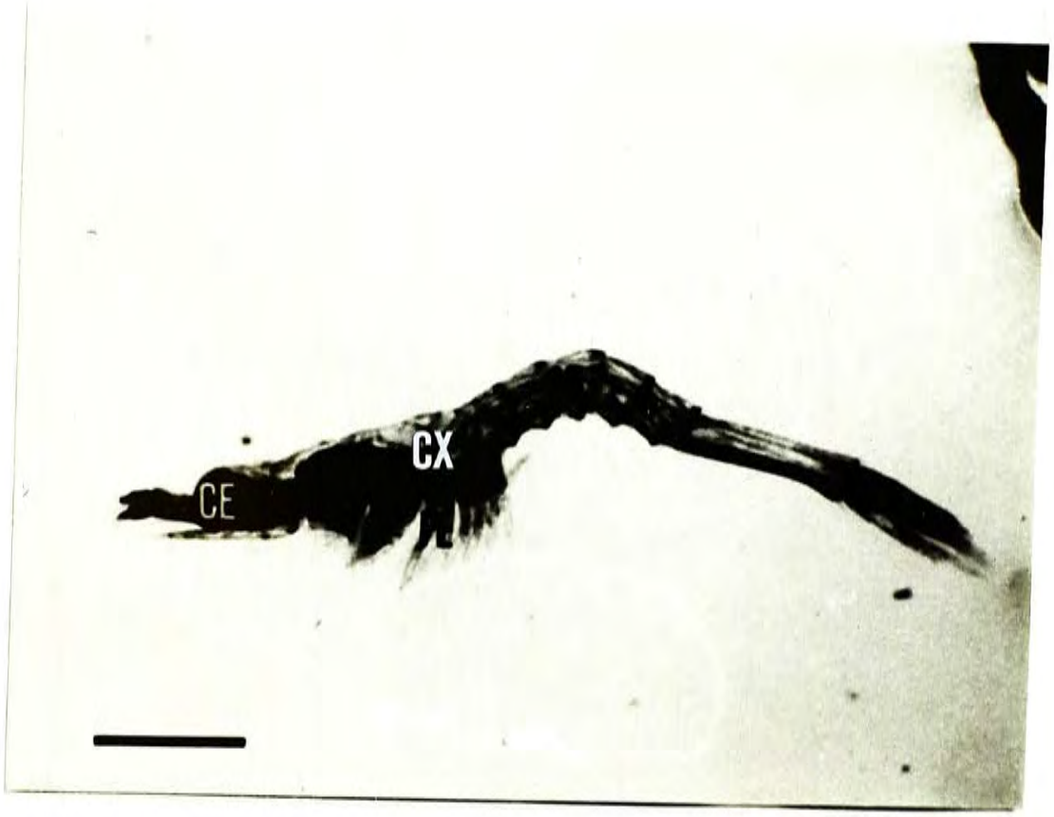
CX
CE

Fig. 16. Metapenaeus ensis at postlarva 30 stage. Scale bar represents 0.5 cm.

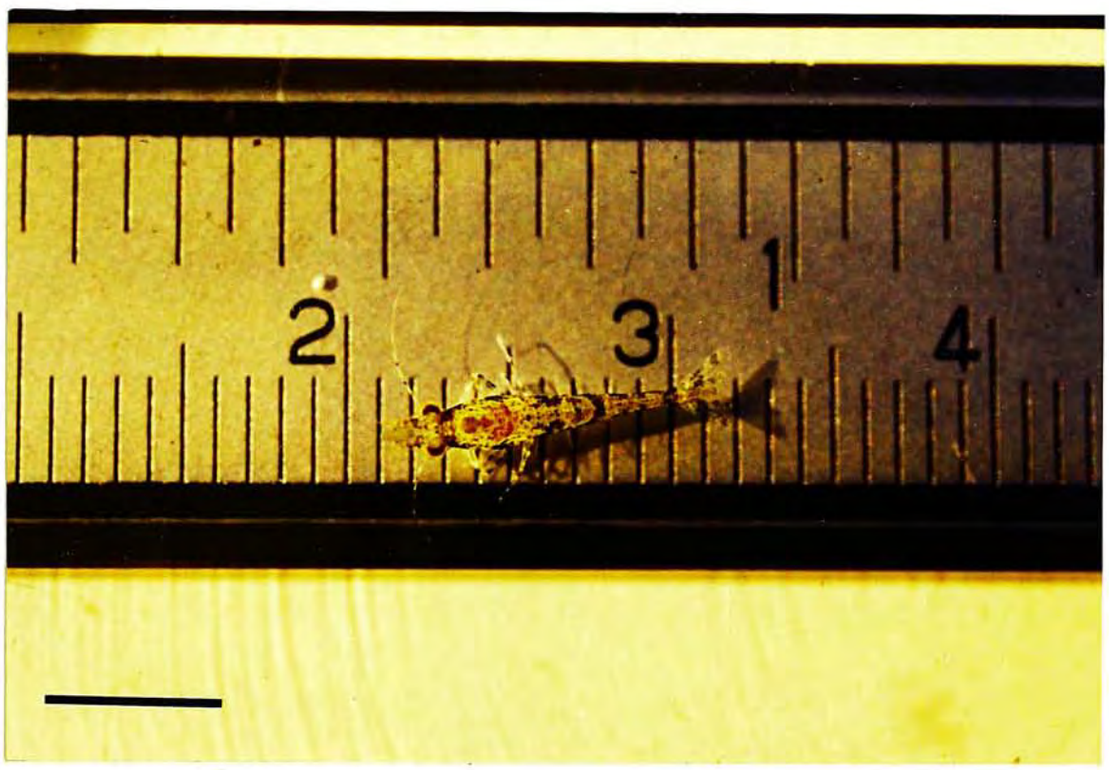
2
3
1
4

Fig. 17. Frontal section of Metapenaeus ensis at nauplius I stage. The body of larva was filled with yolk cells (YC). AN, antenna; MA, mandible. Scale bar represents 50 μm. H & E.


AN
JMA
VC

Fig. 18. Sagittal section of Metapenaeus ensis at nauplius II stage. YC, yolk cell. Scale bar represents 50 μm. H & E.

Fig. 19. Sagittal section of Metapenaeus ensis at nauplius III stage. The gut epithelium (arrow-head) is distinguishable near the posterior end of the larva. AN, antenna; YC, yolk cell. Scale bar represents 50 μm. H & E.

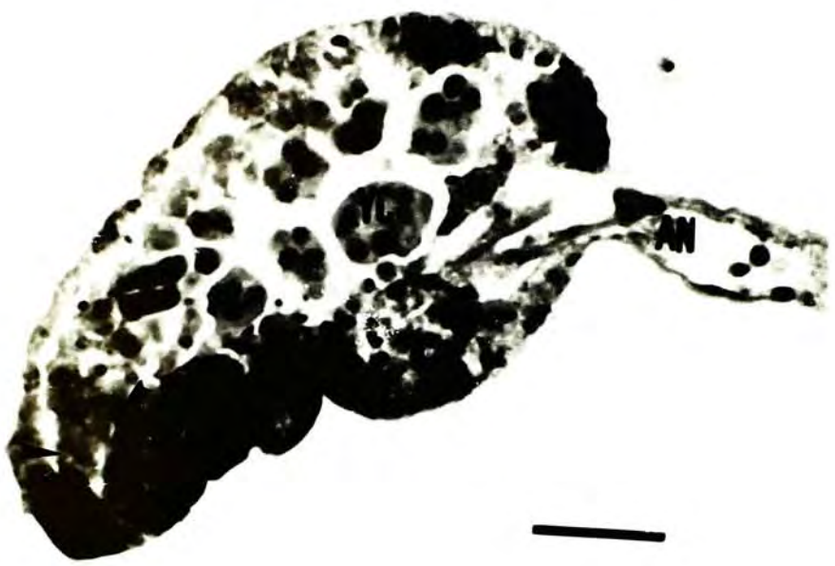
VL
AM

Fig. 20. Sagittal sections of Metapenaeus ensis at nauplius IV stage.

(a) The anterior portion of the gut is filled with yolk cells (YC). GE, gut epithelium. Scale bar represents 50 μm. H & E.

(b) The gut epithelium in the anterior region surrounds the yolk cells forming the yolk sac (YS). FG, foregut; GE, gut epithelium; YC, yolk cell. Scale bar represents 50 μm. H & E.

(c) Two caeca (arrow-heads) in circular shape arise from the gut. AN, antenna; MA, mandible. Scale bar represents 50 μm. H & E.

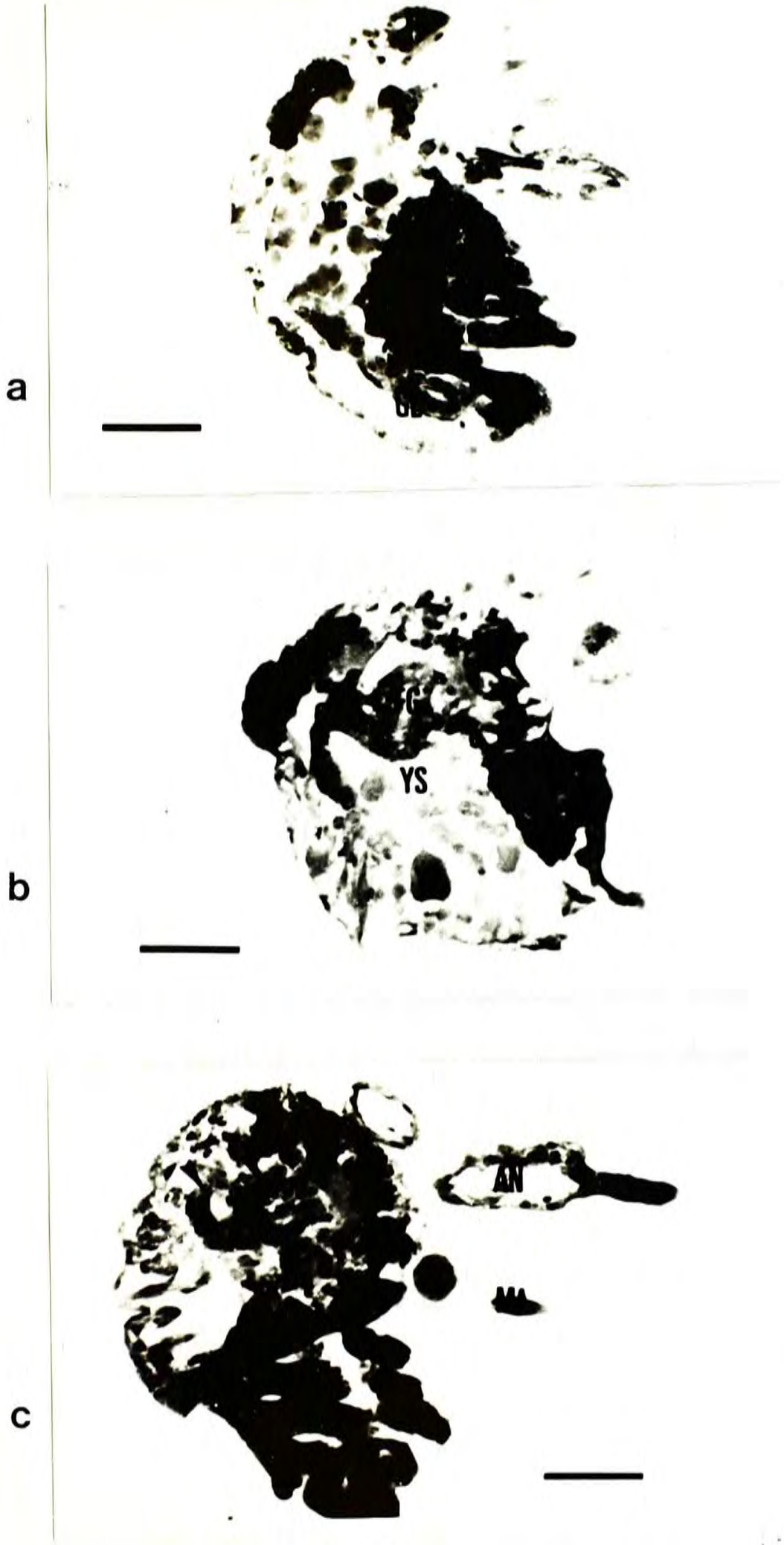
a
b
YS
c
AN

Fig. 21. Sagittal section of Metapenaeus ensis at naupilus V stage. The two gut caeca (arrow-heads) are ovoid in shape. GE, gut epithelium; YC, yolk cell. Scale bar represents 50 μm. H & E.

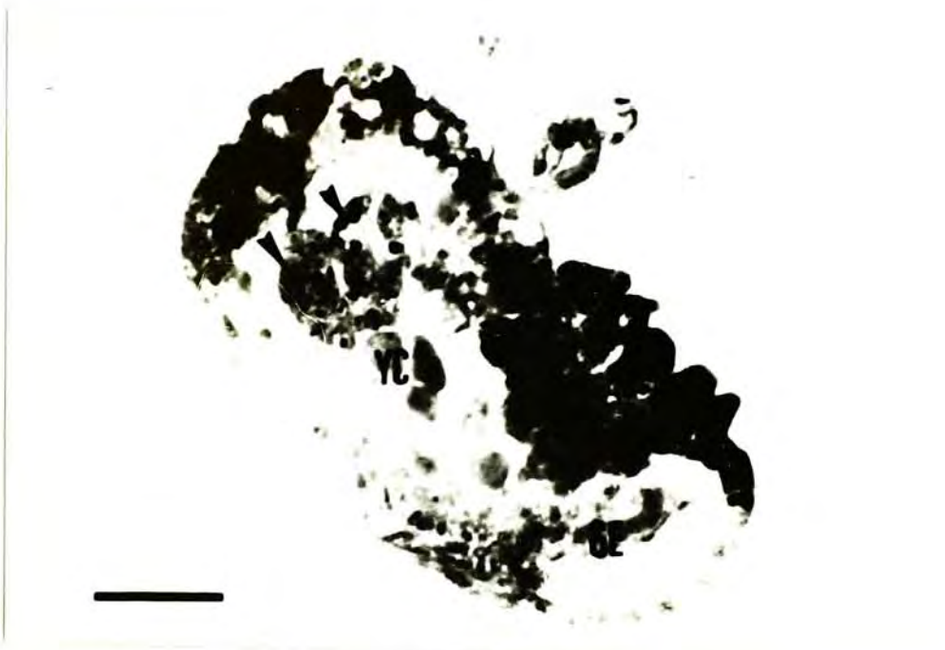

Fig. 22. Sections of Metapenaeus ensis at nauplius VI stage.

(a) Sagittal section. Yolk sac (YS) is nearly devoid of yolk cells. AN, antenna; FG, foregut. Scale bar represents 50 μm. H & E.

(b) Transverse section. The two gut caeca (arrow-heads) arise from the lateral side of the gut. GT, gut; YS, yolk sac. Scale bar represents 50 μm. H & E.

a

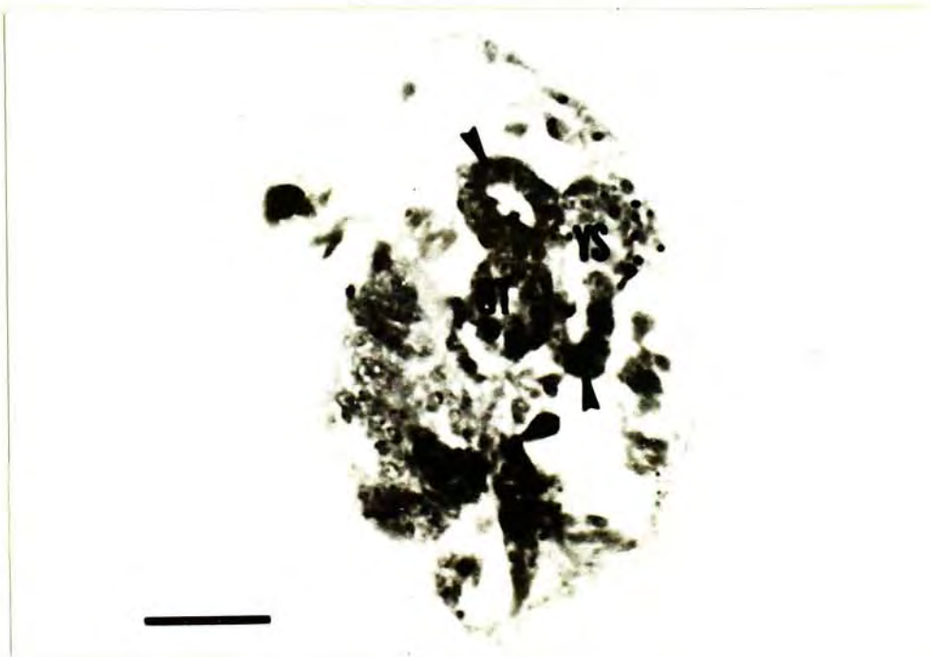

b

Fig. 23. Frontal section of Metapenaeus ensis at protozoea I stage. Two pairs of hepatopancreatic rudiments arise from the tubular midgut gut (MG). AH, anterior hepatopancreatic rudiment; FG, foregut; PH, posterior hepatopancreatic rudiment. Scale bar represents 50 μm. H & E.

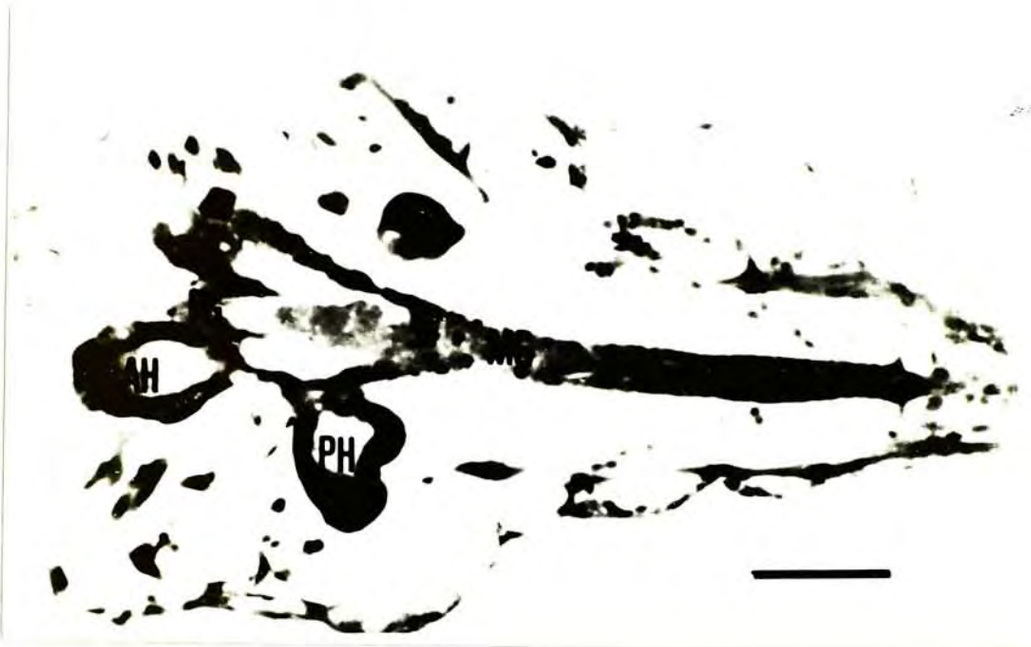
AH
PH

Fig. 24. Sections of Metapenaeus ensis at protozoea II stage.

(a) Sagittal section. The foregut (FG) is not divisible into cardiac and pyloric stomach. OE, oesophagus; PH, posterior hepatopancreatic rudiment. Scale bar represents 50 μm. H & E.

(b) Frontal section. The hepatopancreatic rudiments join to the midgut just beyond the junction of foregut (FG) and midgut (MG) (arrow-heads). AH, anterior hepatopancreatic rudiment; PH, posterior hepatopancreatic rudiment. Scale bar represents 50 μm. H & E.

a

b

Fig. 25. Sections of Metapenaeus ensis at protozoea III.

(a) Sagittal section. The cardiac stomach (CS) and pyloric stomach (PS) are separated by the cardiopyloric valve (arrow). The anterior hepatopancreatic rudiment (AH) lies dorsally on the stomach. The posterior hepatopancreatic rudiment (PH) lies ventrally under the tubular midgut (MG). MO, mouth; OE, oesophagus; arrow-head, orifice of anterior hepatopancreatic rudiment. Scale bar represents 50 μm. H & E.

(b) Frontal section. Interampullary ridge (IR) divides the pyloric stomach into two longitudinal channels (LC) which open to the orifices (arrow-heads) of the hepatopancreatic rudiments. Arrow, proturberance from posterior hepatopancreatic rudiment (PH). AH, anterior hepatopancreatic; CS, cardiac stomach. Scale bar represents 50 μm. H & E.

(c) Frontal section. Proturberance (arrow) emerges from the main lobe of the posterior hepatopancreatic rudiment (PH). Arrow-head, orifice of posterior hepatopancreatic rudiment. AH, anterior hepatopancreatic rudiment; MG, tubular midgut. Scale bar represents 50 μm. H & E.

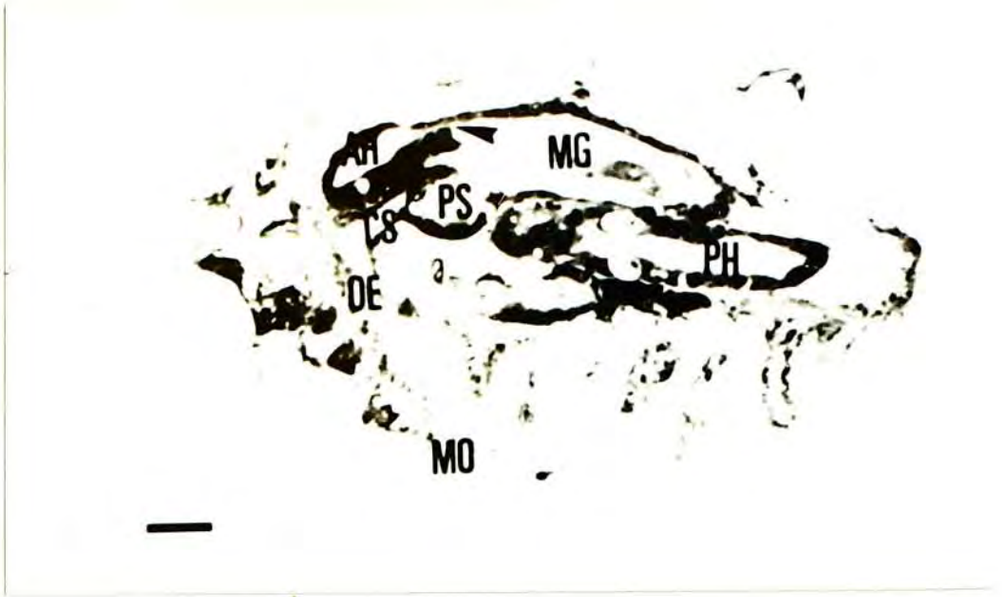

a

b

c

Fig. 26. Sections of Metapenaeus ensis at mysis I stage.

(a) Sagittal section. Anterior midgut caecum (arrow) emerges as a small bulge from the tubular midgut (MG). AH, anterior hepatopancreatic rudiment; CE, compound eye; CS, cardiac stomach; OE, oesophagus; PH, posterior hepatopancreatic rudiment; PS, pyloric stomach. Scale bar represents 50 μm. H & E.

(b) Frontal section. Anterior hepatopancreatic rudiment (AH) enlarges. CE, compound eye; MG, tubular midgut; PH posterior hepatopancreatic rudiment; arrow-head, interampullary ridge. Scale bar represents 50 μm. H & E.

a

b

Fig. 26 (con't).

(c) Transverse section through the pyloric stomach. Anterior hepatopancreatic rudiments (AH) lies dorso-laterally on the stomach. Interampullary ridge (arrow-head) stands vertically on the floor of the pyloric stomach. Scale bar represents 50 μm. H & E.

(d) Lateral lobes (LL) branch from the ventro-lateral lobes (VL) of the posterior hepatopancreatic rudiments branch. MG, tubular midgut. Scale bar represents 50 μm. H & E.

(e) Transverse section of the posterior hepatopancreatic rudiments. MG, tubular midgut; LL, lateral lobe of the posterior hepatopancreatic rudiment; VL, ventro-lateral lobe of the posterior hepatopancreatic rudiment. Scale bar represents 50 μm. H & E.

c

d

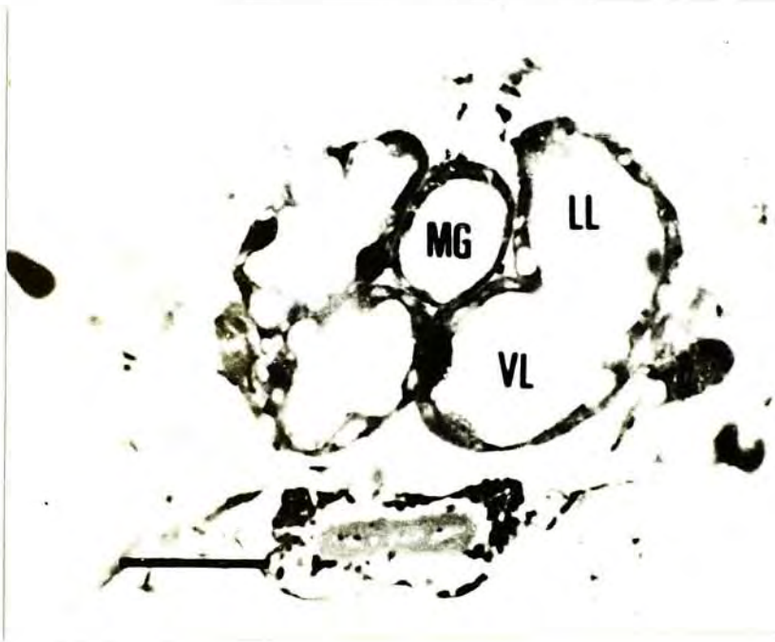

e

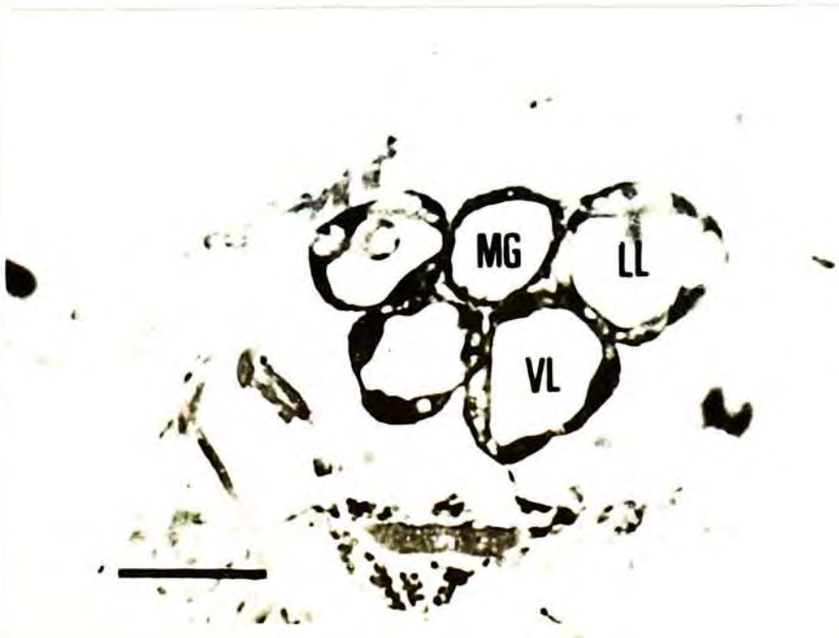

Fig. 27. Sections of Metapenaeus ensis at mysis II stage.

(a) Sagittal section. CS, cardiac stomach; H, heart; MG, tubular midgut; OE, oesophagus; PH, posterior hepatopancreatic rudiment; arrow, anterior midgut caecum. Scale bar represents 50 μm. H & E.

(b) Sagittal section. DL, dorso-lateral lobe of posterior hepatopancreatic rudiment; VL, ventro-lateral lobe of hepatopancreatic rudiment. Scale bar represents 50 μm. H & E.

a

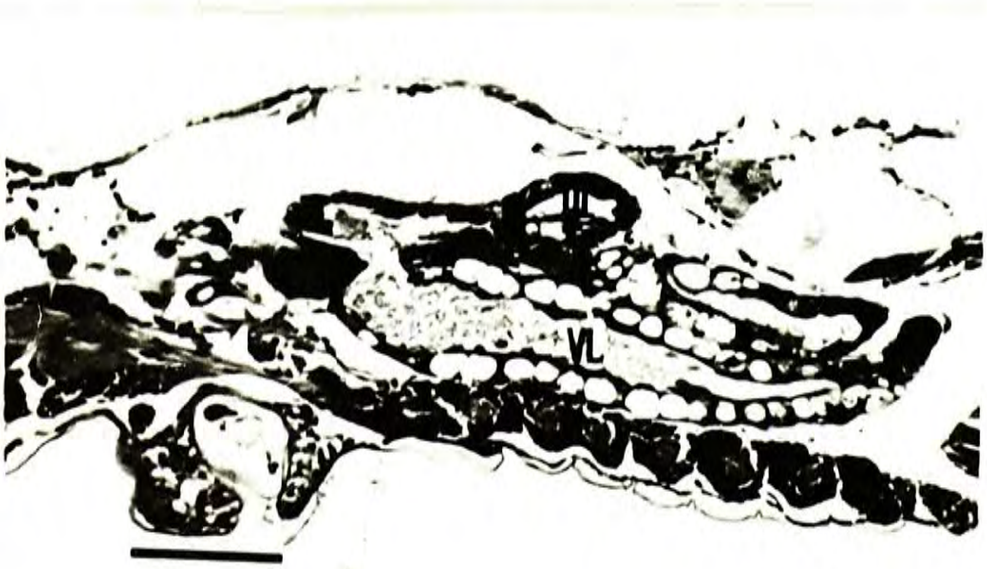

b

Fig. 27 (con't).

(c) Cross section of the posterior hepatopancreatic rudiment. Six lobes are observed. DL, dorso-lateral lobe of posterior hepatopancreatic rudiment; H, heart; LL, lateral lobe of posterior hepatopancreatic rudiment; MG, tubular midgut; VL, ventro-lateral lobe of posterior hepatopancreatic rudiment. Scale bar represents 50 μm. H & E.

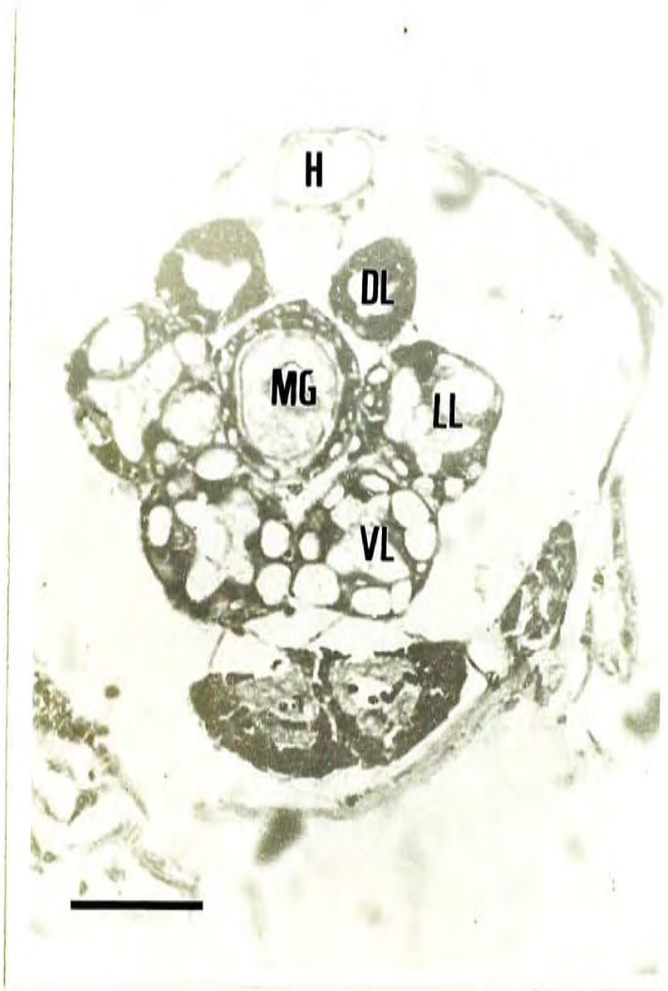

C

Fig. 28. Sagittal section of Metapenaeus ensis at postlarva 1 stage. Anterior hepatopancreatic rudiment (AH) reduces in size. CS, cardiac stomach; GF, gland filter; H, heart; MG, tubular midgut; OE, oesophagus; VL, ventro-lateral lobe of posterior hepatopancreatic rudiment; arrow, anterior midgut caecum. Scale bar represents 50 μm. H & E.

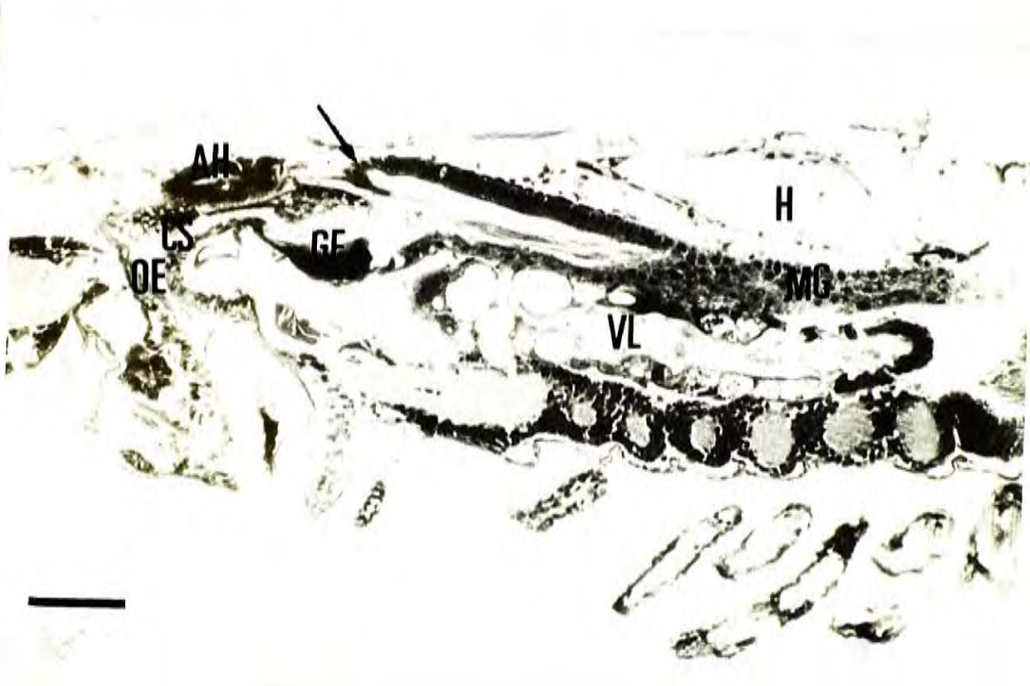
AH
CS
OE
GE
H
MG
VL

Fig. 29. Sagittal sections of Metapenaeus ensis at postlarva 6 stage.

(a) Anterior hepatopancreatic rudiment regresses. The cardiac stomach (CS) is armed with cardiac plate (arrows). GF, gland filter; H, heart; HP, hepatopancreas; PS, pyloric stomach. Scale bar represents 0.1 mm. H & E.

(b) Posterior midgut caecum (PM). HG, hindgut; MG, tubular midgut. Scale bar represents 10 μm. H & E.

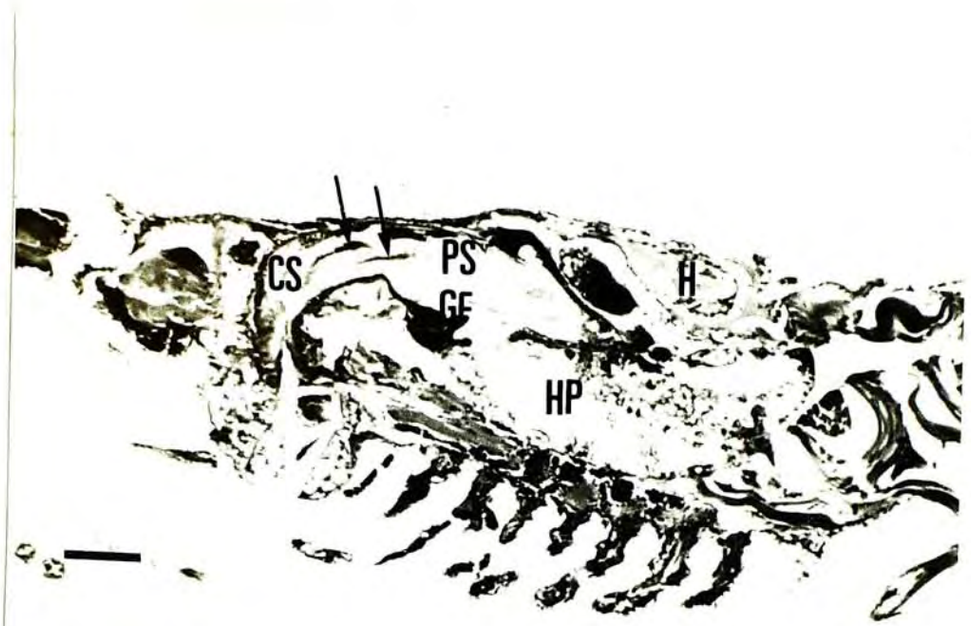

a

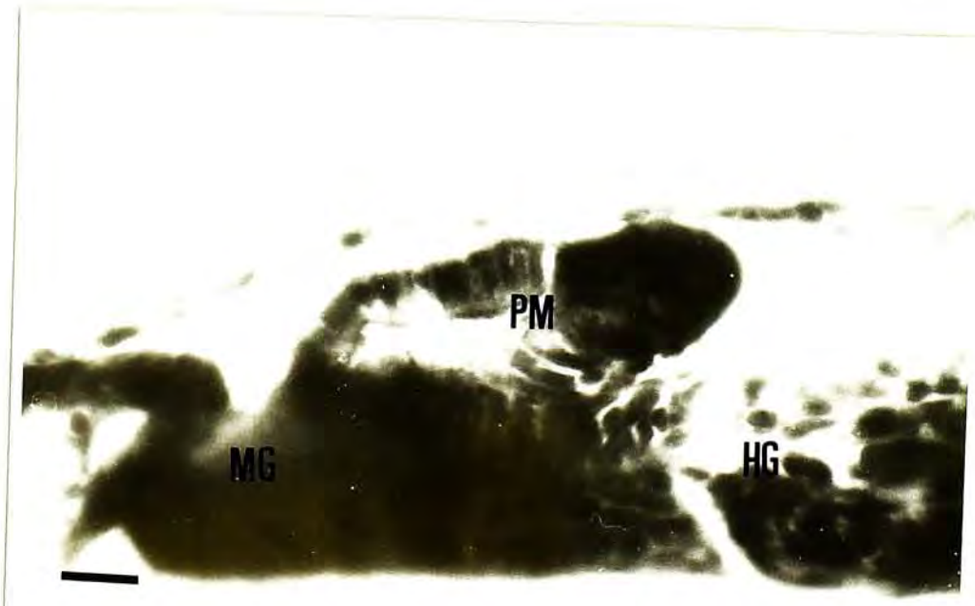

b

Fig. 30. Sections of Metapenaeus ensis at postlarva 10 stage.

(a) The hepatopancreas (HP) ramifies into many short tubules. CS, cardiac stomach; arrow, anterior midgut caecum; H, heart; MG, tubular midgut; PS, pyloric stomach. Scale bar represents 0.1 mm. H & E.

(b) The hepatopancreatic tubules (T) open to a collecting duct (CD). H, heart. Scale bar represents 50 μm. H & E.

(c) Lateral ossicles (LS) develop in the cardiac stomach (CS). HP, hepatopancreas. Scale bar represents 50 μm. H & E.

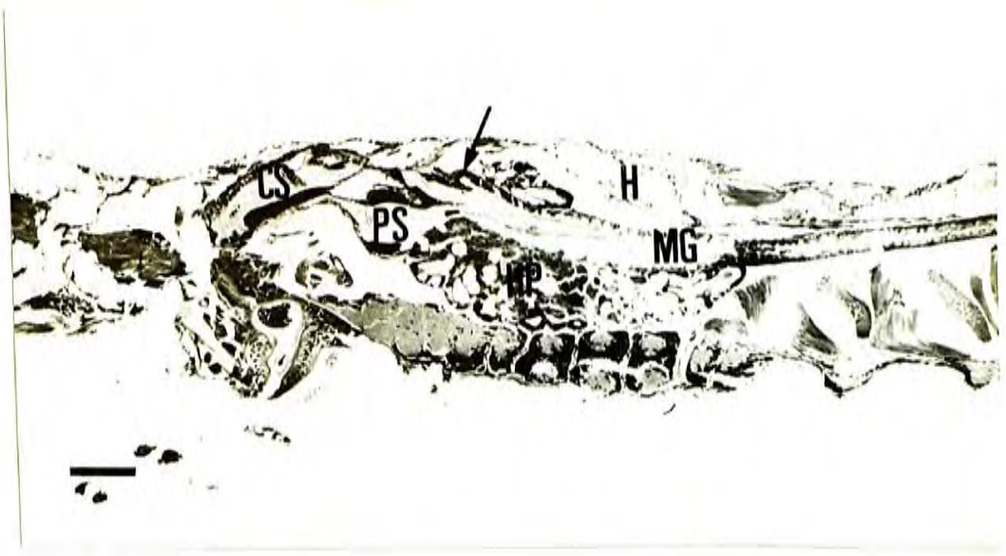

a

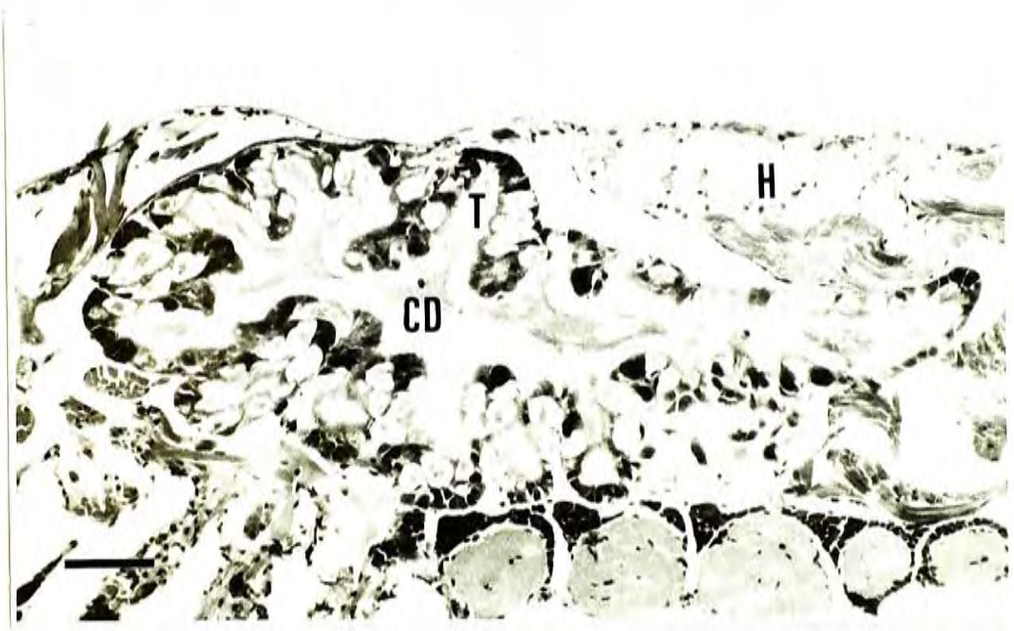

b

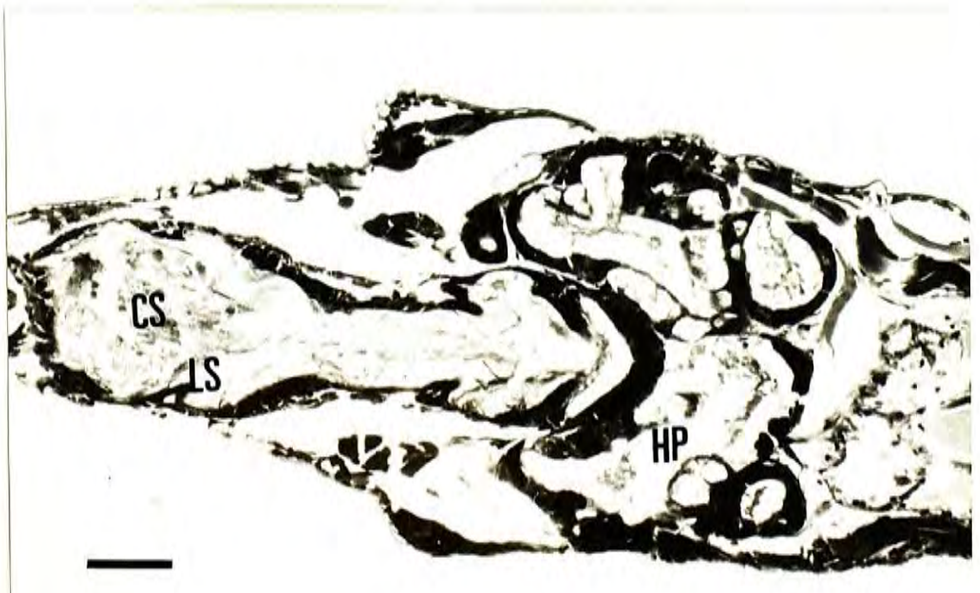

c

Fig. 31. Sagittal section of Metapenaeus ensis at postlarva 20 stage. The dorsal lobe of the hepatopancreas (HP) increases in size wrapping around the pyloric stomach and the anterior portion of the tubular midgut (MG). CS, cardiac stomach; H, heart; MO, mouth; OE, oesophagus; T, tubules of hepatopancreas. Scale bar represents 0.1 mm. H & E.

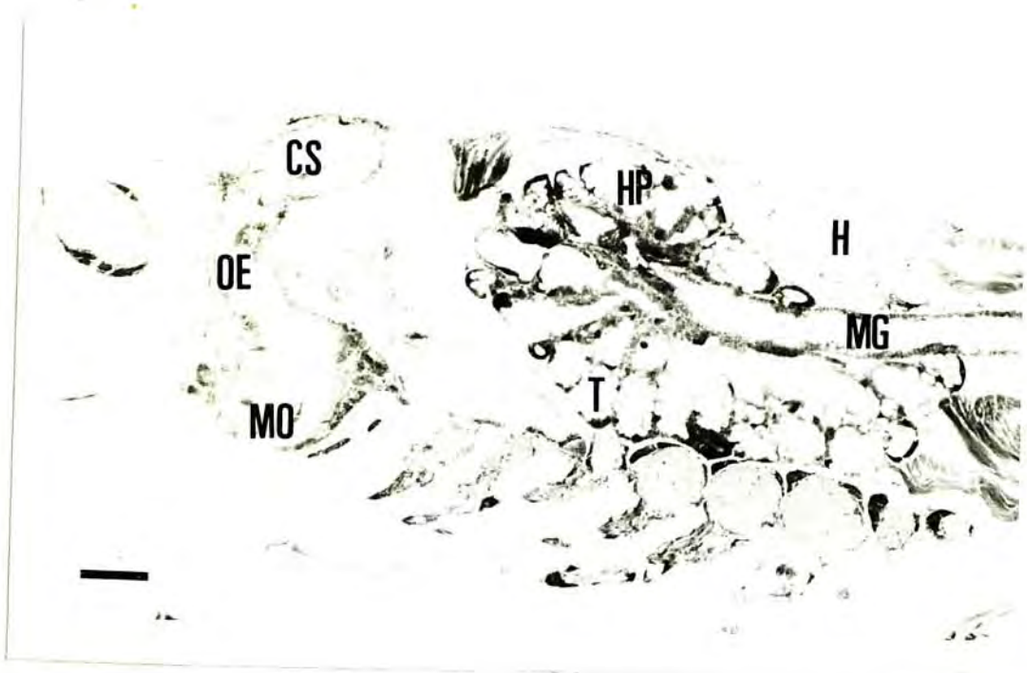
CS
HP
H
OE
MG
T
MO

Fig. 32. Sections of Metapenaeus ensis at postlarva 30 stage.

(a) Sagittal section. CS, cardiac stomach; GF, gland filter; H, heart; MG, tubular midgut; MO, mouth; OE, oesophagus; T, tubule of hepatopancreas. Scale bar represents 0.2 mm. H & E.

(b) Sagittal section. The hepatopancreas consists of numerous tubules (T). H, heart. Scale bar represents 0.2 mm. H & E.

(c) Frontal section. Lateral ossicles (LS) of cardiac stomach (CS) are enlarged. H, heart, HP, hepatopancreas. Scale bar represents 0.2 mm. H & E.

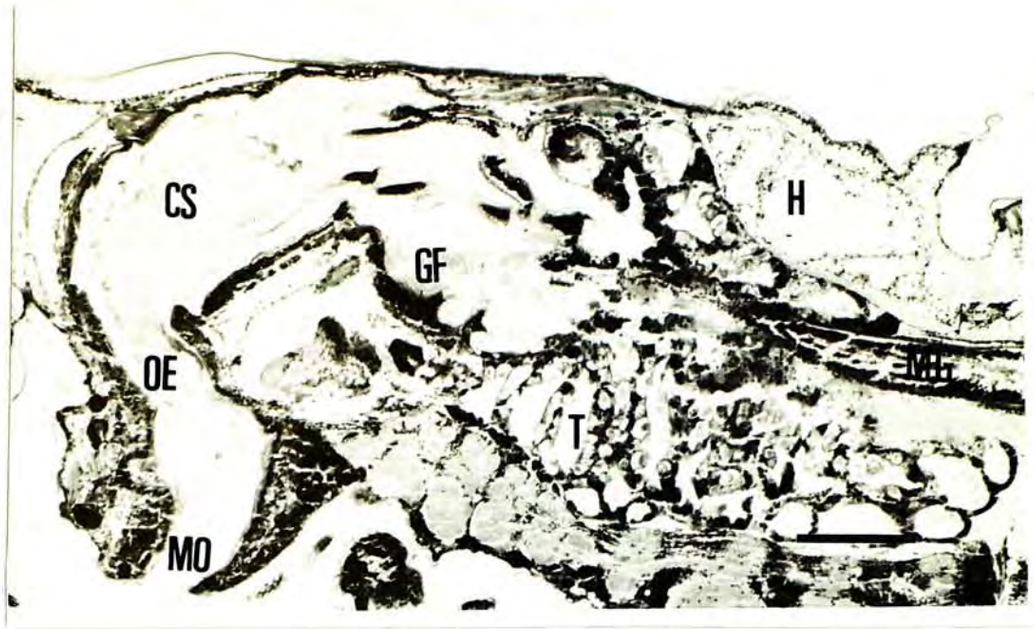

a

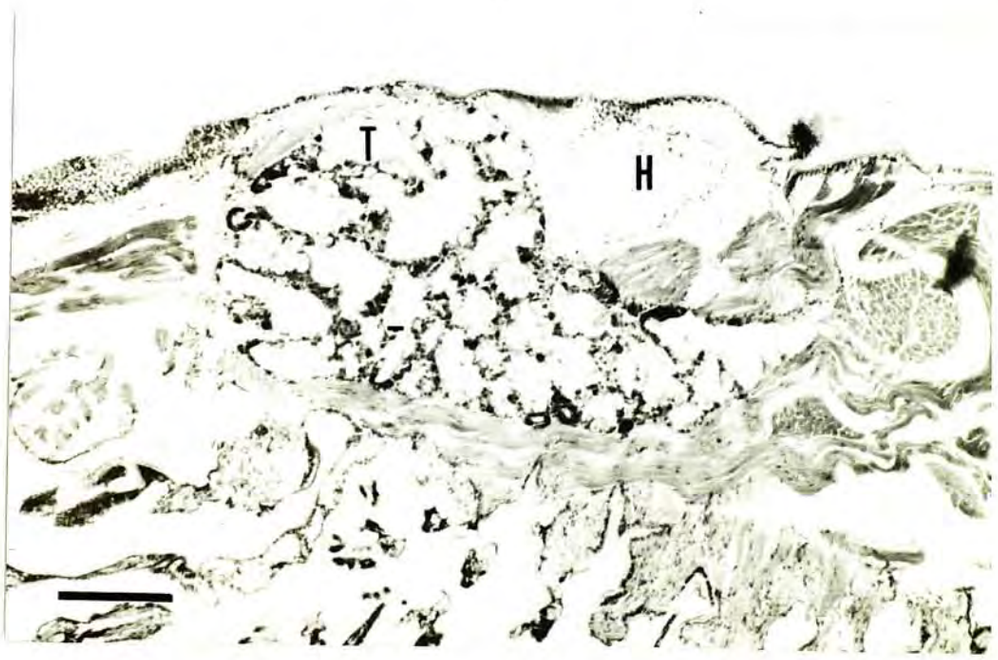

b

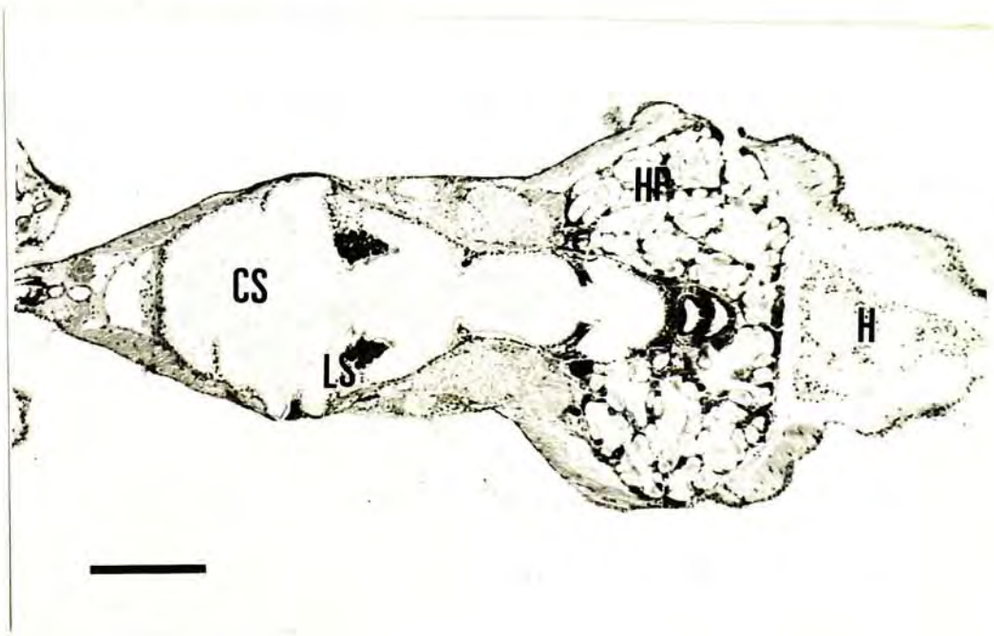

c

Fig.32 (con't) Sections of Metapenaeus ensis at postlarva 30.

(d) Frontal section. Posterior region of the hepatopancreas has less tubules (T). Scale bar represents 0.2 mm. H & E.

(e) Cross section. Tubules in the hepatopancreas tend to run laterally or ventrally in the hepatopancreas. GL, gill; PS, pyloric stomach. Scale bars represents 0.2 mm. H & E.

d

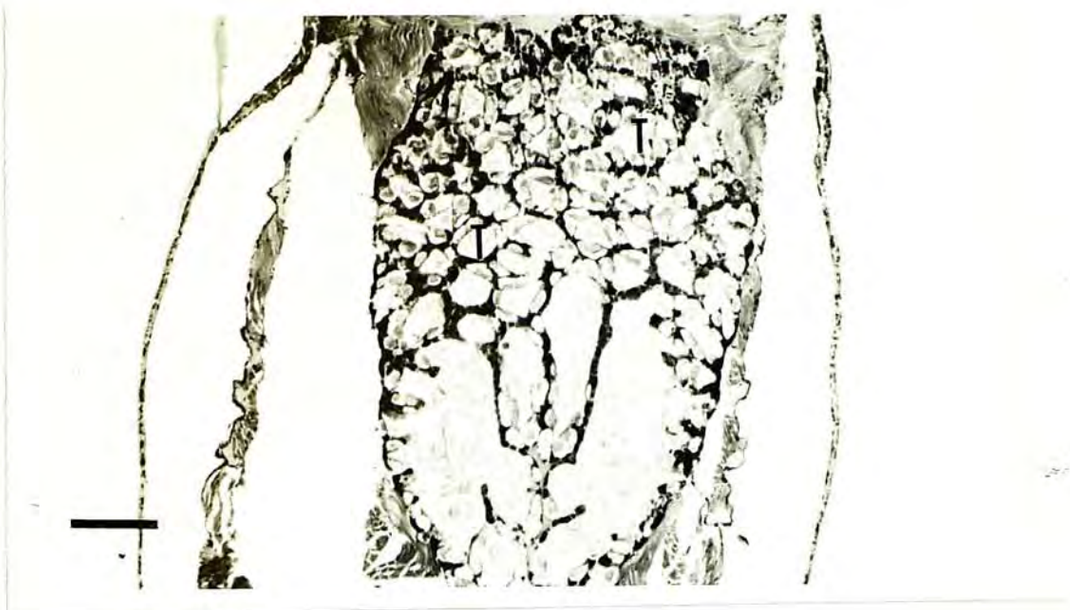

e

Fig. 33. Transmission electron micrograph of gut caeca cell in Metapenaaeus ensis at nauplius VI stage. N, nucleus; M, mitochondrion; MV, microvilli; RE, rough endoplasmic reticulum. Scale bar represents 2 μm.

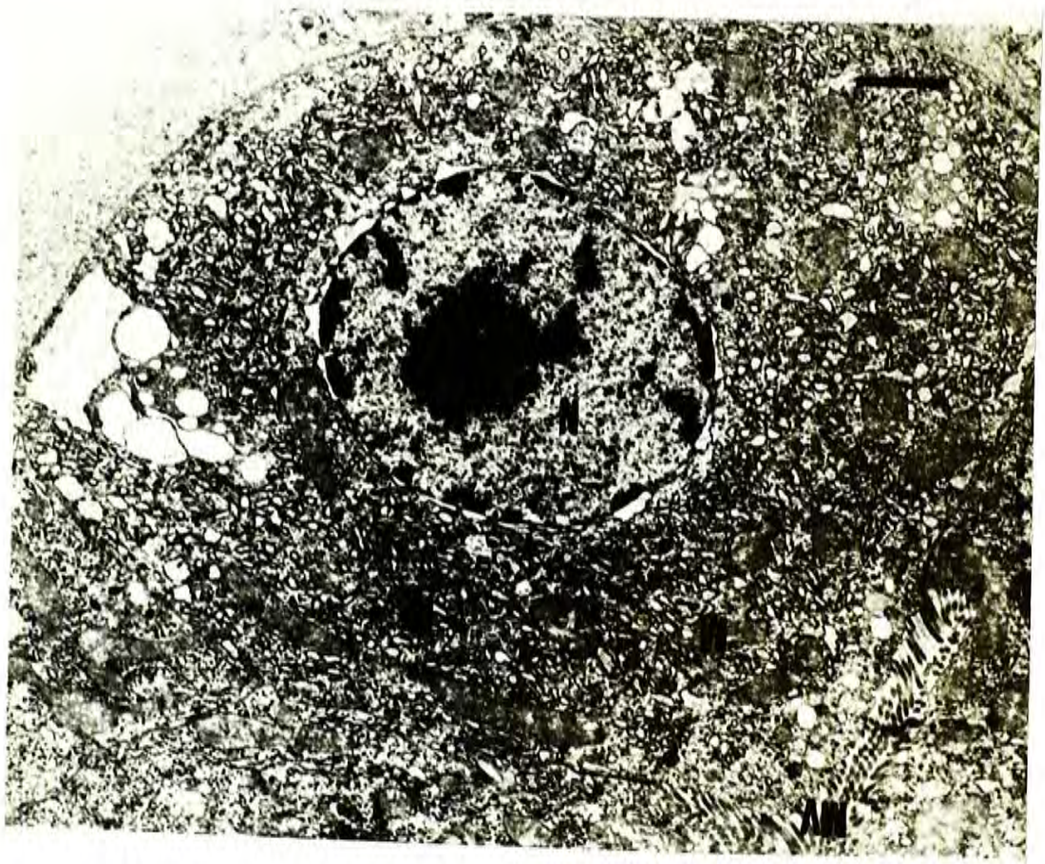

Fig. 34. Transmission electron micrographs of F-cells in the hepatopancreatic rudiments of Metapenaeus ensis.

(a) Protozoea III. G, Golgi body; M, mitochondrion; MF, myofibrils; MV, microvilli; N, nucleus; Scale bar represents 2 μm.

(b) Mysis II. BL, basal lamina; G, Golgi body; M, mitochondrion; MF, myofibrils; MV, microvilli; N, nucleus; NO, nucleolus; R, R-cell; RE, rough endoplasmic reticulum. Scale bar represents 2 μm.

a

b

Fig. 34 (con't).

(c) F-cells in the hepatopancreatic rudiments of Metapenaeus ensis at postlarva 1 stage. BL, basal lamina; G, Golgi body; M, mitochondrion; MF, myofibrils; MV, microvilli; N, nucleus; R, R-cell. Scale bar represents 2 μm.

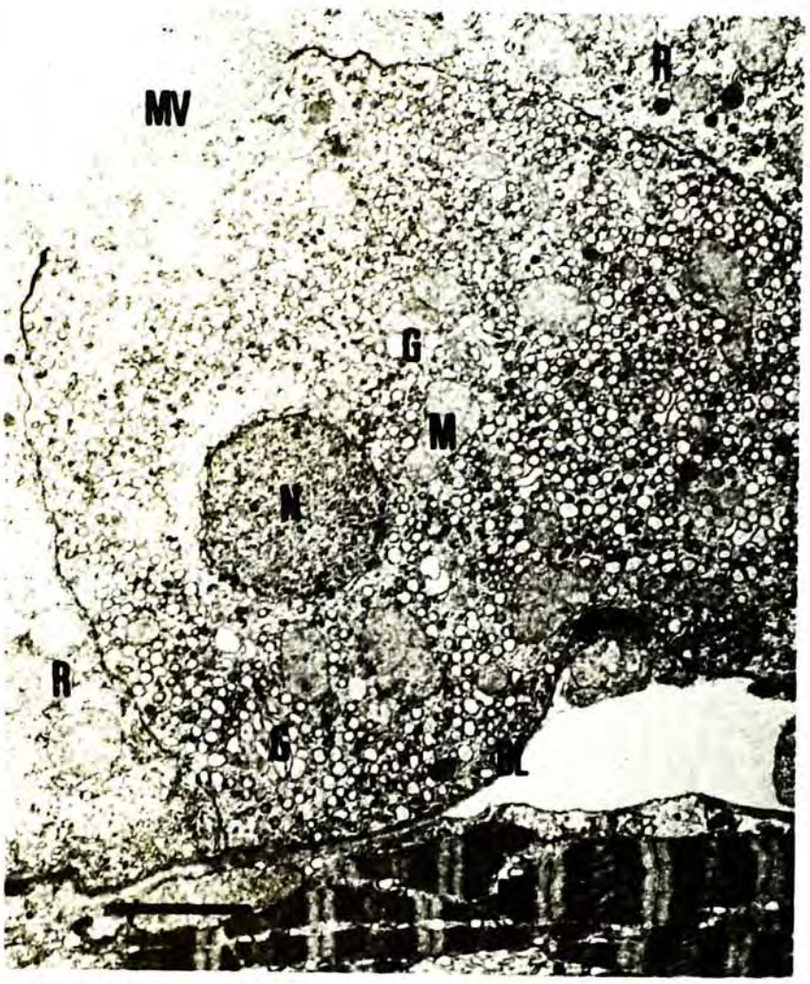

C

Fig. 35. Transmission electron micrographs of B-cells in the hepatopancreatic rudiments of Metapenaeus ensis.

(a) Transforming B-cell in protozoea I stage. DR, dense region; DV, digestive vacuole; F, F-cell; N, nucleus; PV, pinocytotic vesicles; R, R-cell; SA, sub-apical vacuole; arrow-head, pinocytotic channel. Scale bar represents 2 μm.

(b) Mature B-cell in protozoea I stage. DV, digestiv vacuole; F, F-cell; L, lumen of hepatopancreatic rudiment. Scale bar represents 5 μm.

a

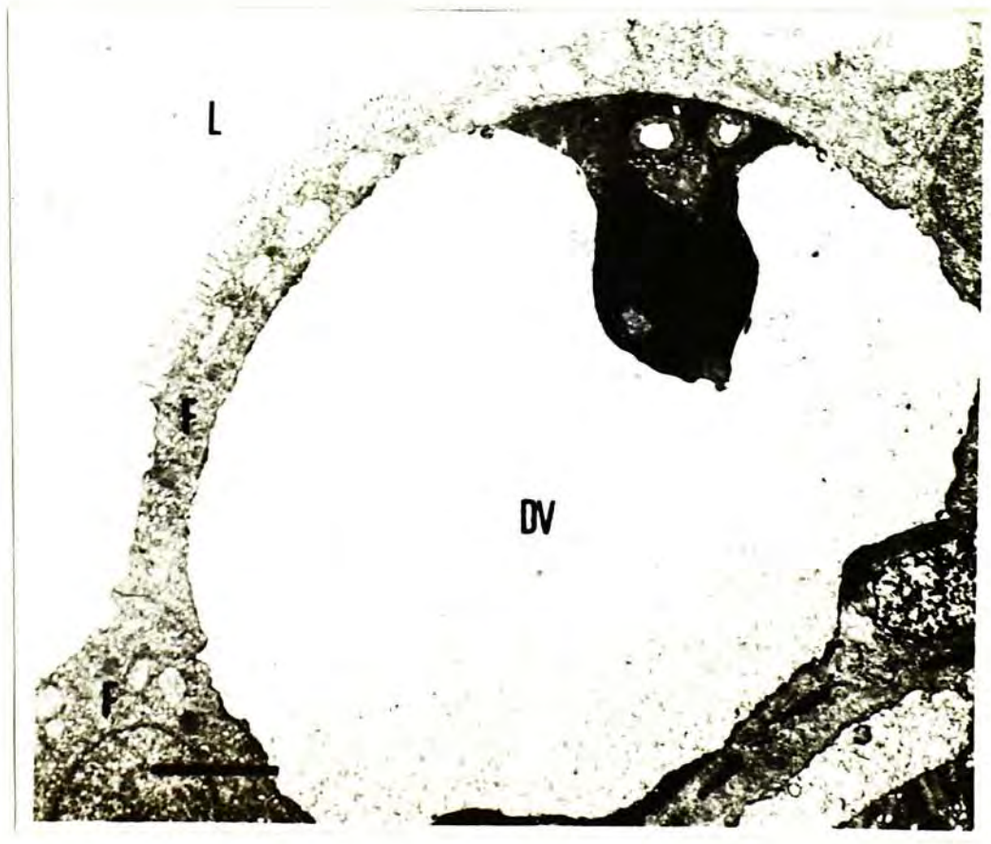

b

Fig. 35 (con't).

(c) Mysis I stage. DV, digestive vacuole; SA, sub- apical vacuole; arrow-head, cytoplasmic strip. Scale bar represents 2 μm.

(d) Postlarva 1 stage. DV, digestive vacuole; MY, myoepithelial cell; MU, muscle; arrow, disoriented microvilli; arrow-head, cytoplasmic strip. Scale bar represents 5 μm.

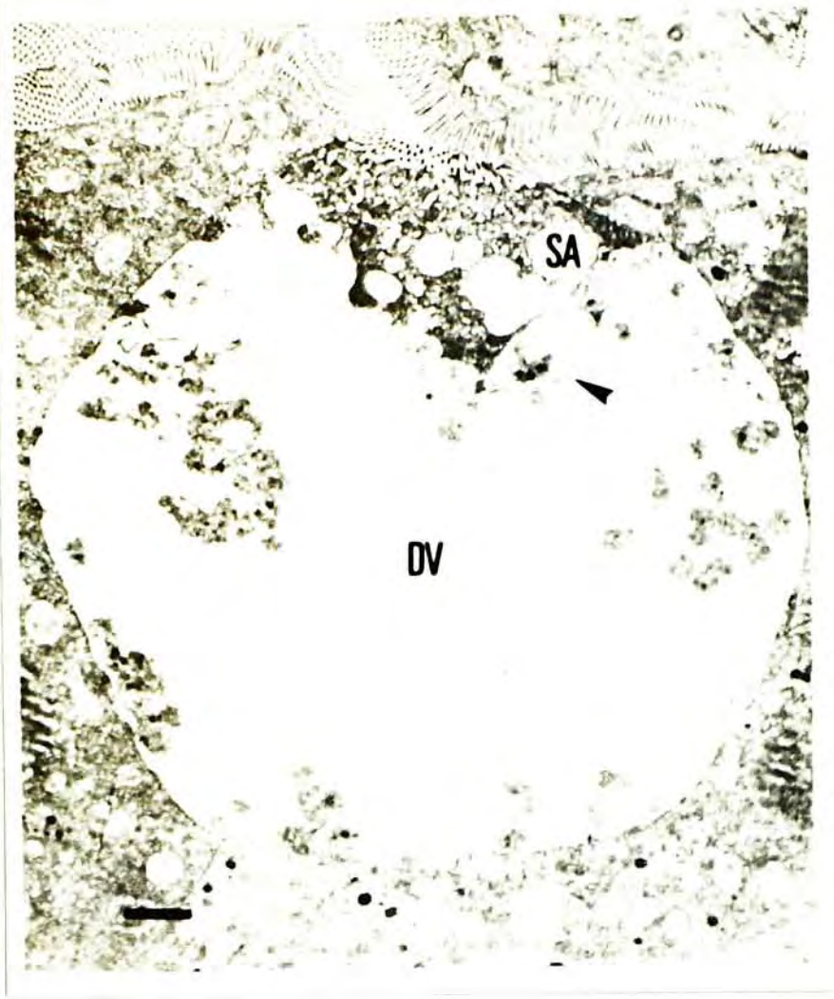

c

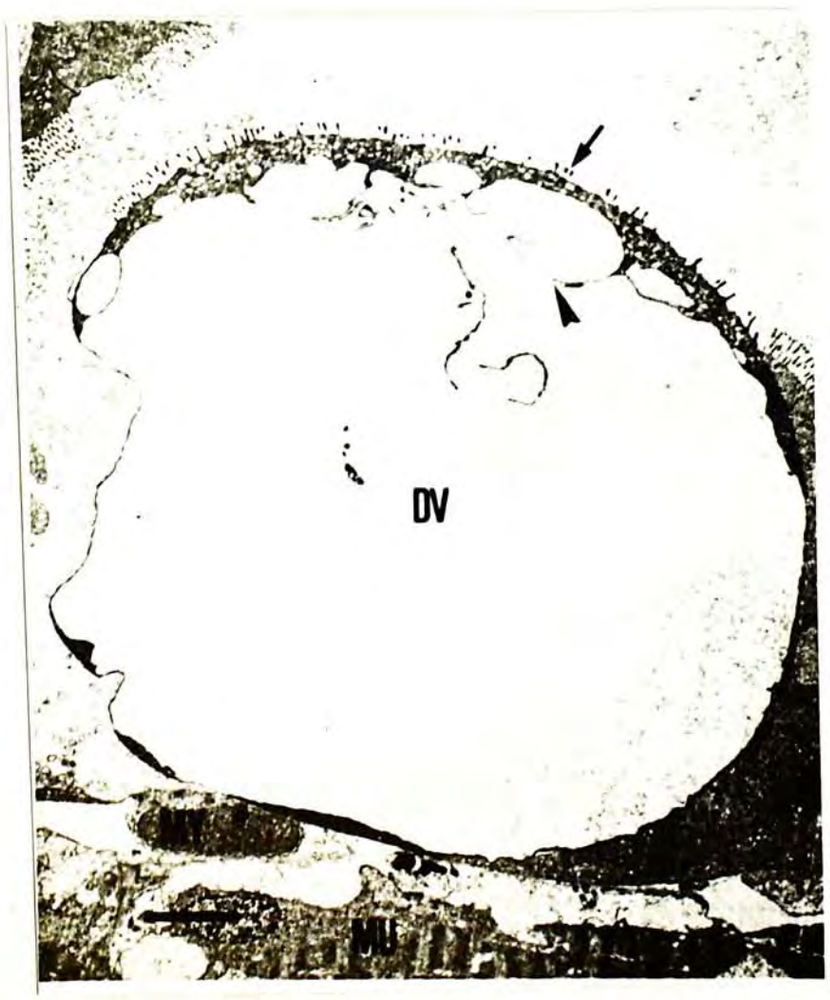

d

Fig. 36. Transmission electron micrographs of R-cells in the hepatopancreatic rudiments of Metapenaeus ensis at mysis II stage.

(a) Supranuclear vacuole (SN) and lipid droplets (LP) are found in the R-cell. F, F-cell; M, mitochondria; MV, microvilli; MY, myoepithelial cell. Scale bar represents 2 μm.

(b) Apical region of R-cell. Numerous mitochondria (M) are accumulated. MV, microvilli; RE; rough endoplasmic reticulum. SN, supranuclear vacuole. Scale bar represents 2 μm.

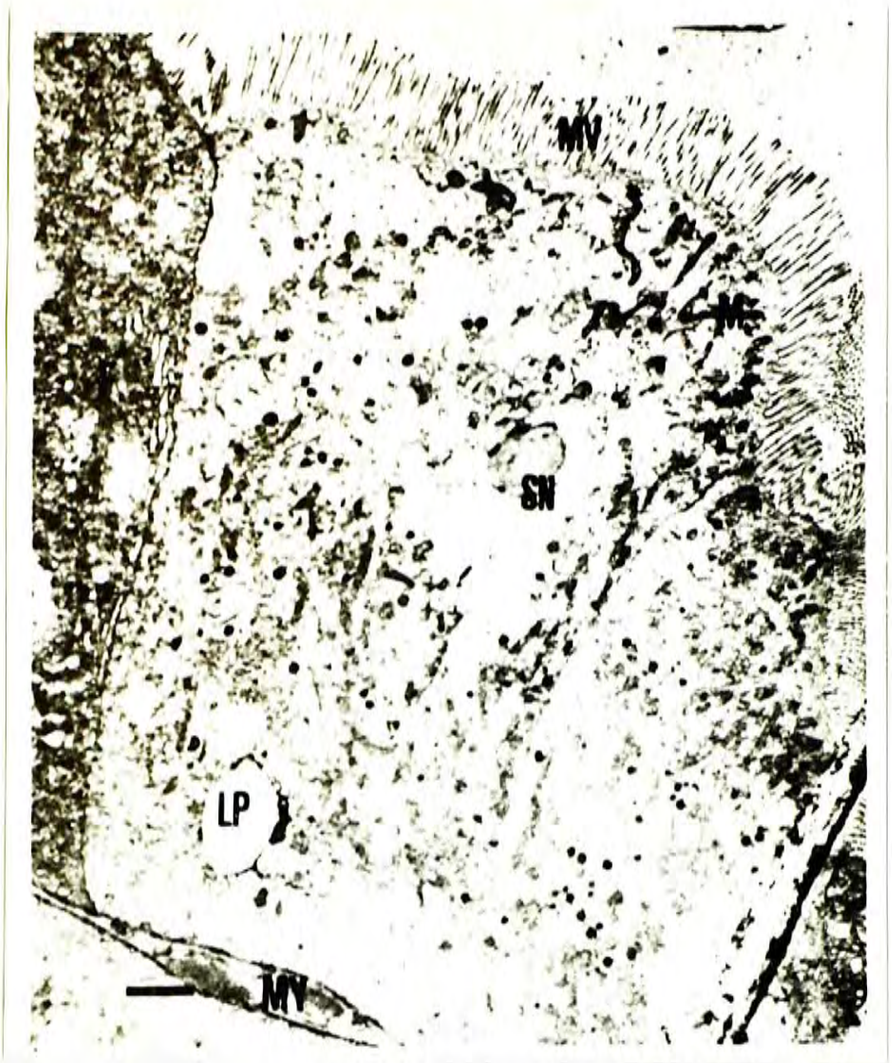

a

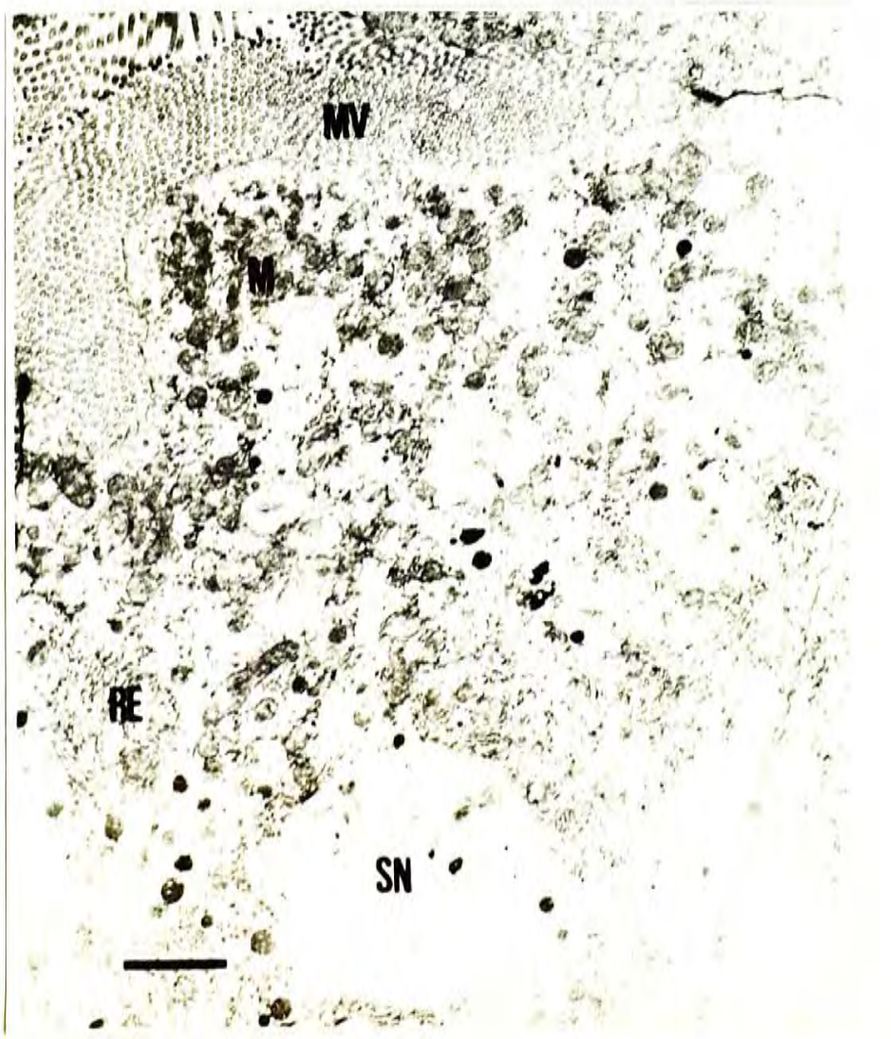

b

Fig. 36 (con't).

(c) Basal region of R-cells in the hepatopancreatic rudiments of Metapenaeus ensis at mysis II stage. Smooth endoplasmic reticulum (SE) is well developed in the basal region of the cell. BL, basal lamina; LP, lipid droplets; M, mitochondrion; MF, myofibrils; N, nucleus; RE, rough endoplasmic reticulum. Scale bar represents 2 μm.

C

Fig. 37. Transmission electron micrographs of E-cells in the hepatopancreatic rudiments of Metapenaeus ensis.

(a) Several E-cells at protozoea I stage. BL, basal lamina; M, mitochondrion; MV, microvilli; MY, myoepithelial cell; N, nucleus. Scale bar represents 2 μm.

(b) A binucleated E-cell at mysis II stage. Scale bar represents 2 μm.

a

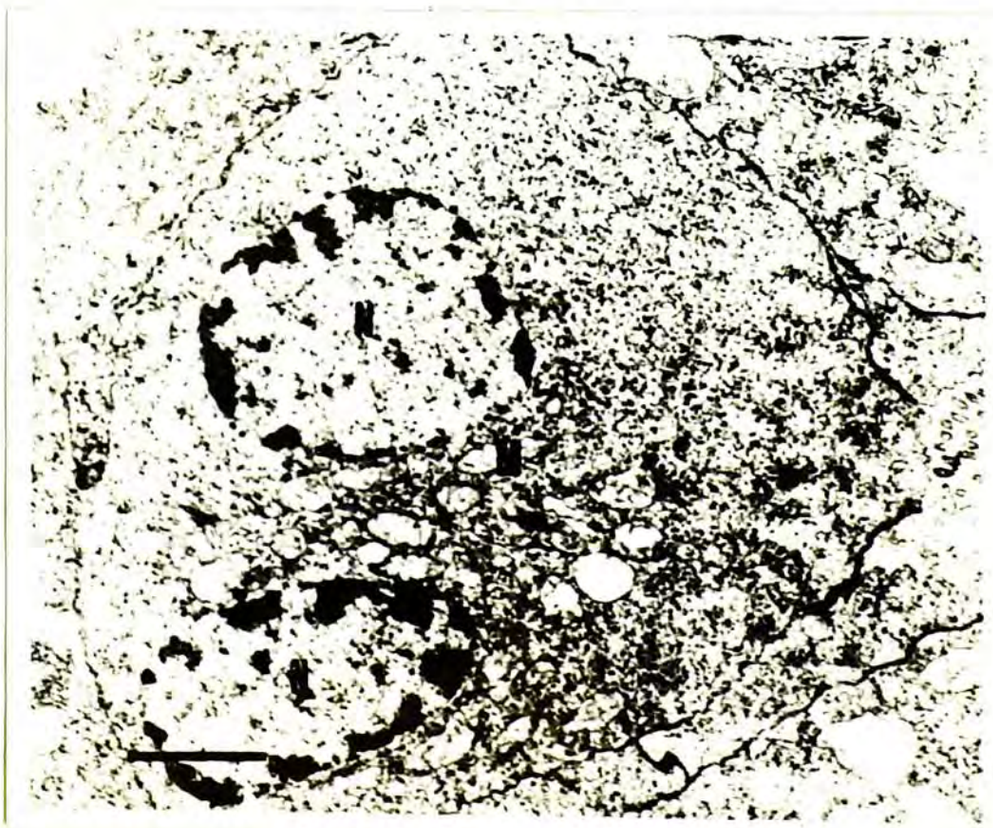

b

CHAPTER V

OPTIMAL PH AND TEMPERATURE FOR THE ASSAYS OF DIGESTIVE ENZYME ACTIVITIES FROM THE HEPATOPANCREAS OF SHRIMP Metapenaeus ensis

5.1 Introduction

Studies on digestive enzymes are useful in understanding digestive physiology. The presence of different digestive enzymes and the different characteristics of digestive enzymes may reflect the feeding habits of the species and the environment to which the species adapts. Amylase can be found in most decapod crustaceans (van Weel, 1970; Gibson & Barker, 1979). The optimum pH is in the range of 5.0 to 7.9. Proteases found in decapod crustaceans include tryptic protease, chymotryptic protease, alkaline protease, collagenase, aminopeptidase, carboxypeptidases, and dipeptidase. Multiple kinds of proteases can be found in a species. Different kinds of proteases found in species of decapod crustaceans were summarized in the reviews by van Weel (1970), Gibson & Barker (1979) and Dall & Morarity (1983).

No information on the digestive enzymes of Metapenaeus ensis has been reported. There have been studies on a closely related species Metapenaeus monoceros (Karunakaran & Dhage, 1977; Tsai et al., 1986). The

Metapenaeus monoceros (Karunakaran & Dhage, 1977; Tsai et al., 1986). The present study investigates the characteristics of amylase and protease of M. ensis and provides basic information on these digestive enzymes for further studies.

5.2 Materials and Methods

Three shrimp fed with mussel (Perna viridis) for one week in the laboratory were sacrificed. The shrimp were at moult stage C. The body weight and body length was 5.0 to 7.0 g and 7.5 to 9.0 cm respectively. The hepatopancreas was isolated and homogenized in 2 ml distilled water. The homogenate was filtered through 5 μm millipore filter. The filtrate collected was used as the crude enzyme extract.

5.2.1 Assay for Amylase Activity

The assay of amylase activity followed the method of Wrint & Stegbauer (1974). Starch was the substrate for amylase in this assay. The concentration of starch solution was 1% in distilled water and 0.25 ml of the starch solution was mixed with 1.75 ml of 0.1M phosphate buffer. Twenty-five μl of the enzyme extract was added to the reaction mixture. After the reaction proceeded for 15 min, 2 ml of dinitrosalicyclic acid reagent was

added to the reaction mixture, which was then boiled for 5 min to stop the reaction. Absorbance was recorded at 540 nm against a maltose standard solution.

To determine the relation of amylase activity and pH, the reaction was conducted at 0.5 pH intervals from pH 5.0 to 7.5 at 25 °C. The relation of amylase activity and temperature was performed at 5 °C intervals from 25 to 50 °C at pH 6.5. The specific activities of amylase were expressed as μmole maltose μg protein^{-1} h^{-1}.

5.2.2 Assay for Protease Activity

Protease activity was determined with the method of Charney & Tomarelli (1947). Azocasein was used as the substrate which was dissolved in distilled water to the concentration of 1 % and 0.25 ml of the substrate solution was added to a centrifuge tube containing 0.2 ml of 0.8% NaCl solution, 0.53 ml of 0.1 M buffer (see below) and 20 μl of enzyme extract. The assay was conducted for 1 h and then the reaction was stopped by adding 2 ml of 5% trichloroacetic acid. The reaction mixture was centrifuged to separate the precipitated protein. Two ml of the supernatant was added to 2 ml of 0.5M sodium hydroxide solution. The absorbance at 440 nm was recorded. The specific activities of protease were expressed as velocity

constant K μg protein^{-1} and calculated from the equation shown below:

$$K = 1/t \times 2.3 \times \log (C1/C2)$$

where K = velocity constant

C1 = initial azocaesin concentration

C2 = final azocaesin concentration (absorbance of the sample)

t = incubation time in minute

C1 is the undigested value for azocaesin. The value is obtained by measuring the absorbance of 100 fold diluted stock solution and adding 2 ml of 0.5M sodium hydroxide solution to 2 ml of the diluted stock solution.

The optimal pH for the assay of protease activity was studied by performing the reaction at 0.5 pH intervals from pH 5.0 to 10.0 at 25 °C. Phosphate buffer was used for pH 5.0 to 7.5 and borate buffer at pH 8.0 to 10.0. The relation of protease and temperature was investigated by conducting the reaction at temperature at 5 °C intervals from 25 to 50 °C, at pH 9.0.

The total protein content of the enzyme extract was determined according to the method of Hartree (1972) modified from Lowry et al. (1951).

5.3.1 Amylase Activity (Figs. 38 & 39)

In the determination of the relation of amylase activity of the extract from the hepatopancreas in Metapenaeus ensis and pH, the maximum activity was found at pH 6.5, indicating that this is the optimum pH for amylase activity (Fig. 38). At this pH, the activity increased with increase in temperature from 25 to 30 °C and decreased from 30 to 45 °C (Fig. 39). The optimum temperature thus observed was 30 °C at pH 6.5.

Amylase from most crustaceans has an optimum pH in the range of pH 5.0 to 7.8 (van Weel, 1970). Different penaeid shrimps appear to have similar pH optimum. The pH optimum for amylase of Penaeus indicus and Metapenaeus monoceros is 6.6 (Karunakaran & Dhage, 1977) and the pH optimum of amylase for Penaeus japonicus is 6.8 (Maugle et al., 1982). The temperature optima appear to vary among different penaeid species. The temperature optima for P. indicus and M. monoceros are 35 to 40 °C (Karunakaran & Dhage, 1977). Amylase of P. japonicus has a temperature optimum at 40 °C (Maugle et al., 1982).

5.3.2 Protease Activity (Figs. 40 & 41)

Protease from M. ensis did not have a specific optimum pH.

Determining activity at different pHs showed a broad range of activity of higher than 10^{-6} K μg protein^{-1} from pH 6.0 to 9.0 (Fig. 40). The highest activity was found at pH 9.0. Thus, pH 9.0 was chosen for the study of protease activity in subsequent experiments in Chapters VI and VII.

The lack of a pH optimum in protease activity may be due to the presence of more than one proteases in the hepatopancreas of M. ensis. Biesiot & Capuzzo (1990) demonstrated that there are two pH optima at pH 5.3 and 6.4 for the protease from Homarus americanus. Study on the protease from the hepatopancreas of Callinectes sapidus also showed two pH optima at 6.2 and 7.5 (Dendinger, 1987). Proteases in most crustaceans have alkaline pH optima and acid proteases are rare (van Weel, 1970). In the review of Dall & Moriarty (1983), Astacus, Cambarus and Uca have trypsin-like proteinases with pH optima at pH 7 to 9. The pH optima for protease activity from Penaeus kerathurus and Penaeus japonicus were at alkaline pH from 8.5 to 9.0 and pH 8.0 to 8.3 respectively (Galgani et al., 1984, 1985). Tsai et al. (1986) showed that a number of shrimp species, including Penaeus monodon, P. japonicus, P. penicillatus, Metapenaeus monoceros and Macrobrachium rosenbergii, have highest chymotrypsin activities at pH 7 to 8.

The activity of protease in M. ensis increased with increase in temperature from 25 to 50 °C at pH 9.0 (Fig. 41). Protease from P. japonicus has a optimum assay temperature at 40 °C (Magule et al., 1982). The protease activity of P. kerathurus increased to 50 °C and dropped abruptly at

temperature higher than 50 °C (Galgani et al., 1984). Tsai et al. (1986) found that shrimp proteases were unstable at temperature higher than 50 °C. Protease from H. americanus was also able to function at this high temperature (Biesiot & Capuzzo, 1990). The protease activity of H. americanus increased from 25 to 50 °C and started to decrease at 50 °C. The protease of M. ensis appears to have similar thermo-tolerance and functional temperature range.

Fig. 38. Relation of amylase activity of extract from the hepatopancreas in Metapenaeus ensis and pH. Reaction conditions are 25 °C, 15 min.

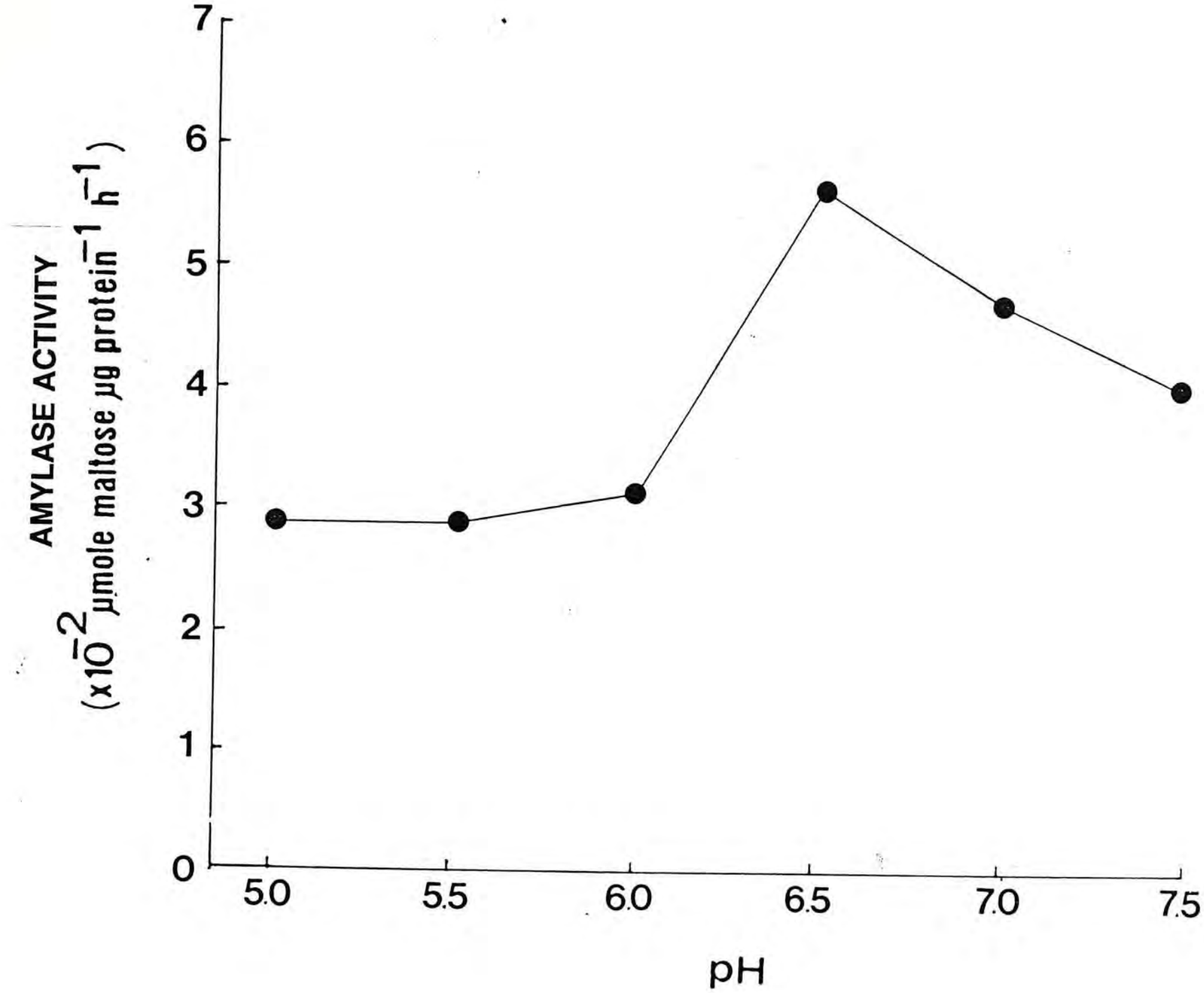
AMYLASE ACTIVITY
(x10⁻² µmole maltose µg protein⁻¹ h⁻¹)
7
6
5
4
3
2
1
0
5.0
5.5
6.0
6.5
7.0
7.5
pH

Fig. 39. Relation of amylase activity of extract from the hepatopancreas in Metapenaeus ensis and temperature. Reaction conditions are pH 6.5, 15 min.

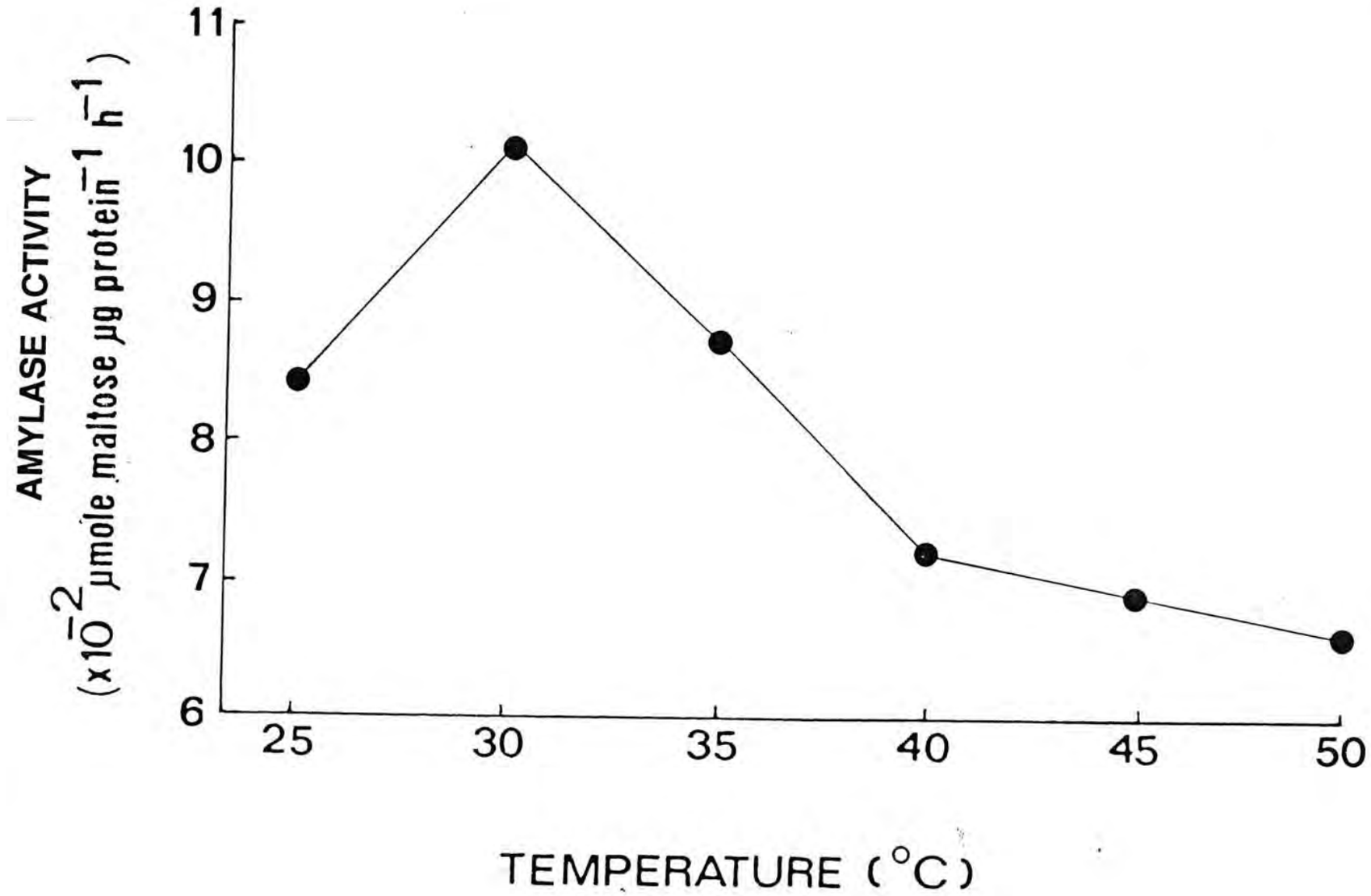
AMYLASE ACTIVITY
(x10⁻² µmole maltose µg protein⁻¹ h⁻¹)
11
10
9
8
7
6
25
30
35
40
45
50
TEMPERATURE (°C)

Fig. 40. Relation of protease activity of extract from the hepatopancreas in Metapenaeus ensis and pH. Reaction conditions are pH 25 °C, 1 h.

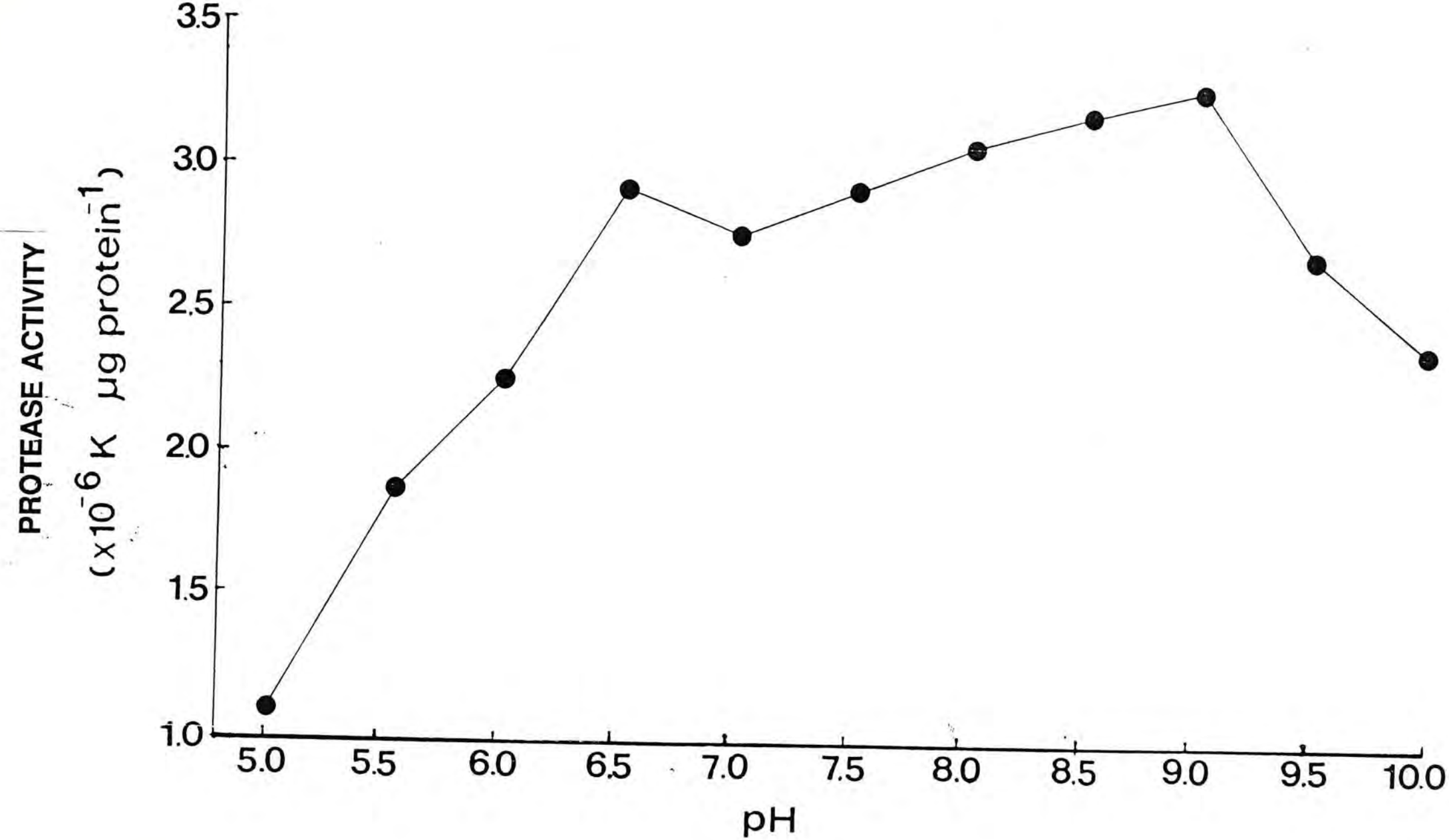
PROTEASE ACTIVITY
(x10⁻⁶ K µg protein⁻¹)
3.5
3.0
2.5
2.0
1.5
1.0
5.0
5.5
6.0
6.5
7.0
7.5
8.0
8.5
9.0
9.5
10.0
pH

Fig. 41. Relation of protease activity of extract from the hepatopancreas in Metapenaeus ensis and temperature. Reaction conditions are pH 9.0, 1 h.

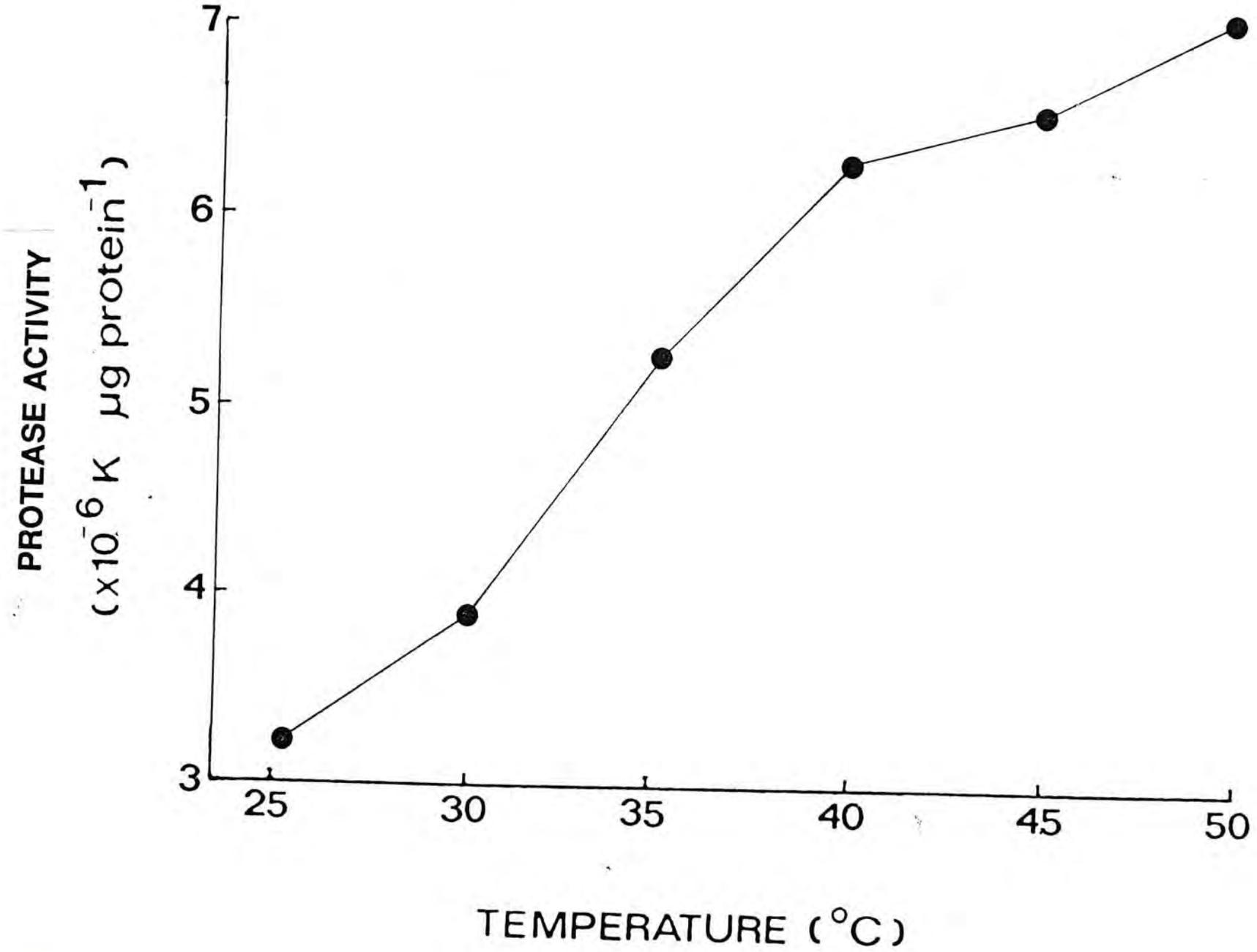
PROTEASE ACTIVITY
(x10⁻⁶ K µg protein⁻¹)
7
6
5
4
3
25
30
35
40
45
50
TEMPERATURE (°C)

CHAPTER VI

CHANGES IN THE HEPATOPANCREAS OF SHRIMP Metapenaeus ensis DURING THE DIGESTIVE CYCLE

6.1 Introduction

The hepatopancreas is the principal organ for digestion in decapod crustaceans. The organ should respond cytologically or enzymatically to food intake in order to digest, absorb and assimilate the food. The changes in the ultrastructure of the hepatopancreas during the digestive cycle were studied in Carcinus maenas (Hopkin & Nott, 1980), Penaeus semisulcatus (Al-Mohanna & Nott, 1986, 1987a), Homarus gammarus and Scylla serrata (Barker & Gibson 1977, 1978). Barker & Gibson (1977, 1978) also demonstrated the changes in digestive enzymatic activities in the hepatopancreas of H. gammarus and S. serrata during the digestive cycle. The changes in the ultrastructure of the hepatopancreas during the cycle may reflect the functions of different cell types in the organ. The present study investigates the ultrastructural changes of the hepatopancreas and the accompanied changes in digestive enzyme activities of the shrimp Metapenaeus ensis.

6.2 Materials and Methods

Metapenaeus ensis at moult stage C or D_0 of body weight 5.5 to 7.0 g and body length 7.5 to 9.0 cm were used in the present study. Shrimp were initially fed with mussel Perna viridis for one week before experiments. The animals were kept in seawater of temperature at 24 °C and salinity at 33 ppt.

6.2.1 Gut Clearance Time

The duration of food mass passing along the gut of M. ensis was studied. Since the exoskeleton of the shrimp is rather transparent, food materials in the gut are observable through the exoskeleton. Two groups of shrimp containing six individuals each were used. They were kept in two separate buckets filled with 10 l of seawater. One of the groups was fed with mussel Perna viridis, and the other was fed with eel meal stained with fast green in order to locate clearly the position of the food materials in the gut. Fast green stain was added in the proportion of 0.1 g fast green stain powder to 20 g eel meal powder. The position of food materials in the gut was checked every 2 h in the first 12 h period after feeding and then at 16 h, 24 h, 30 h, and 36 h after feeding.

6.2.2 Digestive Enzymes Acitivies

Changes in the activies of amylase and protease during the digestive cycle were studied. The hepatopancreas from 4 individuals were isolated at 1, 2, 4, 8, 12, 24 and 36 h after feeding. The hepatopancreas was homogenized in 2 ml of distilled water. The extract was passed through a 5 μm millipore mesh. The filtrate was analysed for the activities of amylase and protease. The activities of amylase and protease were determined according to the methods described in Chapter V.

Amylase activity was determined at pH 6.5 (in 0.1M phosphate buffer), 25 °C and the reaction was conducted for 15 min. Specific activity of amylase was reported as μmole maltose μg protein^{-1} h^{-1}. Protease activity was determined at pH 9.0 (in 0.1M borate buffer), 25 °C and the reaction was proceeded for one hour. Specific activity of protease was expressed as velocity constant K μg protein^{-1}. The total protein was determined according to the method of Hartree (1972) modified from Lowry et al. (1951).

6.2.3 Ultrastructural Study

The method used in ultrastructural study was the same as described in Chapter III. Hepatopancreas from three individuals were excised at 1, 2, 4, 8, 12, 24, 36 h after feeding. The specimens were observed with Zeiss EM9S-2

or Jeol JEM-100 CXII transmission electron microscope.

6.3 Results

6.3.1 Gut Clearance Time

Shrimp fed on the two diets showed similar results. The stomach was filled with food mass in the first hour after feeding. Food mass stayed in the stomach for about six hour and then the stomach became emptied. The food material extended to occupy the whole length of the tubular midgut and to the hindgut by 12 h after feeding. The food material tended to break in the stomach-midgut junction after 16 h when egestion began. After 24 h, most of the shrimp had empty gut or a short faecal column in the rear end of the tubular midgut and the hindgut.

6.3.2 Digestive Enzyme Activites (Figs. 42 & 43)

There was a tendency for the amylase activity to increase from 1 to 4 h after feeding and decreased at 8 h after feeding (Fig. 42). The activity was similar from 12 to 36 h after feeding. The highest activity appeared to occur in the period between 4 to 8 h after feeding. However, there are no significant differences in amylase activity in the hepatopancreas for animals sacrified at difference times after feeding (ANOVA, $P>0.05$).

The changes in the activity of protease were similar to those for

amylase (Fig. 43). The highest activity was found between 4 to 8 h after feeding. The activity then dropped and maintained at a level similar to that at 1 h after feeding. There was no significant difference in the protease activity during the 36-h period (ANOVA, $P>0.05$).

6.3.3 Ultrastructural Changes in the Hepatopancreas

a) Transformation of F-cells to B-cells (Figs. 44-51)

At 1-2 h after feeding, pinocytotic vesicles and dense granules were accumulated in the apical region of F-cells (Fig. 44). The plasma membrane in the apical region of F-cells invaginated to form pinocytotic channels. The pinocytotic vesicles were larger in size in the sub-apical region. During the same period, dense granules of similar size were found to be crowded under the apical border of the F-cells (Fig. 44).

At 4 h after feeding, numerous pinocytotic vesicles accumulated in the apical region of F-cells giving the cell a foamy appearance (Fig. 45). The pinocytotic vesicles tended to vary in sizes and are irregular in shape. The dense granules observed earlier persisted in the apical region of the cell.

At 8 h after feeding, pinocytotic channels could still be observed in the apical region of F-cells (Fig. 46). The pinocytotic vesicles were larger in size

towards the basal region of the cell. Sub-apical vacuoles were formed. The shape of the sub-apical vacuoles was oval to irregular. The sub-apical vacuoles fused together to form digestive vacuoles. The digestive vacuoles then coaleced to become bigger. The content of the digestive vacuoles might consist of granular substances. The cell at this stage might be regarded as an intermediate between F- and B-cell. The cell was slightly distended in the mid-region.

By 12 h after feeding, less pinocytotic channels were observed. Fusion among the pinocytotic vesicles, sub-apical vacuoles and digestive vacuoles was evident and the digestive vacuoles increased in size (Fig. 47). The digestive vacuole eventually became a single large vacuole which greatly distended the cell, giving it the characteristic appearance of a B-cell (Fig. 48). Condensed materials appeared in the sub-apical vacuoles and the digestive vacuole. Dense region might be found in the digestive vacuole of some of the B-cells. Clear zone might occur within the dense region. The digestive vacuole might be partitioned by strips of cytoplasm. Cytoplasm became dense and the volume of cytoplasm was reduced. The cell was transformed into a barrel-shape. The nucleus was being compressed and deflated laterally or basally.

By 24 h after feeding, dense regions in the digestive vacuole of B-cells disappeared and small fragments left in the vacuole. The digestive vacuole was being filled with granular materials (Fig. 49). The digestive vacuole

expanded and distended the cell very much. The cytoplasm was greatly condensed and became just a thin rim surrounding the vacuole. The nucleus was further compressed into ovoid shape and very much condensed. Microvilli became disoriented and lost. Cell adhesions between adjacent cells were disrupted and the cell tended to be extruded (Fig. 50). Extruded B-cells and the digestive vacuoles were observed in the lumen of the tubules (Fig. 51). The microvilli of the extruded B-cell were lost.

b) Changes in R-cells (Figs. 52-55)

By 1-2 h after feeding, mitochondria and small vesicles accumulated apically (Fig. 52a). No apical pinocytosis could be observed in R-cells. Smooth endoplasmic reticulum was found in the central region of R-cell, mostly around the nucleus (Fig. 52b) but was poorly developed in the basal region of the cell. By 4-8 h, the rough endoplasmic reticulum system was extensively developed and extended throughout the cell (Fig. 53). Lipid droplets appeared to increase in size and became numerous at 8 h after feeding. The rough endoplasmic reticulum regressed by 12 h after feeding. At that time smooth endoplasmic reticulum proliferated in the basal region of the cell (Fig. 54). By 24 h Golgi bodies with dilated cisternae were observed. Vacuoles of low density content and small vesicles with high density content were found to pinch off from the Golgi body (Fig. 55).

6.4 Discussion

The digestive cycle of Metapenaeus ensis takes about 24 h. This is consistent with the observation in Penaeus semisulcatus (Al-Mohanna & Nott, 1987a), Homarus americanus and Scylla serrata (Barker & Gibson, 1977, 1978). Food mass stayed in the stomach of M. ensis for about 6 h. During this period, the digestive enzyme activities in the hepatopancreas appeared to increase to maximum. Ingestion of food possibly induced secretion of digestive enzymes from the hepatopancreas.

Pinocytosis was observed in F-cells at 1-8h after feeding which might correspond to the absorption of digested food. Smooth endoplasmic reticulum in R-cells of M. ensis proliferated from 2-8 h after feeding. It was proposed in P. semisulcatus that R-cells absorb luminal nutrients by diffusion and the proliferation of smooth endoplasmic reticulum and associated rough endoplasmic reticulum were responsible for transferring the absorbed metabolites (Al-Mohanna & Nott, 1987a). The digestive enzyme activities appeared to drop 8 h after feeding when the stomach was emptied. By 16 h after feeding, the food material broke from the junction between the stomach and the tubular midgut, indicating undigested food no longer emerged from the stomach so that the process of digestion is probably completed in 16 h.

Sub-apical vacuoles in the B-cells in M. ensis, were similar to those

reported in P. semisulcatus, which were regarded as an intermediate stage in the fusion of small pinocytotic vesicles to produce large digestive vacuoles (Al-Mohanna & Nott, 1986). A clear zone appeared in the dense region in the digestive vacuole of the B-cell in M. ensis by 12 h after feeding was probably a sign of intracellular digestion and assimilation as suggested in P. semisulcatus (Al-Mohanna & Nott, 1986). Intracellular digestion in B-cells of M. ensis was probably completed at 24 h after feeding since the dense region in the digestive vacuole of B-cells disappeared. The B-cells tended to be extruded during this period. B-cells were extruded by 24 h after feeding in P. semisulcatus (Al-Mohanna & Nott, 1986), and by 12 to 24 h after feeding in Carcinus maenas (Hopkin & Nott, 1980). The condensed materials in the digestive vacuole of M. ensis may contain residue of undigested materials. The extrusion of B-cells possibly eliminated the wastes stored in the digestive vacuole.

The transformation of B-cells from F-cells was also reported by Loizzi (1971), Hopkin & Nott (1980), Al-Mohanna & Nott (1986). The transformation process generally involves the uptake of luminal nutrients by apical pinocytosis in F-cells resulting in many vesicles. After the fusion of the vesicles and intracellular digestion, the digestive vacuole formed and distended the cell. Wastes from digestion or assimilation may be accumulated in the digestive vacuole. The mature B-cells tend to be extruded from the tubular epithelium, eliminating the metabolic wastes in the vacuole and probably releasing the digestive enzymes stored in the cell.

R-cell did not show any sign of transformation from F-cell and appeared to have its own activities during the digestive cycle. In contrast to F-cells, apical pinocytosis did not occur in R-cells. No digestive vacuole formation was observed in R-cells. Lipid droplets in R-cells increased in size and amount when digestion proceeded.

There is a tendency for the digestive enzyme activities in M. ensis to increase upon the uptake of food and to reach maximum between 4 to 8 h after feeding, although this change was not statistically significant. During this period, pinocytosis ocurred in F-cells and rough endoplasmic reticulum proliferated in R-cells. These ultrastructural changes are consistent with the absorption of nutrients. The digestive enzyme activities dropped at 8 h after feeding while the stomach became emptied. It was reported that there are three bursts of enzyme activities in Homarus gammarus at 0-15 min, 1-2 h and 3.5-5 h after feeding (Barker & Gibson, 1977) and also three waves of activities in Scylla serrata at 0.5-1 h, 3 h and 8 h after feeding (Barker & Gibson, 1978). With the sampling time of the present study, burst of enzymes within the first hour after feeding could not be detected.

The differentiation route of different cell types in hepatopancreas is in dispute for many years. Many routes of cellular differentiation were proposed and summarized in the review of Gibson & Barker (1977). Almost all the routes assume E-cells as the mother cells for other cell types, either directly or indirectly. Recent studies support the differentiation of B-cells from F-cells

(Loizzi, 1971; Hopkin & Nott, 1980; Caceci et al., 1988). The present study is in agreement with these studies. R-cells appear to originate from another route of differentiation from E– cells.

Fig. 42. Amylase activity in the hepatopancreas of Metapenaeus ensis during the digestive cycle.

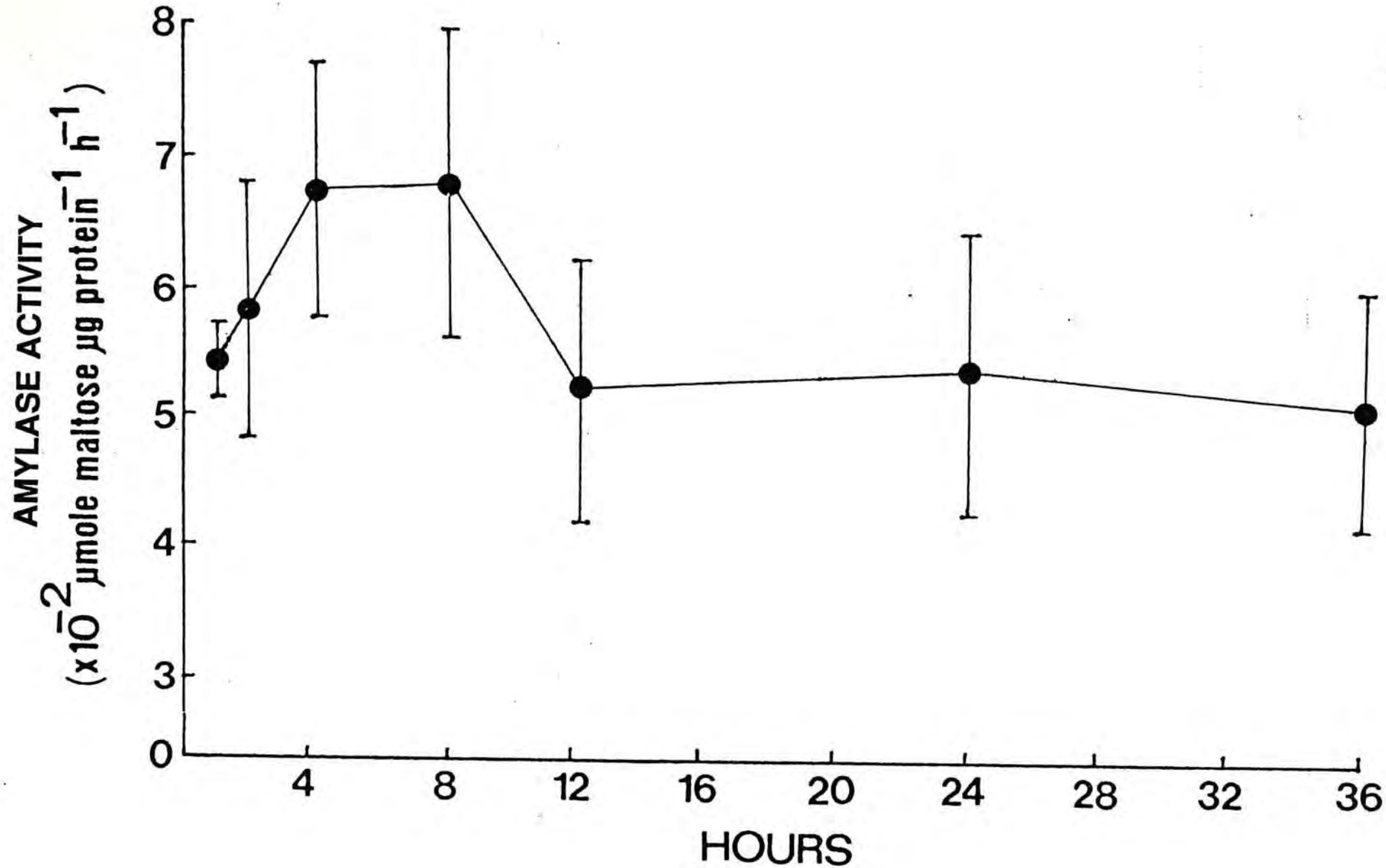
AMYLASE ACTIVITY
(x10⁻² µmole maltose µg protein⁻¹ h⁻¹)
0
3
4
5
6
7
8
4
8
12
16
20
24
28
32
36
HOURS

Fig. 43. Protease activity in the hepatopancreas of Metapenaeus ensis during the digestive cycle.

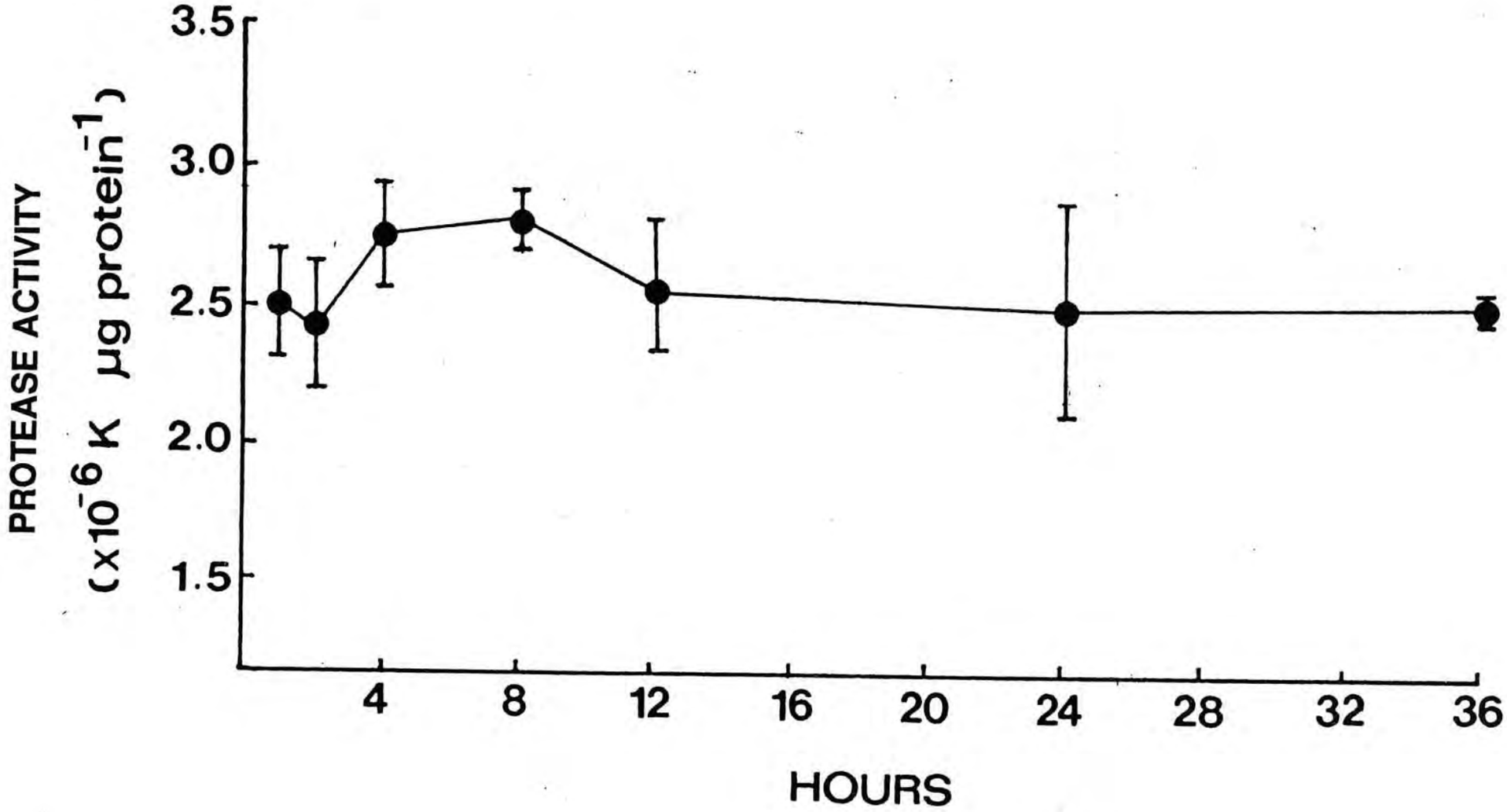
PROTEASE ACTIVITY
(x10⁻⁶ K µg protein⁻¹)
3.5
3.0
2.5
2.0
1.5
4
8
12
16
20
24
28
32
36
HOURS

Fig. 44. Transmission electron micrograph of F-cell in the hepatopancreas of Metapenaeus ensis at 1 h after feeding. Pinocytosis takes place apically and gives rise to numerous pinocytotic vesicles (PV). Numerous dense granules (DG) aggregate in the apical region of F-cell. M, mitochondrion; MV, microvilli; PC, pinocytotic channel. Scale bar represents 1 μm.

M
PV
PC
M

Fig. 45. Transmission electron micrograph of F-cell in the hepatopancreas of Metapenaeus ensis at 4 h after feeding. Continued pinocytosis results in numerous pinocytotic vesicles (PV) and gives the cell a foamy appearance. M, mitochondrion; MV, microvilli; PV, pinocytotic vesicle; R, R-cell; arrow-head, pinocytotic channel. Scale bar represents 1 μm.

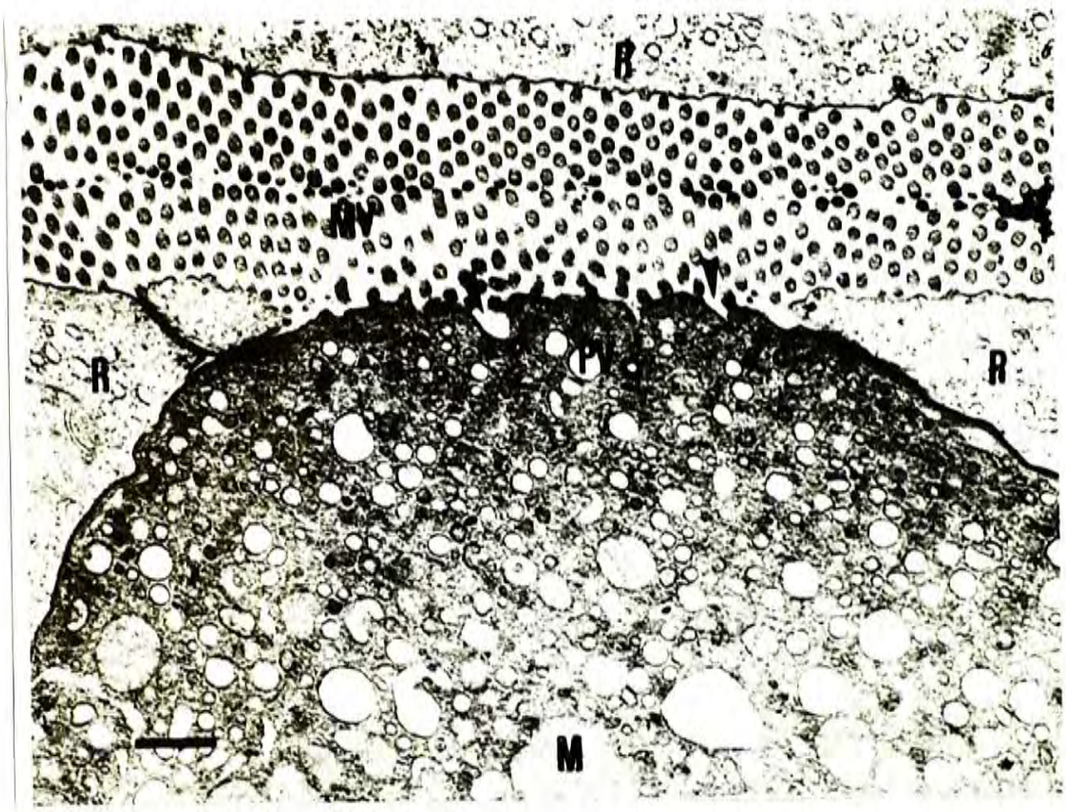
R
AV
R
PV
R
M

Fig. 46. Transmission electron micrograph of intermediate between F- & B-cell in the hepatopancreas of Metapenaeus ensis at 8 h after feeding. Vesicles are larger towards basal region. Sub-apical vacuoles (SA) coalece to form digestive vacuole (DV). M, mitovchondrion; PV, pinocytotic vesicles; R, R-cell. Scale bar represents 2 μm.


R
SA
R
PV
DV

Fig. 47. Transmission electron micrograph of intermediate between F- and B-cell in the hepatopancreas of Metapenaeus ensis at 12 h after feeding. Pinocytosis ceased. Sub-apical vacuoles (SA) fuse together. M, mitochondrion; arrow-heads, fusion of vaucoles. Scale bar represents 2 μm.


SA
SA

Fig. 48. Transmission electron micrograph of B-cell in the hepatopancreas of Metapenaeus ensis at 12 h after feeding. Fusion among vacuoles continues. The digestive vacuole (DV) is partitioned by strips of cytoplasm (arrow-heads). Dense regions (DR) are found in the digestive vacuole. Clear zone (CZ) may appear inside the dense region. N, nucleus; R, R-cell; SA, sub-apical vacuole. Scale bar represents 5 μm.

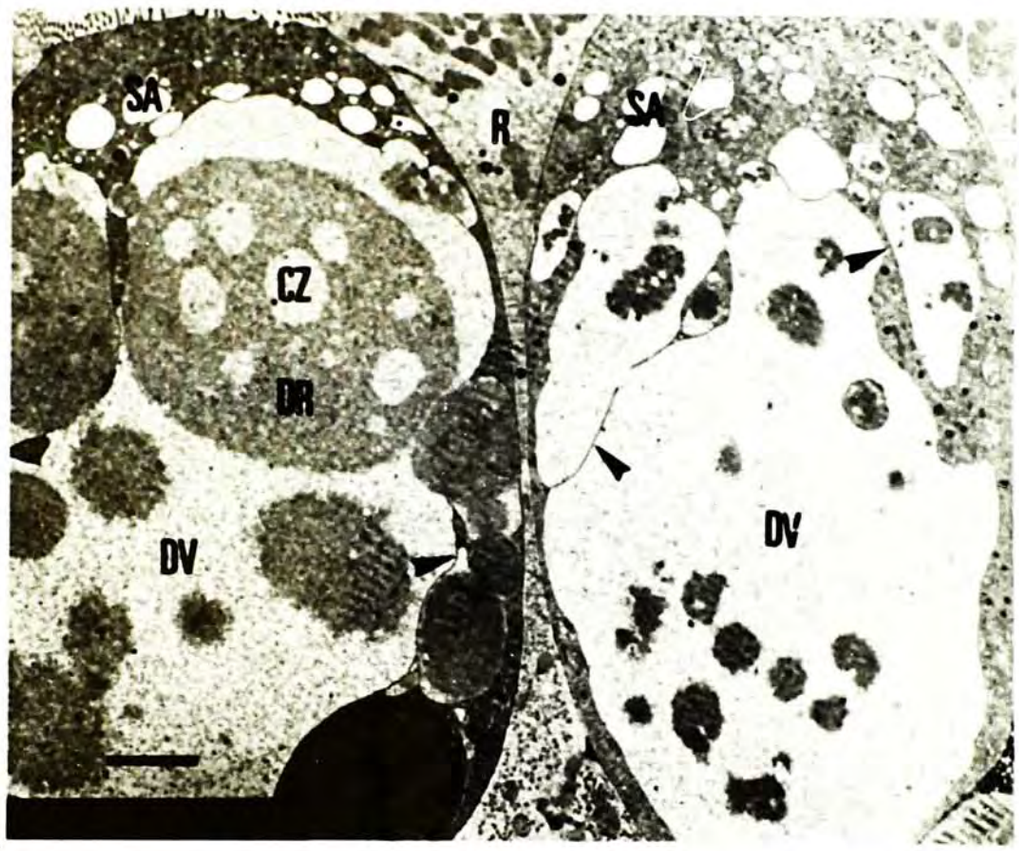
SA
R
SA
CZ
DR
DV
DV

Fig. 49. Transmission electron micrograph of a mature B–cell in the hepatopancreas of Metapenaeus ensis at 24 h after feeding. The cytoplasm (arrow-heads) becomes a thin shell surround the digestive vacuole (DV). The nucleus (N) is compressed and deflated laterally. Microvilli (arrow) are disoriented and losing. R, R–cell. Scale bar represents 5 μm.


DV
R
R
Q

Fig. 50. Transmission electron micrograph of mature B-cell prior to extrusion at 24 h after feeding. Cell adhesion between adjacent cell and the B-cell is disrupted (arrow-head). DV, digestive vacuole; F, F-cell; R, R–cell. Scale bar represents 2 μm.


R
DV

Fig. 51. Extruded B-cell found in the tubular lumen in the hepatopancreas of Metapenaeus ensis. Microvilli are lost. DV, digestive vacuole; N, nucleus. Scale bar represents 5 μm.

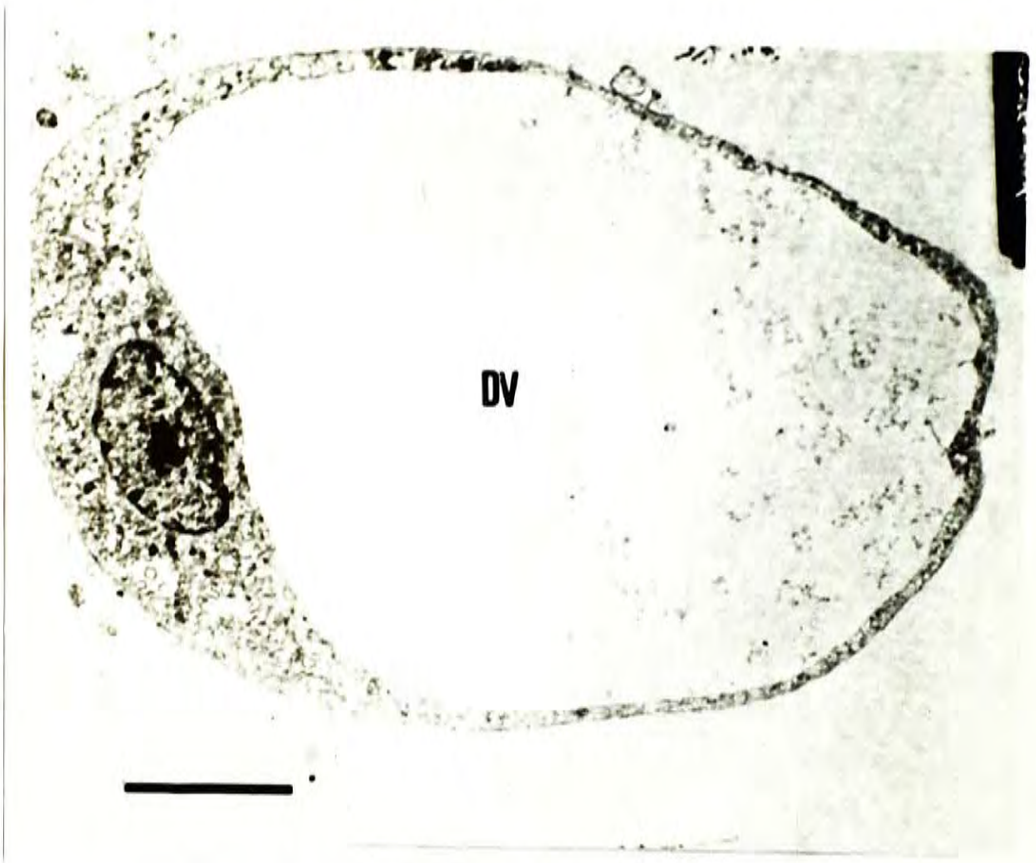
DV

Fig. 52. Transmission electron micrographs of R-cells in the hepatopancreas of Metapenaeus ensis at 2 h after feeding.

(a) Apical region. Mitochondria (M) accumulate in the apical region. MV, microvilli. Scale bar represents 2 μm.

(b) Basal region. Smooth endoplasmic reticulum (SE) is found around the nucleus (N) in the central region of the cell. BL, basal lamina; LP, lipid droplet. Scale bars represents 2 μm.

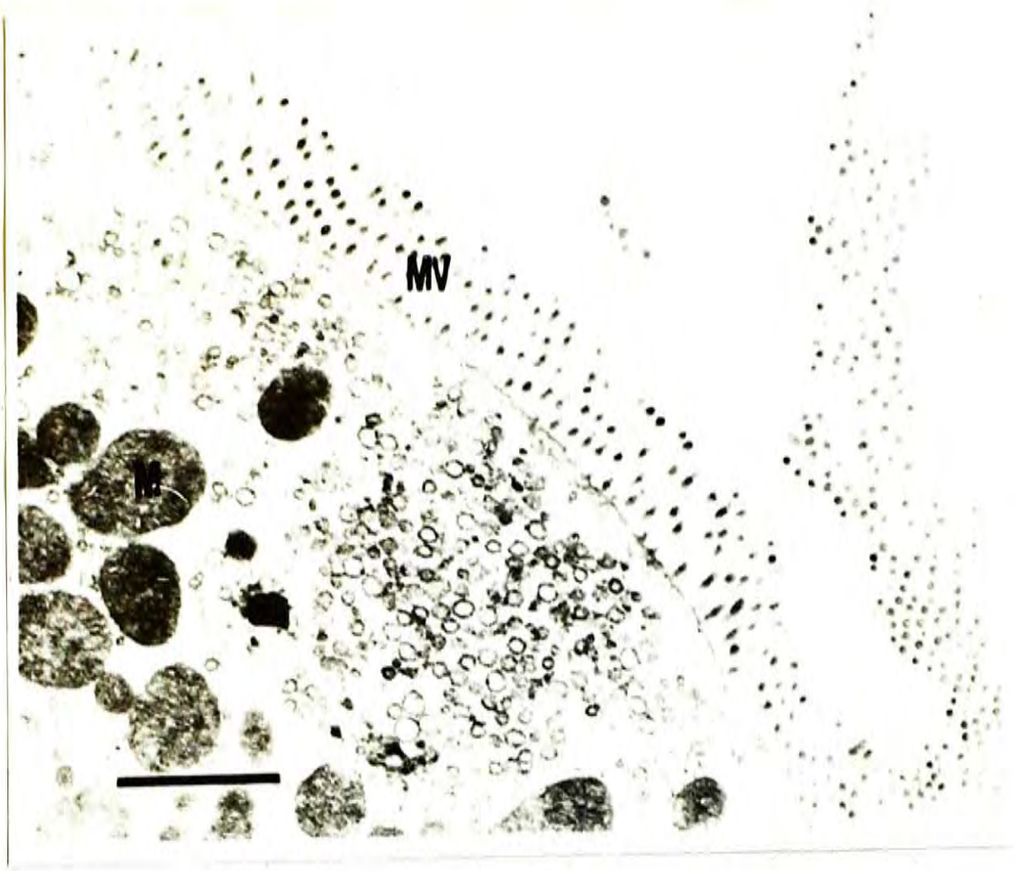

a

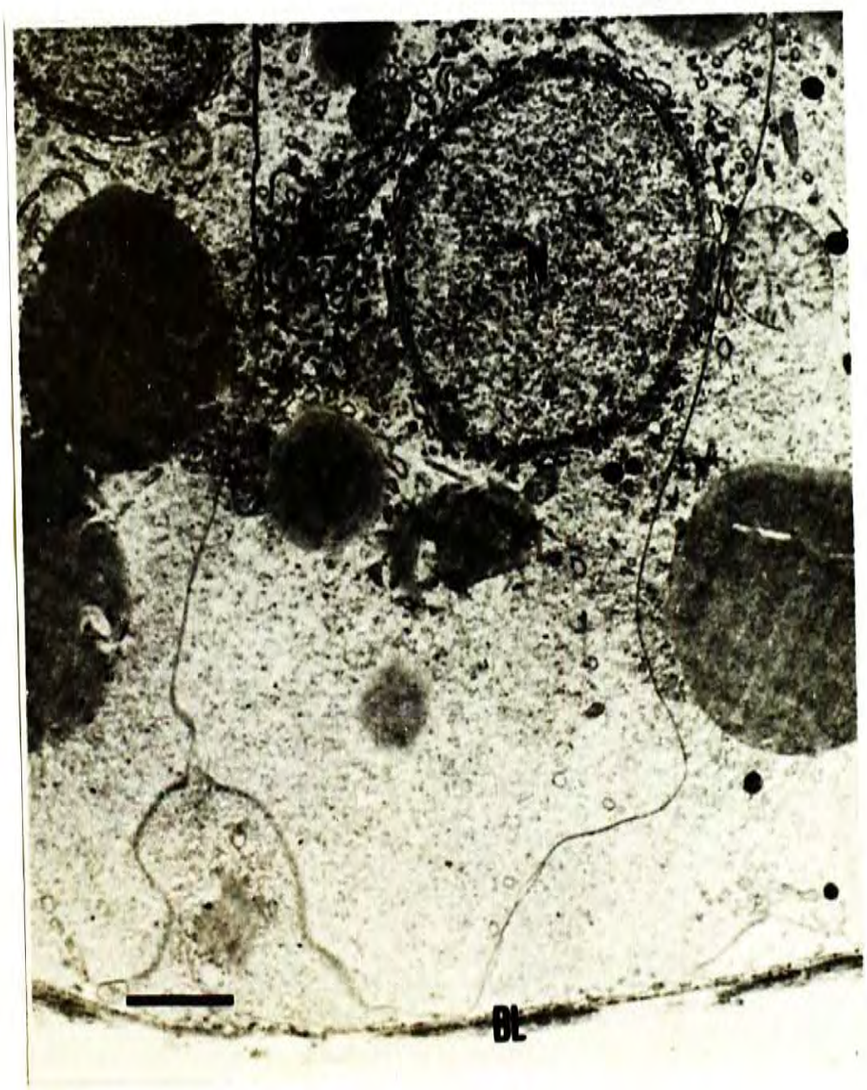

b

Fig. 53. Transmission electron micrograph of R-cell in the hepatopancreas of Metapenaeus ensis at 8 h after feeding. Rough endoplasmic reticulum (RE) extensively develop throughout the cell. Lipid droplets (LP) are more and become larger. M, mitochondrion. Scale bar represents 5 μm.

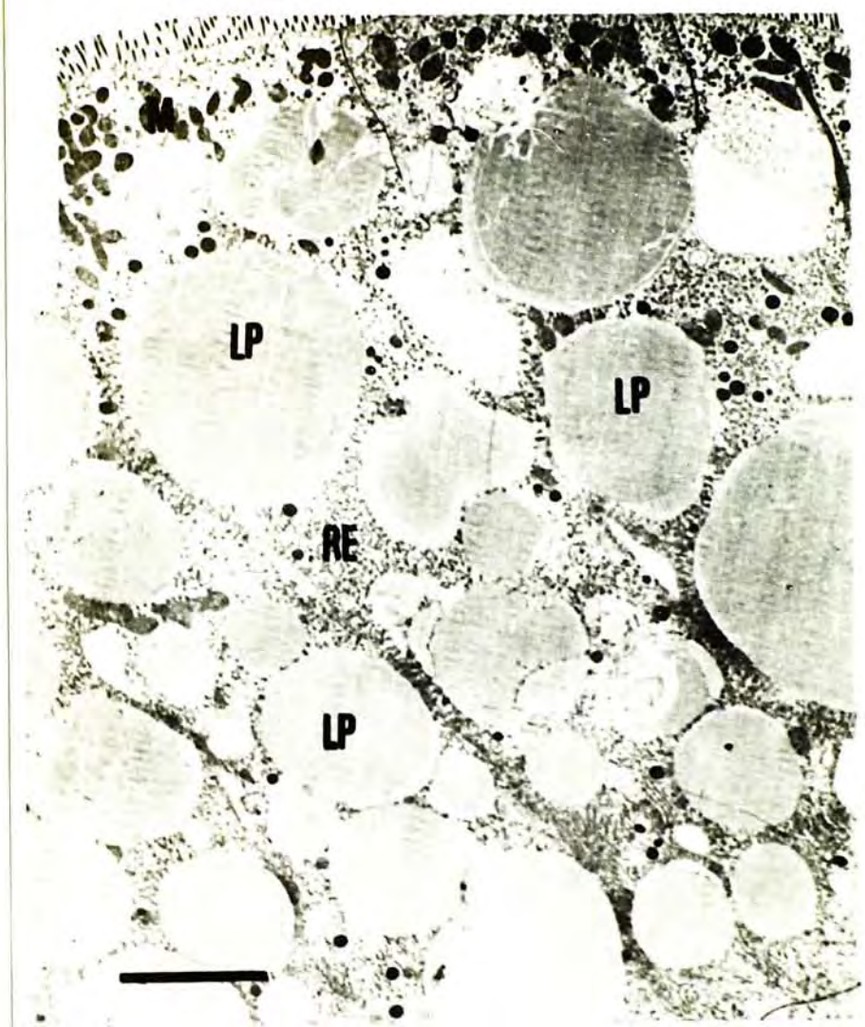
LP
LP
RE
LP

Fig. 54. Transmission electron micrograph of basal region of R-cell in the hepatopancreas of Metapenaeus ensis at 12 h after feeding. Rough endoplasmic reticulum regressed. Smooth endoplasmic reticulum (SE) proliferates in the basal region. BL, basal lamina; LP, lipid droplet; N, nucleus. Scale bar represents 1 μm.


LP
N

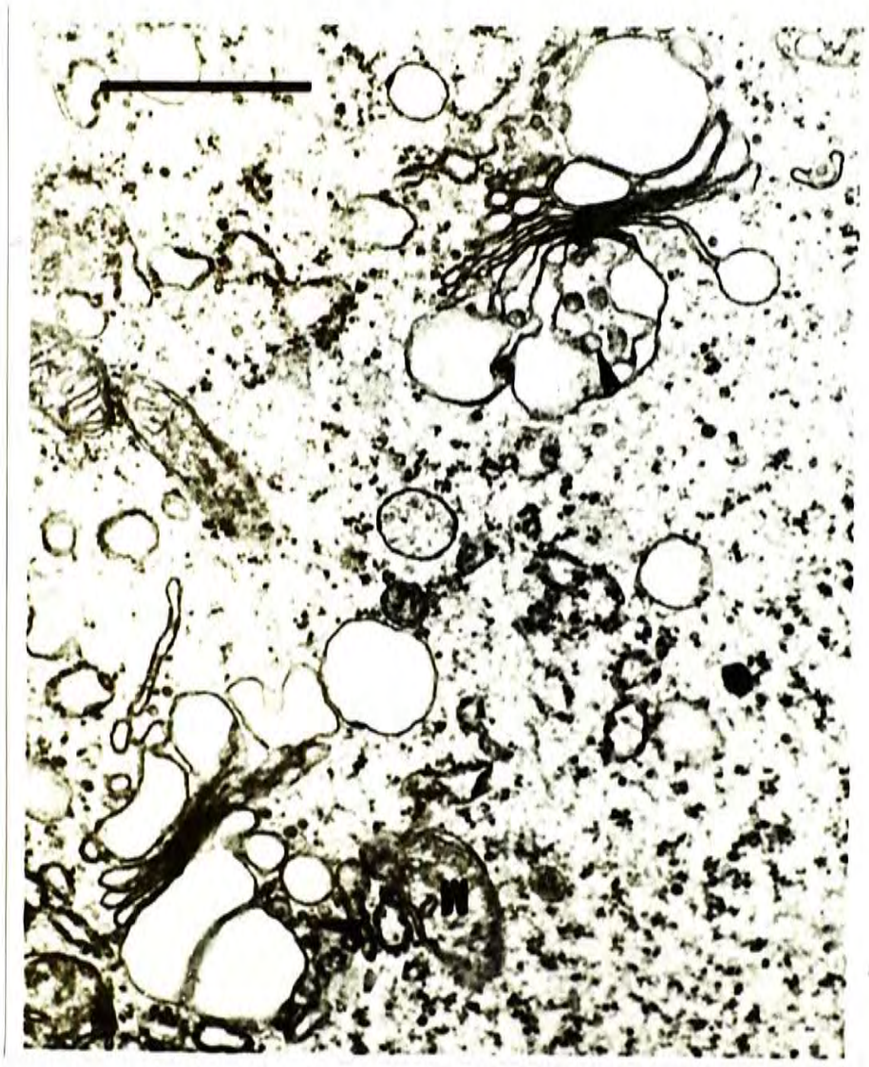

Fig. 55. Transmission electron micrograph showing Golgi bodies in the R-cell at 24 h after feeding. The cisternae are dilated. Vesicles (V) and dense granules (arrow-heads) appeared to pinch off from the Golgi bodies (G). M, mitochondrion. Scale bar represents 1 μm.

CHAPTER VII

EFFECTS OF STARVATION ON THE HEPATOPANCREAS IN THE SHRIMP Metapenaeus ensis

7.1 Introduction

The biochemical composition of decapod hepatopancreas is dependent on various factors, such as body size, season, moult stage and dietary stress. Starvation affects the biochemical composition (Cuzon et al., 1980; Barclay et al., 1983), digestive enzyme activities (Cuzon et al., 1980) and histological structure (Papathanassiou & King, 1984) of the hepatopancreas in shrimp. It has been suggested that the histology of the hepatopancreas may be used to indicate dietary stress (Papathanassiou & King, 1984; Vogt et al., 1985, 1986). Yet dietary status may also be reflected by the amount of organic reserves in the hepatopancreas. In the present study, the effects of starvation on the biochemical composition, digestive enzyme activities and the histological structure and ultrastructure of the hepatopancreas in the shrimp Metapenaeus ensis were investigated. This species is commonly cultured in southern China. The results from this study may be used to assess the dietary status of the animals under culture conditions. Part of the results of this study has previously been reported (Leung et al., 1990).

7.2 Materials and Methods

7.2.1 Experimental Condition

Metapenaeus ensis were hatchery raised or acquired from local fish markets. The body weight and body length of shrimp ranged from 2.3 to 4.0 g and 6.0 to 7.5 g, respectively. They were fed with mussels (Perna viridis) for at least 1 week before the experiment. Shrimp at moult stage C or D_o were then placed individually in plastic compartments (14.5 cm x 9.5 cm) on a water table. The water depth was maintained at about 6 cm. The temperature and salinity of the seawater was 18 to 22 °C and 31 to 33 ppt, respectively. The shrimp were either fed daily with mussel or starved. The hepatopancreas was excised from the shrimp after 0, 2, 4, 8, or 16 days of starvation. Some shrimp starved for 16 days were then refed with mussel for 2 days. The hepatopancreas was isolated for analyses. Daily-fed shrimp were also sacrificed on the same days. The moult stage of the shrimp might change during the experiment. Only shrimp at stage C or D_o were taken for analyses.

7.2.2 Determination of Biochemical Composition

Three to six individuals were sacrificed for the determination of hepatosomatic index and biochemical composition. The hepatopancreas and the rest of the body were freeze-dried and weighed. The hepatosomatic index was expressed as the freeze-dried weight of the hepatopancreas divided by the total freeze-dried body weight. Protein concentration in the hepatopancreas was determined according to the method of Hartree (1972), modified from Lowry et al. (1951). Lipids were extracted by the procedure of Sasaki & Capuzzo (1984) and the concentration was determined by the method of Barnes & Blackstock (1973). Carbohydrate concentration was measured by the method of Dubois et al. (1956). The biochemical composition was expressed as mg g^{-1} of the freeze-dried weight of the hepatopancreas.

7.2.3 Determination of Digestive Enzyme Activities

Hepatopancreas freshly isolated from the daily-fed and starved shrimp was homogenized and the extract was passed through 5 μm mesh. Activities of amylase and protease were determined with the methods described in Chapter V. The enzyme activities of daily-fed shrimp were determined 6 h after feeding. Previous experiments showed that the activities reached maximum from 4 to 8 h after food intake (see Chapter VI). Amylase activity

was measured according to Wrint & Stegbauer (1974). The reaction mixture was incubated at 25 °C, pH 6.5, for 15 min. Protease activity was determined with the method of Charney & Tomarelli (1947). The reaction mixture was incubated at 25 °C, pH 9, for 1 h. The activities of amylase and protease were expressed as μg maltose μg protein^{-1} h^{-1} and velocity constant K μg protein^{-1}, respectively.

7.2.4 Histological Study

Structural changes in the hepatopancreas under starvation were studied with histological and histochemical methods. The results were compared with the samples before starvation. Three shrimp were sampled at each time interval. The method for histological study followed Humason (1974) as described in Chapter III. Hepatopancreas fixed in cold Bouin's fluid were embedded in paraffin wax and stained with hematoxylin and eosin (H & E). Hepatopancreas fixed in cold 5% formalin for 24 hours were cut into frozen sections of 10 μm thick and stained in Sudan black B (Humason, 1974) to examine the amount of lipid reserve. The number of B-cells in paraffin sections was counted in randomly selected fields under the magnification of 100x and expressed as a percentage of the total number of cells. The total number of cells in a field was about 300.

7.2.5 Ultrastructural Study

Three starved shrimp were sacrificed at the specific time intervals. The samples were studied with transmission electron microscopy. The procedures for ultrastructural study were those described in Chapter III. The samples were observed with Zeiss EM9S-2 or Jeol JEM-100 CXII transmission electron microscope.

7.3 Results

7.3.1 Biochemical Studies (Figs. 56-59)

The shrimp were inactive when starved. Some starved shrimp proceeded to late premoult stages as the daily-fed shrimp do. Yet only 3 out of 21 shrimp (14.3%) moulted during 16 days of starvation, whereas 4 out of 15 (26.7%) of the daily-fed shrimp moulted during the same period.

The hepatosomatic index, protein, lipid and carbohydrate concentrations (Figs. 56 to 59) in the hepatopancreas did not vary significantly (ANOVA, $P>0.05$) among the daily-fed shrimp during the period of experiment. The hepatosomatic index was around 0.044 to 0.059. Mean protein, lipid and carbohydrate concentrations were 460 to 520 mg g^{-1}, 105 to 118 mg g^{-1} and

46 to 51 mg g^{-1} respectively. The hepatosomatic index of the shrimp after 4 or more days of starvation (Fig. 56) was significantly lower than that of daily-fed shrimp (Student's t-test, $P<0.05$). After 16 days of starvation, the hepatosomatic index was less than 50% of the value in daily-fed shrimp. The hepatosomatic index of the shrimp refed for 2 days after 16 days of starvation increased but is significantly lower than the daily-fed value. Protein concentration in the hepatopancreas of starved shrimp (Fig. 57) did not vary significantly during the starvation period (ANOVA, $P>0.05$) and was not significantly different from the corresponding values in daily-fed shrimp (Student's t-test, $P>0.05$). Lipid concentration in the hepatopancreas of shrimp after 2 or more days of starvation (Fig. 58) is significantly lower than that of daily-fed shrimp (Student's t-test, $P<0.05$). After starved for 16 days, the lipid concentration was 30% of the value in daily-fed shrimp. Carbohydrate concentration (Fig. 59) is significantly lower than that of daily-fed shrimp after 4 or more days of starvation (Student's t-test, $P<0.05$). After 16 days, the concentration was 60% of the daily-fed value. Lipid and carbohydrate concentrations in the hepatopancreas of shrimp refed for 2 days after 16 days of starvation increased to the level of the daily-fed shrimp.

7.3.2 Digestive Enzyme Activities (Figs. 60 & 61)

The activities of amylase and protease (Figs. 60 & 61) did not vary significantly in daily-fed shrimp (ANOVA, $P>0.05$) during the experimental

period. The mean amylase and protease activity varied from 0.063 to 0.069 μmole maltose μg protein^{-1} h^{-1} and from 4.4 to 4.7x10^{-6} K μg protein^{-1} respectively. Amylase activity was significantly lower in shrimp after 8 and 16 days of starvation (Fig. 60); it was about 30% of the daily-fed value after 16 days. Protease activity of the starved shrimp was significantly lower than that of daily-fed shrimp after 4 or more days of starvation (Fig. 61). After 16 days of starvation, the protease activitiy was 50% of the daily-fed value. The activities of both amylase and protease increased to the level of daily-fed shrimp after refeeding for 2 days after starvation.

7.3.3 Histological Study (Figs. 62-64)

The hepatopancreas of daily-fed shrimp (Fig. 62a) did not differ markedly from that of shrimp after 16 days of starvation (Fig. 62b). The hepatopancreas of shrimp after 16 days of starvation did not show severe destruction although cell lysis and karyolysis were occasionally observed. For shrimp refed for 2 days after 16 days of starvation, the tubules of the hepatopancreas were similar to those of the daily-fed shrimp (Fig. 62c). The percentage of B-cells decreased after starvation (Fig. 63). Frozen sections stained with Sudan black B showed numerous lipid droplets in the cells of hepatopancreas of daily-fed shrimp (Fig. 64a). The amount of lipid droplets was less after 4 days of starvation. The lipid droplets could hardly be detected after 16 days of starvation (Fig. 64b). When the shrimp was refed for 2 days after starvation, the percentage of B-cells and the amount of lipid droplets increased (Figs. 63 & 64c).

7.3.5 Ultrastructural Study (Figs. 65-75)

After 2 days of starvation, lipid droplets in R-cells diminished in size and decreased in amount (Fig. 65) as compared to the R-cells of daily-fed shrimp shown in Chapter III. The lipid droplets were surrounded by rough endoplasmic reticulum (Fig. 66). Smooth endoplasmic reticulum was only confined to basal region of the cell. The nucleus was surrounded by a layer

of vesicles.

Abundant residual bodies of lysosomes appeared in the apical cytoplasm of R-cells after 4 days of starvation (Fig. 67). Whorls of rough endoplasmic reticulum with a dense granule in the centre were found in the central to basal region of the cell (Fig. 68). Some rough endoplasmic reticulum just formed whorls of multilayered structure without granule in the centre (Fig. 69). Mitochondria tended to enlarge after starvation. The cisternae of smooth endoplasmic reticulum in the basal region of R-cells became constricted after 16 days starvation and appeared as long strings of double membrane (Fig. 70). Upon refeeding after starvation, the size of lipid droplets increased after refeeding. Smooth endoplasmic reticulum became proliferated and no constriction of the cisternae was observed (Fig. 71a). The layer of vesicles around the nucleus tended to diminish (Fig. 71b).

F-cells showed little changes under starvation. Their mitochondria enlarged to great size (Fig. 72). When the shrimp was refed after starvation, the ultrastructure tended to be similar to those of daily-fed shrimp (Fig. 73a, b). The cytoplasm was filled with numerous vesicles. The mitochondria became smaller than during starvation and were about the size of those in the daily-fed shrimp.

B-cells observed in starved shrimp had little difference from those of daily-fed shrimp. Lamellated structure was observed in the digestive vacuole

after 4 days of starvation (Fig. 74). The B-cell appeared to be similar to those of daily-fed shrimp after refeeding (Fig. 75). Sub-apical vacuoles and digestive vacuoles were formed.

7.4 Discussion

The decrease in the activity of starved Metapenaeus ensis suggests that the energy demand would be lower so that they may tolerate a long period of fasting. The oxygen consumption of M. ensis has been shown to decrease upon starvation (Ovsianico-Koulikowsky, 1987). A decrease in hepatosomatic index during starvation as found in this study was also reported in Penaeus japonicus (Cuzon et al., 1980). A lower hepatosomatic index of starved shrimp indicates that the hepatopancreas regresses as nutrient reserves are utilised. The failure to accumulate nutrients may preclude the shrimp to undergo ecdysis, resulting in a lower moult frequency observed in starved shrimp. The hepatosomatic index could not recover to the daily-fed level after 2 days of refeeding, suggesting that the hepatopancreas needed more time to recover.

Protein concentration in the hepatopancreas of M. ensis did not vary significantly during the starvation period, whereas lipid and carbohydrate concentrations decreased. These results show that lipids and carbohydrate

were metabolised during the onset of starvation. The level of lipids was higher than that of carbohydrate and decreased more rapidly during starvation, indicating that lipids are more important than carboydrates as an energy reserve. The decrease in lipid and carbohydrate concentrations tended to level off after 4 days of starvation. It could be estimated that the decrease in lipid and carbohydrate accounted for no more than 40% of the decrease in the weight of the hepatopancreas as shown by the decrease in hepatosomatic index. Thus, it is likely that protein in the hepatopancreas was also metabolized. As protein is the major constituent in the hepatopancreas, a substantial decrease in the amount of protein would be accompanied by a decrease in the weight of the whole organ so that a change in protein concentration might not be observed. It has been shown that in starved Penaeus esculentus the total amount of lipids and protein in hepatopancreas decreases (Barclay et al., 1983). Organic reserves from body tissues other than the hepatopancreas may also be metabolized during starvation. Barclay et al. (1983) showed in P. esculentus protein and lipids in the abdomen are the most important energy reserves utilised during starvation. In Nephros norvegicus, lipid content in the hepatopancreas and the rest of the body do not change upon starvation, suggesting protein is metabolised in preference to lipids (Dall, 1981). Cuzon et al. (1980) suggested that in starved P. japonicus energy reserves are utilised in the order of carbohydrate, lipids and protein. Thus, the type of biochemical components preferentially metabolized in starved decapod crustaceans appears to depend on the duration of starvation and may also be species specific, possibly relating to the feeding habits of the

animal.

The decrease in amylase and protease activities in M. ensis apparently resulted from the absence of food. Amylase and trypsin level in the hepatopancreas of starved P. japonicus also decreased (Cuzon et al., 1980). In agreement with previous studies (Papathanassiou & King, 1984; Rosemark et al., 1980), it was showed that fewer B-cells were present in the tubules of the hepatopancreas in starved M. ensis. It is generally believed that the secretion of digestive enzymes in crustaceans can be induced by food intake (Gibson & Barker, 1979). B-cells are believed to secrete digestive enzymes, so that a decrease in the amount of B-cells would lead to decrease in digestive enzyme activities. After refeeding, the amount of B-cells in the hepatopancreas of M. ensis increased to the level before starvation. Therefore, the amount of digestive enzymes secreted may restore to the level before starvation so that food could be digested and reserves could be built up again. The activities of the two digestive enzymes were apparently induced by the availability of food.

Ultrastructurally, F- and B-cells in M. ensis were slightly affected under starvation. These results are consistent with those of previous studies on Palaemon serratus (Papathanassiou & King, 1984) and Penaeus monodon (Vogt et al., 1985).

The decrease in the apical activities of R-cells in starved M. ensis is

apparently due to the lack of nutrients to be absorbed. The smooth endoplasmic reticulum in R-cells regressed in the apical region and was confined to the basal region. The cisternae of the basal endoplasmic reticulum were constricted as strings of double membrane in M. ensis after starvation for 16 days. The apical smooth endoplasmic reticulum is postulated to transfer digested metabolites from the tubular lumen into the R-cells (Al-Mohanna & Nott, 1987a). The lack of metabolites for assimilation in R-cells is possibly related to the constriction of cisternae of basal endoplasmic reticulum in starved shrimp.

Enlargement of mitochondria appears to be a common feature under starvation. This phenomenon has been reported in Palamon serratus (Papathanassiou & King, 1984), P. monodon (Vogt et al., 1985) and H. americanus (Anger et al., 1985).

The whorls of multilayered rough endoplasmic reticulum surrounding a dense granule in the centre found in the R-cells of M. ensis under starvation was also reported by Papathanassiou & King (1984) in the R-cells of starved Palamon serratus. The dense granule in the centre was found to consist of lipid in their study. The whorls of rough endoplasmic reticulum may thus relate to lipid metabolism.

The layer of vesicles surrounding the nucleus of R-cells in M. ensis under starvation had not been reported in other similar studies. The reason

for the appearance of this layer was unknown.

Since the hepatopancreas of M. ensis starved for 16 days did not suffer from severe structural destruction as shown in the histological study, the organ could recover when food was available.

The decrease in hepatosomatic index, lipid and carbohydrate concentration and digestive enzyme activities indicate that these parameters may be used to monitor dietary status of shrimp under culture conditions. However, since these parameters may vary with other factors such as body size, age, moult stage and season, comprehensive studies on the effects of these factors are necessary before the biochemical parameters can be used as an indicator for dietary conditions.

Fig. 56. Hepatosomatic index of daily-fed (squares), starved (closed circles) Metapenaeus ensis during starvation, and refed shrimp after starvation (open circles). Data are expressed as means of 3-6 individuals and vertical bars represent $\pm$ 1 S.E. In some cases, half of the bar is omitted for clarity. Asterisks indicate significant differences between values in daily-fed and starved shrimp (Student's t-test, $P<0.05$).

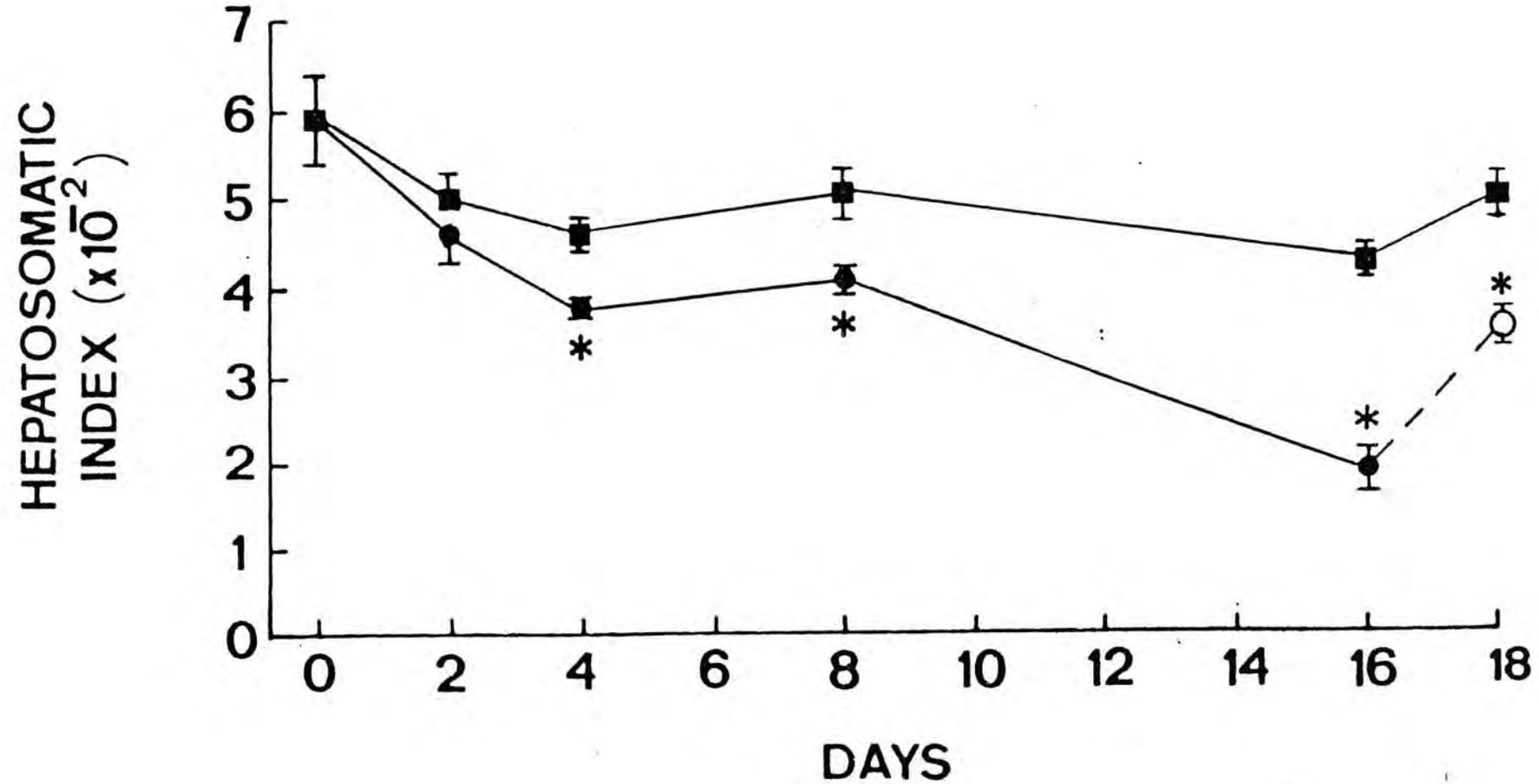
HEPATOSOMATIC INDEX (x10⁻²)
7
6
5
4
3
2
1
0
0
2
4
6
8
10
12
14
16
18
DAYS
*
*
*
*

Fig. 57. Protein concentration of the hepatopancreas in daily-fed (squares), starved (closed circles) Metapenaeus ensis during starvation, and refed shrimp after starvation (open circles). Data are expressed as means of 3-6 individuals and vertical bars represent ± 1 S.E. In some cases, half of the bar is omitted for clarity.

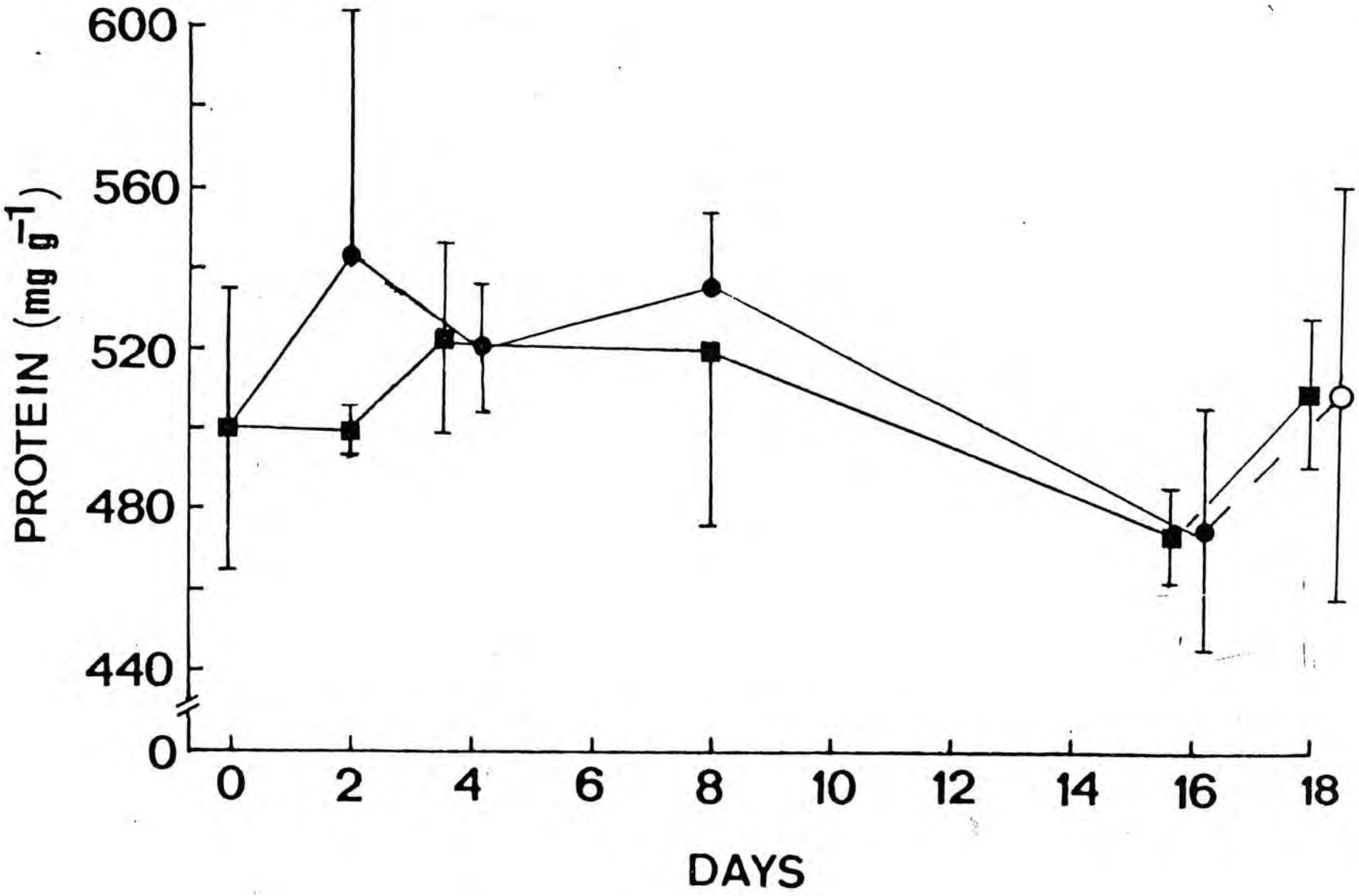
600
560
520
480
440
0
PROTEIN (mg g⁻¹)
0
2
4
6
8
10
12
14
16
18
DAYS

Fig. 58. Lipid concentration of the hepatopancreas in daily-fed (squares), starved (closed circles) Metapenaeus ensis during starvation, and refed shrimp after starvation (open circles). Data are expressed as means of 3-6 individuals and vertical bars represent $\pm$ 1 S.E. In some cases, half of the bar is omitted for clarity. Asterisks indicate significant differences between values in daily-fed and starved shrimp (Student's t-test, $P<0.05$).

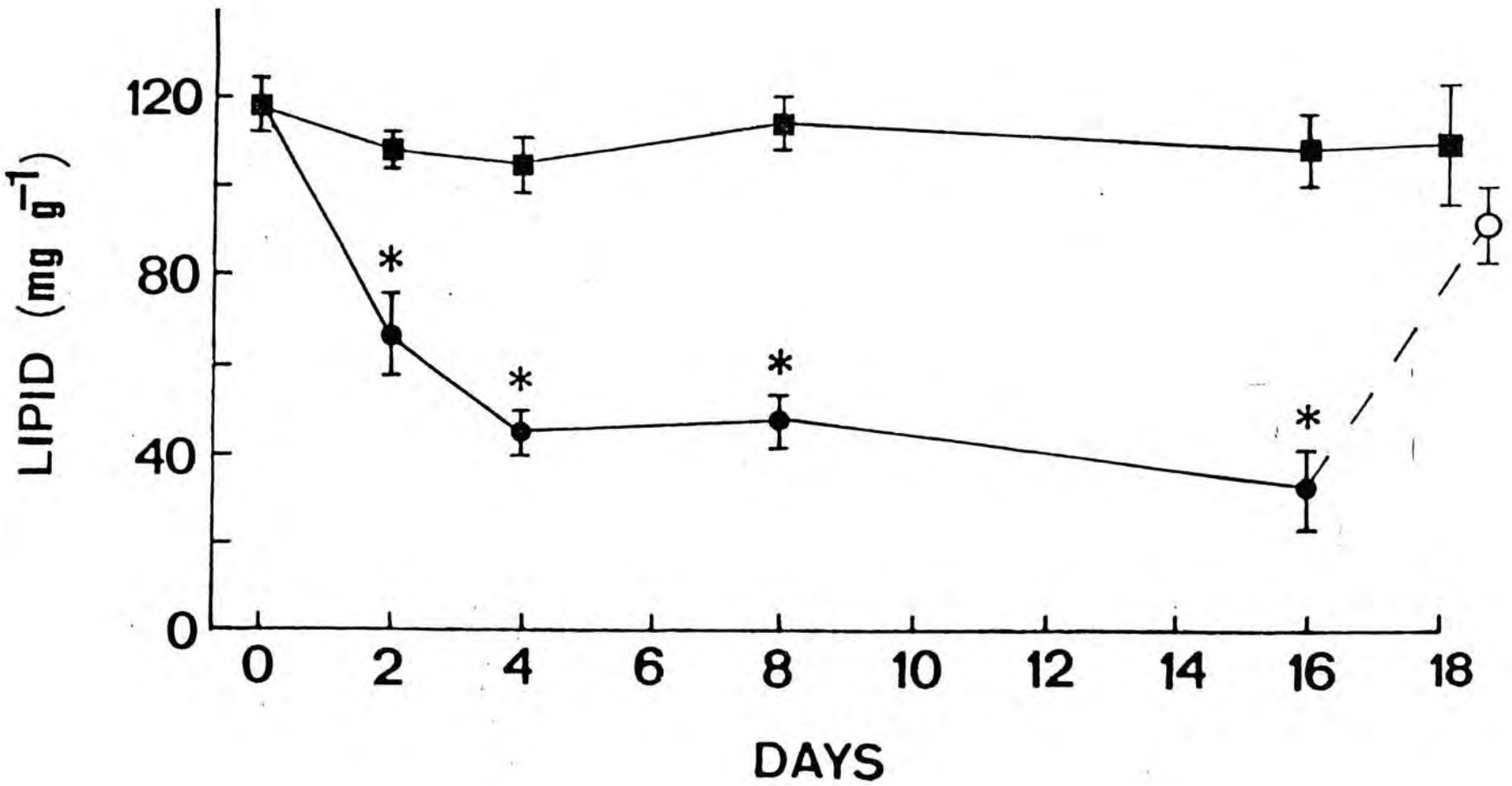
LIPID (mg g⁻¹)
120
80
40
0
0
2
4
6
8
10
12
14
16
18
DAYS
*
*
*
*

Fig. 59. Carbohydrate concentration of the hepatopancreas in daily-fed (squares), starved (closed circles) Metapenaeus ensis during starvation, and refed shrimp after starvation (open circles). Data are expressed as means of 3-6 individuals and vertical bars represent $\pm$ 1 S.E. In some cases, half of the bar is omitted for clarity. Asterisks indicate significant differences between values in daily-fed and starved shrimp (Student's t-test, $P<0.05$).

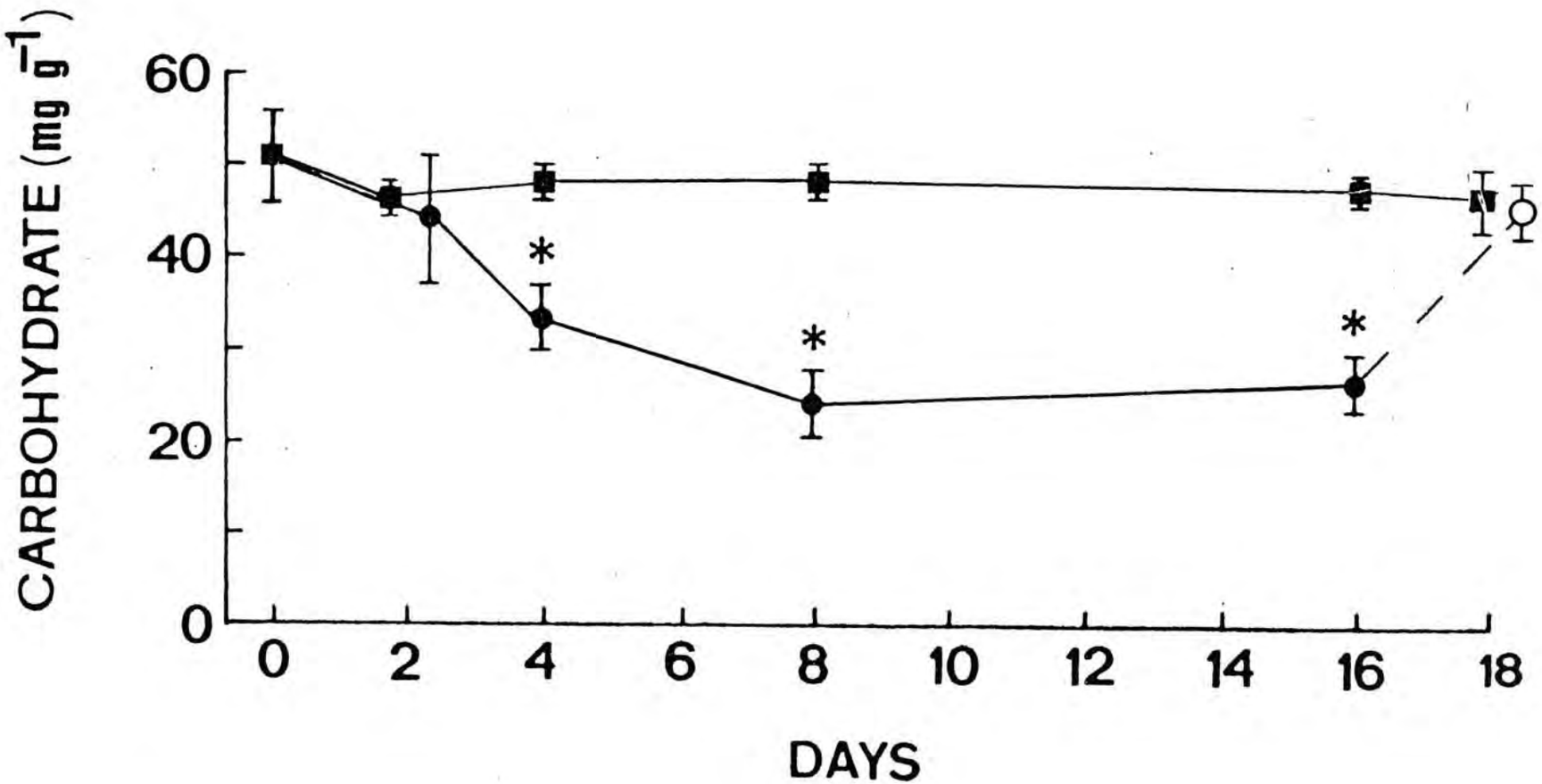
CARBOHYDRATE (mg g⁻¹)
60
40
20
0
0
2
4
6
8
10
12
14
16
18
DAYS
*
*
*

Fig. 60. Amylase activities in the hepatopancreas of daily-fed (squares), starved (closed circles) Metapenaeus ensis during starvation, and refed shrimp after starvation (open circles). Data are expressed as means of 3-8 individuals and vertical bars represent ± 1 S.E. In some cases, half of the bar is omitted for clarity. Asterisks indicate significant differences between values in daily-fed and starved shrimp (Student's t-test, $P<0.05$).

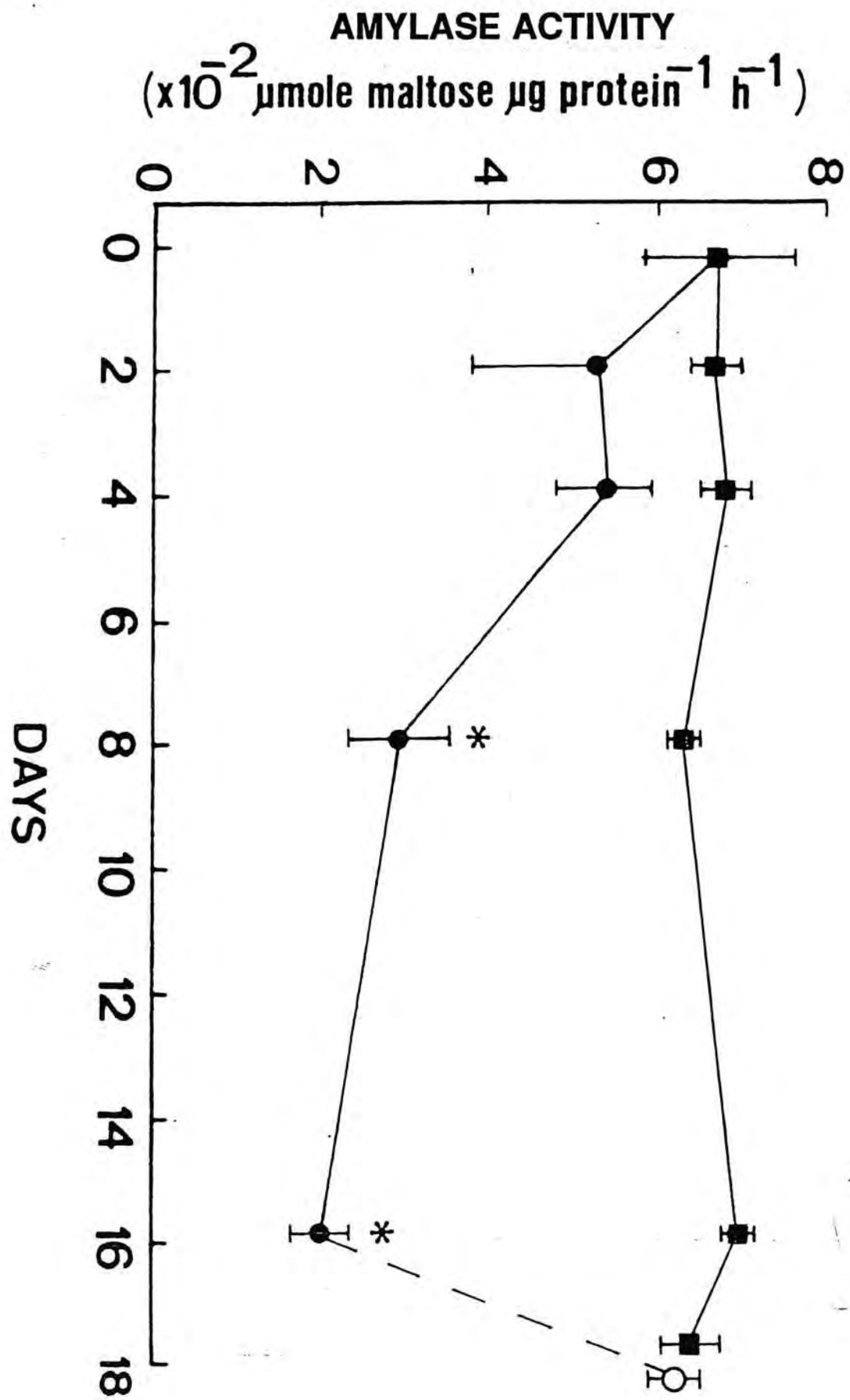
AMYLASE ACTIVITY
(x10⁻² µmole maltose µg protein⁻¹ h⁻¹)
0
2
4
6
8
DAYS
0
2
4
6
8
10
12
14
16
18
*
*
♂

Fig. 61. Protease activities in the hepatopancreas of daily-fed (squares), starved (closed circles) Metapenaeus ensis during starvation, and refed shrimp after starvation (open circles). Data are expressed as means of 3-8 individuals and vertical bars represent $\pm$ 1 S.E. In some cases, half of the bar is omitted for clarity. Asterisks indicate significant differences between values in daily-fed and starved shrimp (Student's t-test, $P<0.05$).

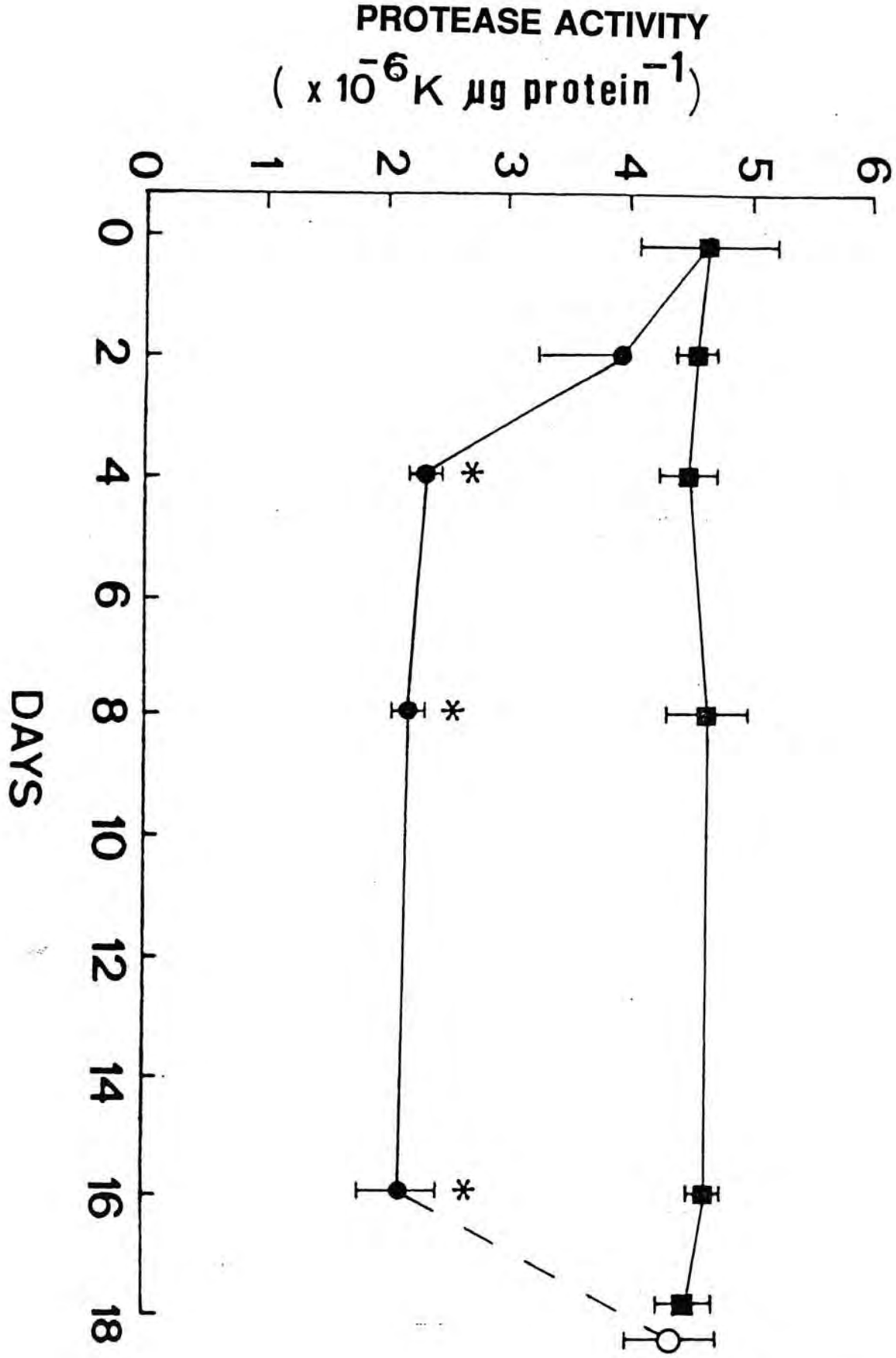
PROTEASE ACTIVITY
(x 10⁻⁶K µg protein⁻¹)
0
1
2
3
4
5
6
DAYS
0
2
4
6
8
10
12
14
16
18
*
*
*

Fig. 62. Hepatopancreas of daily-fed and starved Metapenaeus ensis.

(a) Daily-fed shrimp. Tubules consist of numerous B-cells (B). R, R-cell. Scale bar represents 5 μm. H & E.

(b) Shrimp starved for 16 days. The number of B-cells is less. The tubules does not suffer from severe distruction after starvation. B, B-cell; CT, connective tissue sheath; E, E-cells. Scale bar represents 5 μm. H & E.

(c) Shrimp refed for 2 days after 16 days of starvation. The number of B-cells appears to be increased. B, B-cell, F, F-cell; R, R-cell. Scale bar represents 5 μm. H & E.

a

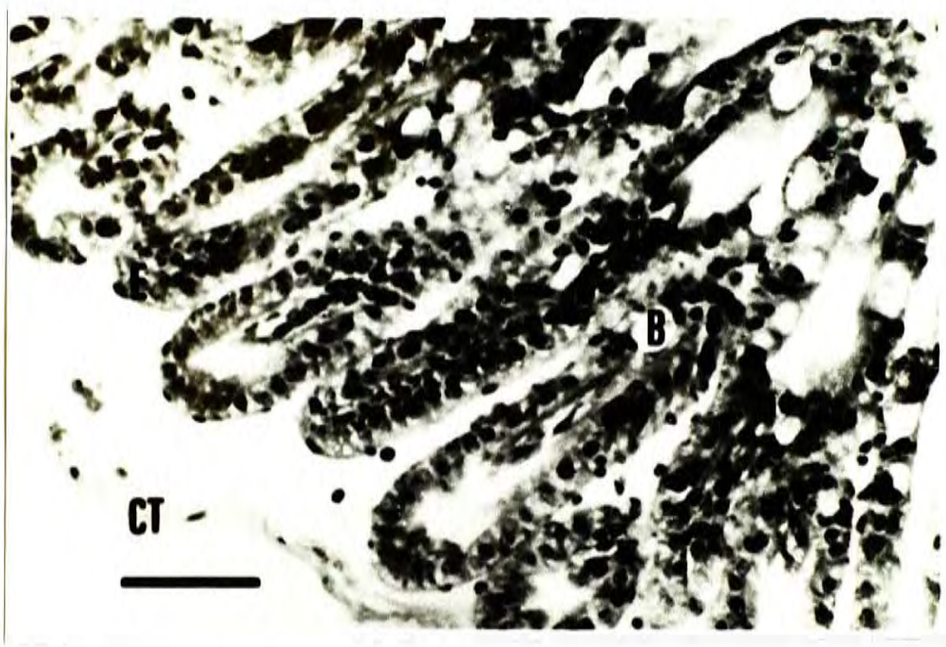

b

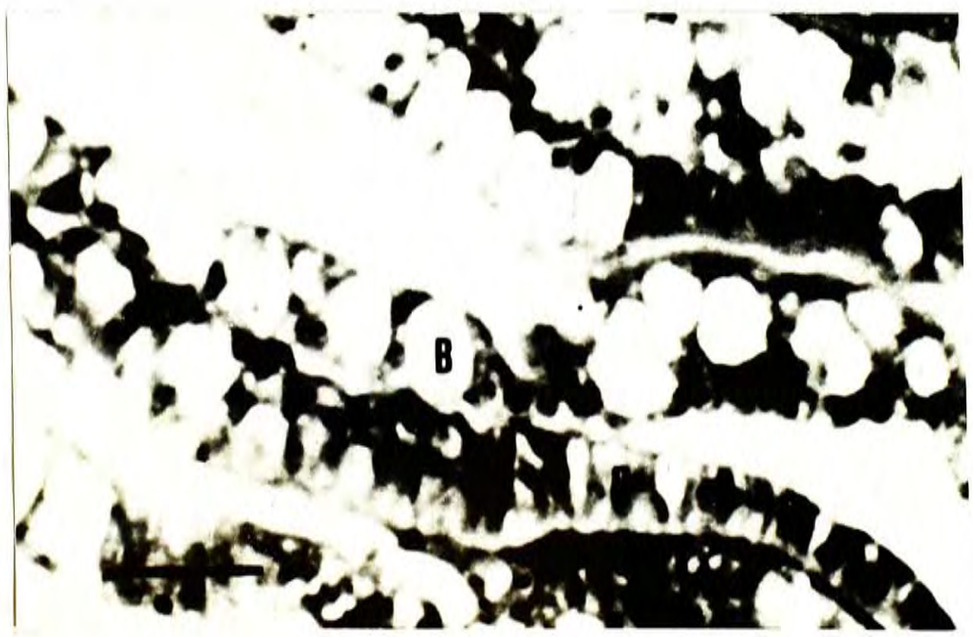

c

Fig. 63. Amount of B-cells as percentage of total number of cells in the hepatopancreas of Metapenaeus ensis during starvation (closed circles) and in M. ensis refed for 2 days after 16 days of starvation (open circles). Asterisks indicate significant differences between values in shrimp before starvation (Day 0) and starved shrimp (Student's t-test, $P<0.05$).

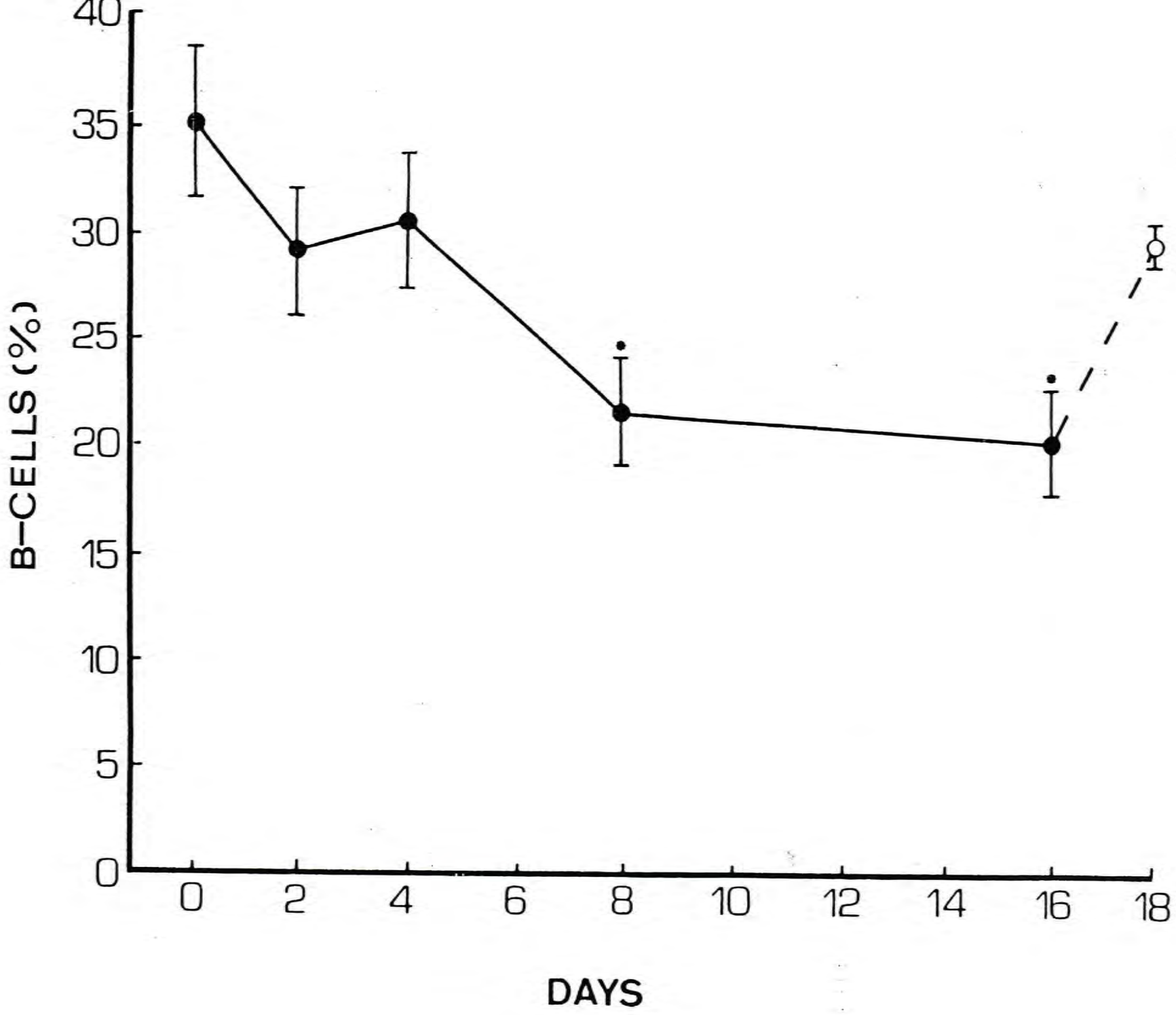
B–CELLS (%)
40
35
30
25
20
15
10
5
0
0
2
4
6
8
10
12
14
16
18
DAYS

Fig. 64. Sections of hepatopancreas in Metapenaeus ensis showing lipid reserve in the tubules. The sections were stained with Sudan black B.

(a) Daily-fed shrimp. Numerous lipid droplets (arrow–heads) are found in the tubules (T). Scale bar represents 5 μm.

(b) Shrimp starved for 16 days. Lipid droplets are hardly be detected. T, tubules of hepatopancreas. Scale bar represents 5 μm.

(c) Shrimp refed for 2 days after 16 days of starvation. Lipid droplets (arrow-heads) are numerous. T, tubules of hepatopancreas. Scale bar represents 5 μm.

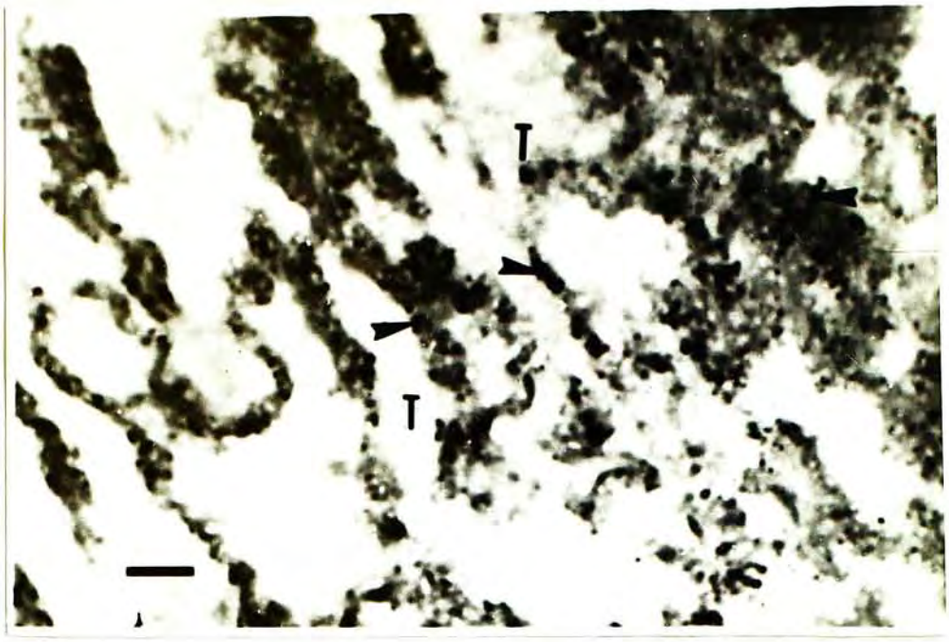

a

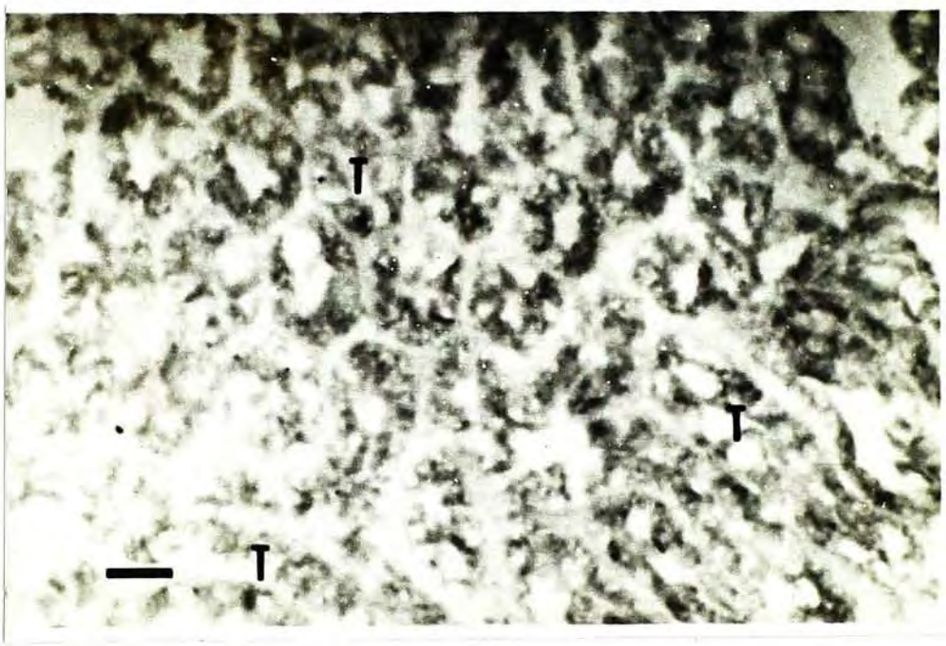

b

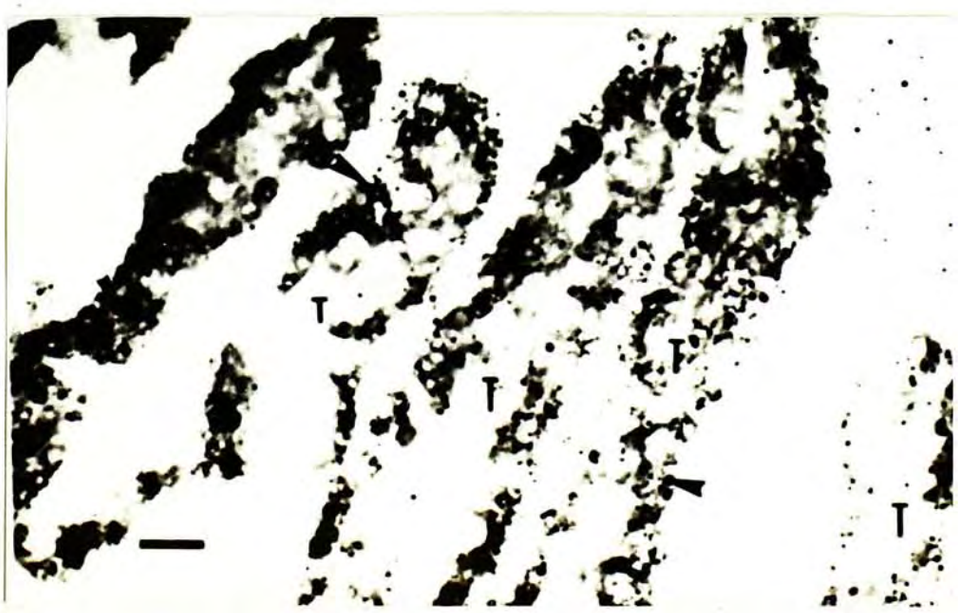

c

Fig. 65. Transmission electron micrograph of R-cells in the hepatopancreas of Metapenaeus ensis after 2 days of starvation. Lipid droplets (LP) decreases in number and becomes smaller in size. Nucleus (N) is surrounded by a layer of vesicles (V). BL, basal lamina; M, mitochondrion; RE, rough endoplasmic reticulum; SE, smooth endoplasmic reticulum. Scale bar represents 2 μm.

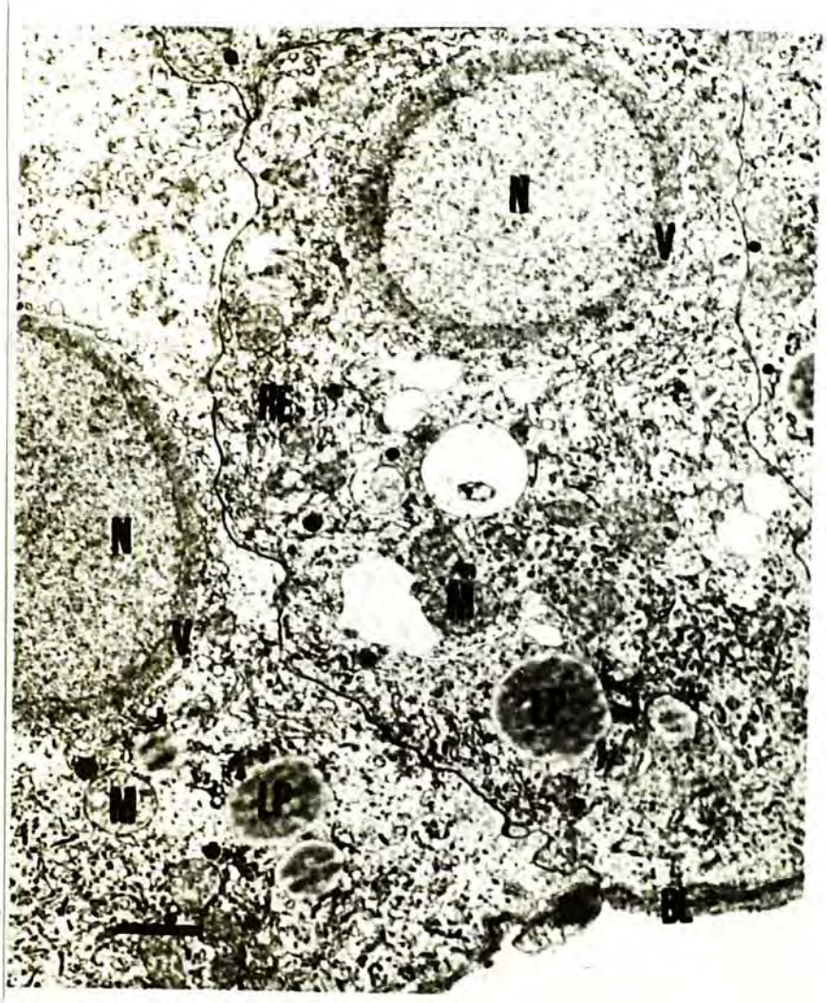
N
V
M
N
V
M
M
LP

Fig. 66. Transmission electron micrograph showing lipid droplets surrounded by rough endoplasmic reticulum in R-cell in the hepatopancreas of Metapenaeus ensis after 2 days of starvation. LP, lipid droplet; M, mitochondrion; N, nucleus; RE, rough endoplasmic reticulum; V, vesicles. Scale bar represents 1 μm.

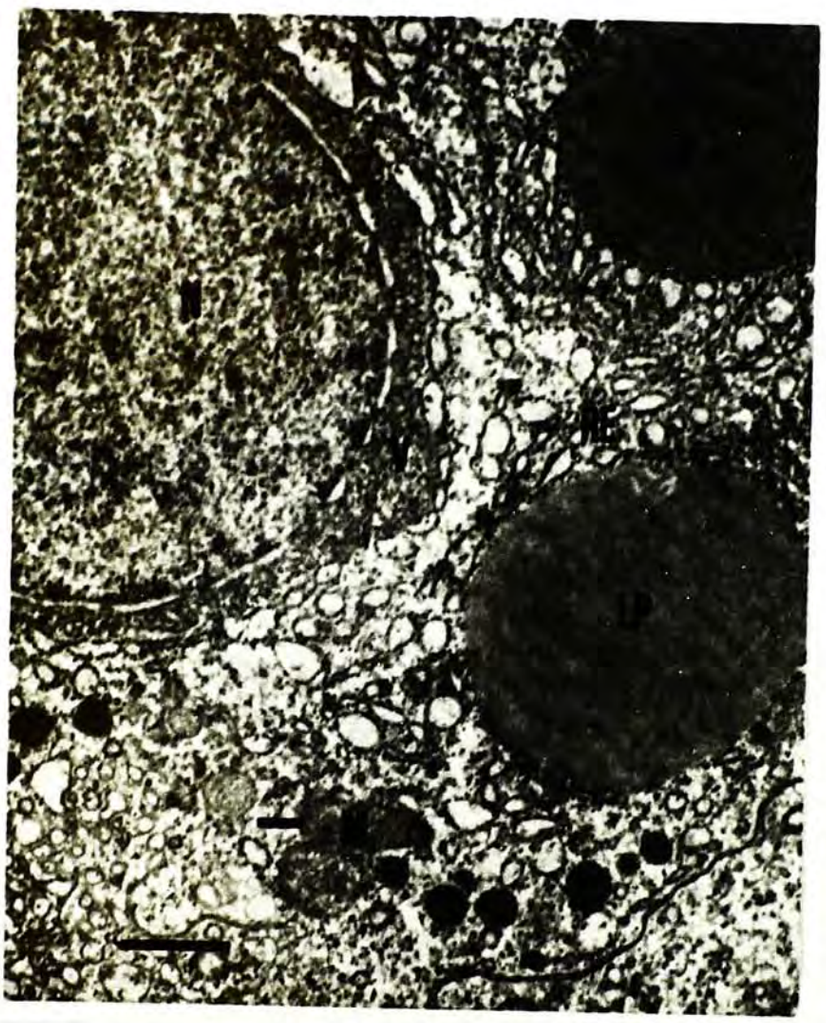

Fig. 67. Transmission electron micrograph of the apical region of R-cell in the hepatopancreas of Metapenaeus ensis after 4 days of starvation. Many residual bodies of lyzosomes (LY) are found. M, mitochondrion; MV, microvilli. Scale bar represents 2 μm.

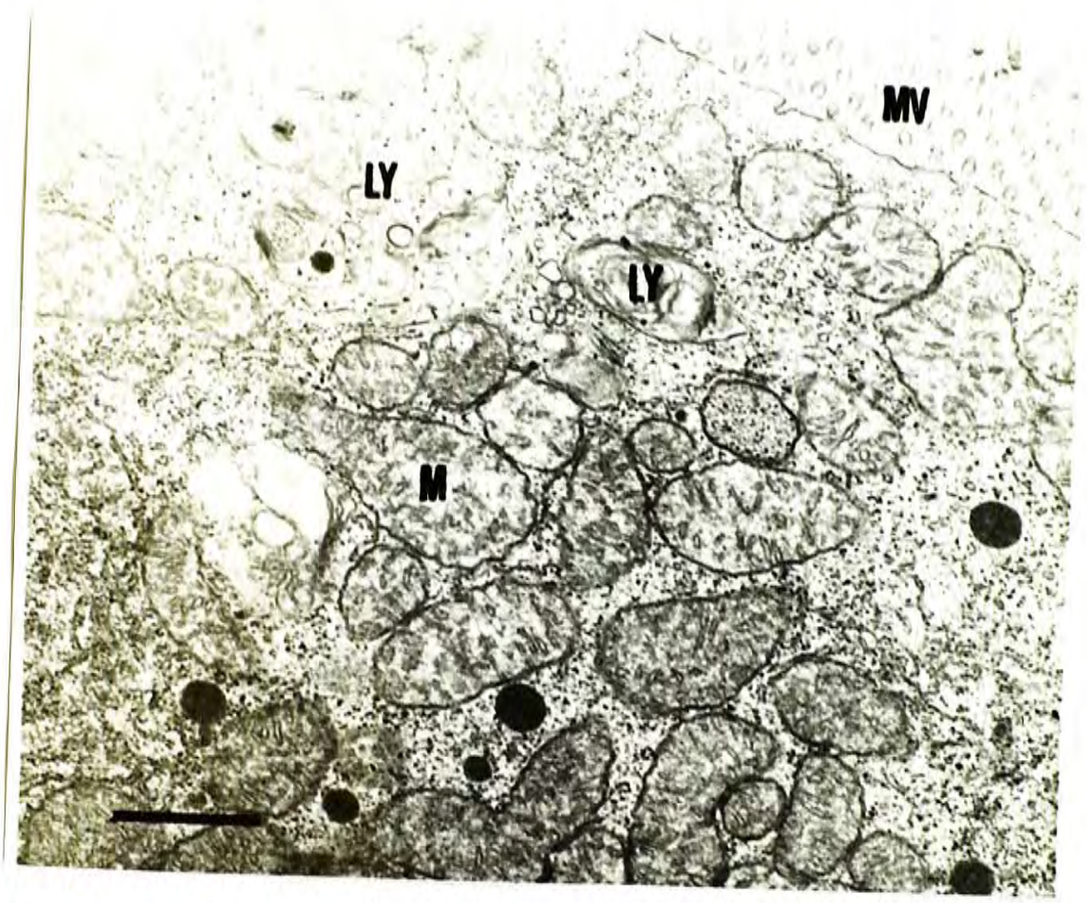
MV
LY
LY
M

Fig. 68. Transmission electron micrograph of the basal region of R-cell in the hepatopancreas of Metapenaeus ensis after 4 days of starvation. Rough endoplasmic reticulum (RE) forms multi-layered whorls surrounding dense granules (DG) in the center. LY, residual body of lyzosome; M, mitochondrion; MV, microvilli. Scale bar represents 2 μm.


LY

Fig. 69. Transmission electron micrograph of the multi-layered whorls in the basal region of R-cell in the hepatopancreas of Metapenaeus ensis after 4 days of starvation. No dense granule is surrounded in the center. BL, basal lamina; RE, rough endoplasmic reticulum. Scale bar represents 1 μm.

Fig. 70. Transmission electron micrograph of R-cell in the hepatopancreas of Metapenaeus ensis after 16 days of starvation. Smooth eodoplasmic reticulum (SE) becomes constricted and locates basally. Mitochondria (M) tends to be dilated. BL, basal lamina; N, nucleus. Scale bar represents 1 μm.


N
M

Fig. 71. Transmission electron micrographs of R-cells in the hepatopancreas of Metapenaeus ensis refed for 2 days after 16 days of starvation.

(a) Smooth endoplasmic reticulum (SE) proliferates in the basal region. Constricted endoplasmic reticulum disappears. BL, basal lamina; LP, lipid droplet; M, mitochondrion. Scale bar represents 1 μm.

(b) The layer of vesicles surrounding the nucleus (N) tends to diminsh. Mitochondria (M) had slight dilation. Scale bar represents 1 μm.

a

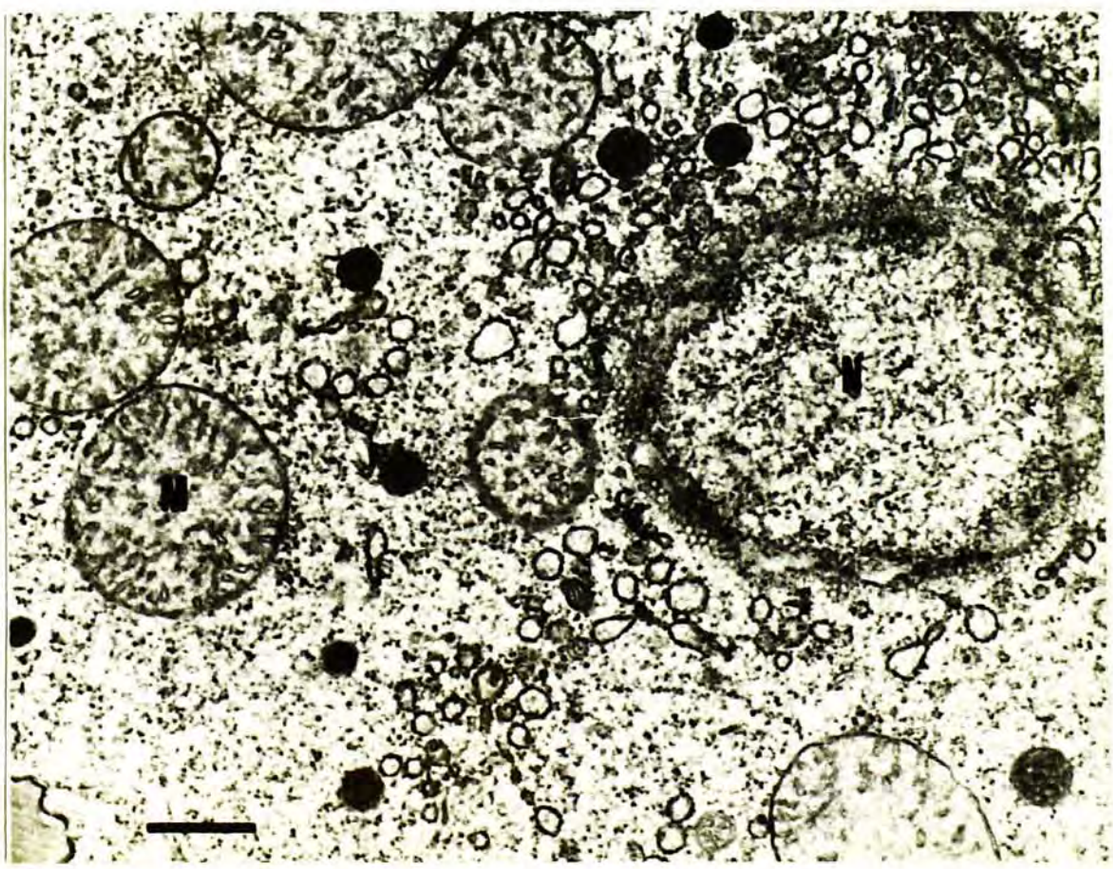

b

Fig. 72. Transmission electron micrograph of F-cell in the hepatopancreas of Metapenaeus ensis after 16 days of starvation. Mitochondria (M) are extremely dilated. BL, basal lamina; MV, microvilli. Scale bars represent 1 μm.

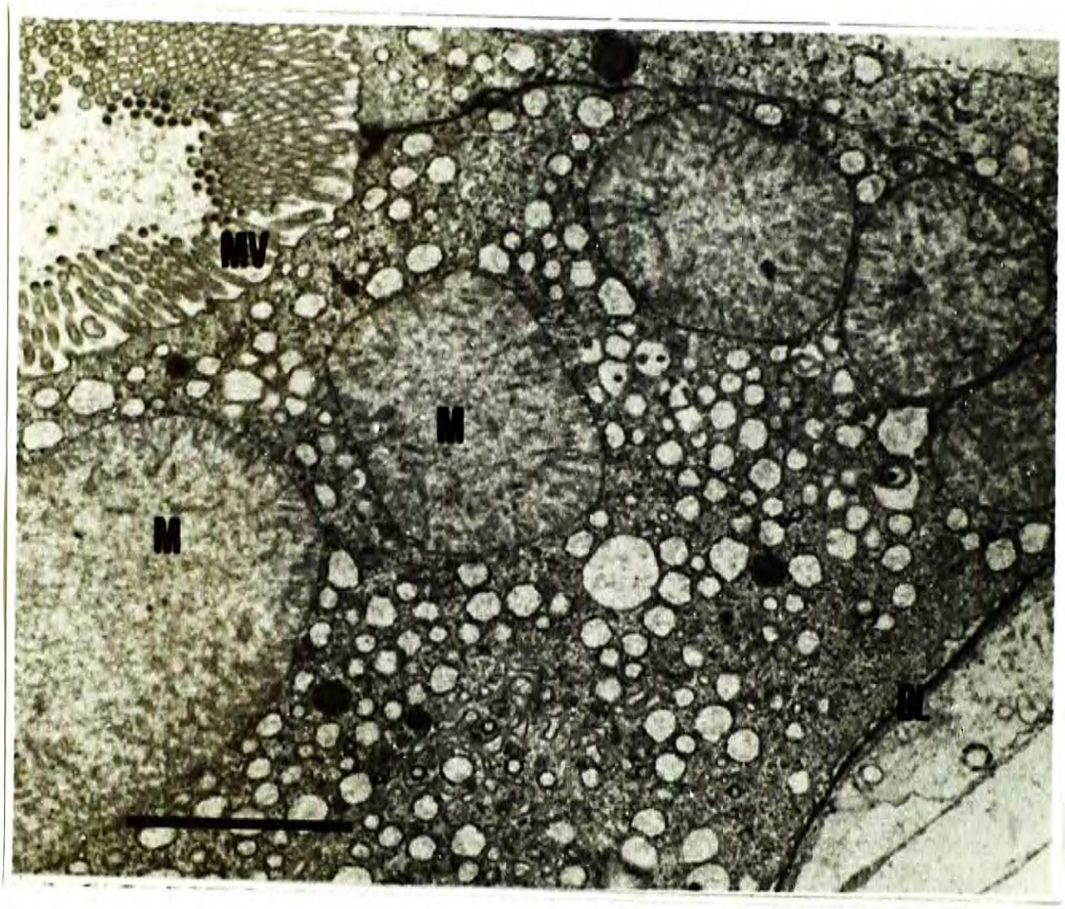
MV
M
M
M

Fig. 73. Transmission electron micrographs of F-cells in the hepatopancreas of Metapenaeus ensis refed for 2 days after 16 days of starvation.

(a) Apical region. G, Golgi body; M, mitochondrion; MV, microvilli. Scale bar represents 1 μm.

(b) Basal region. BL, basal lamina; M, mitochondiron;N, nucleus. Scale bar represents 1 μm.

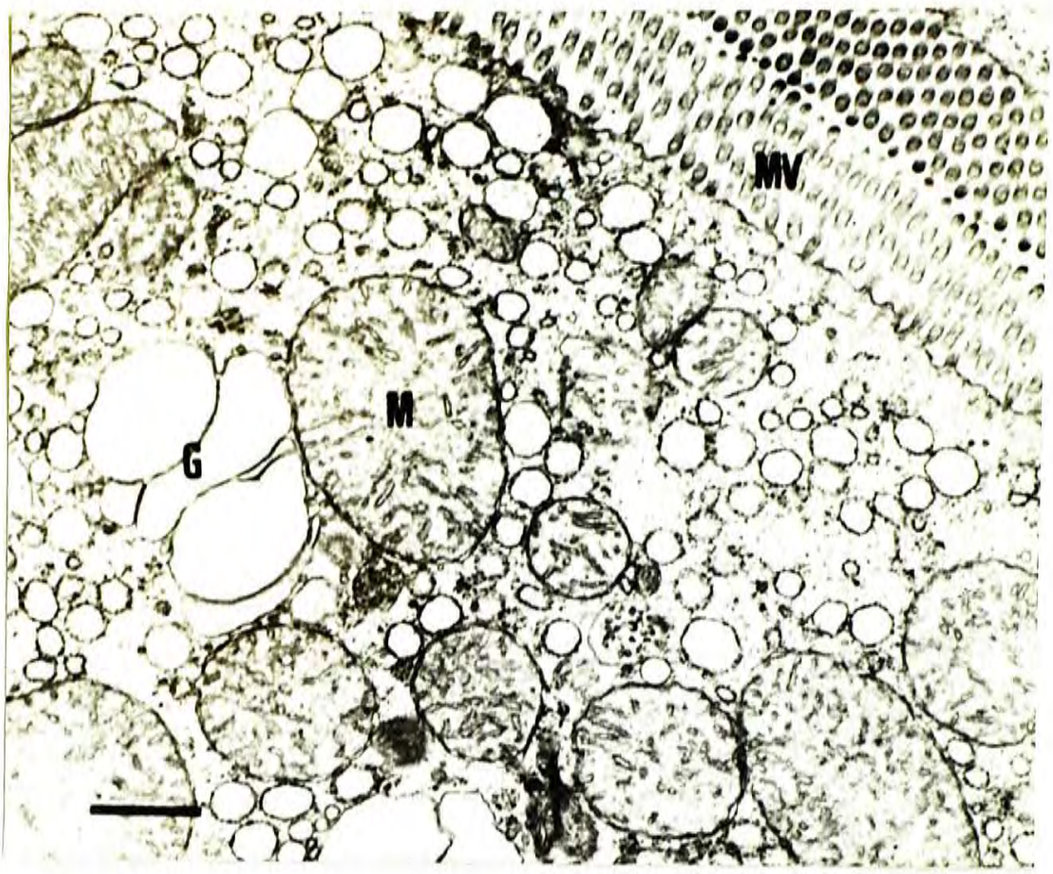

a

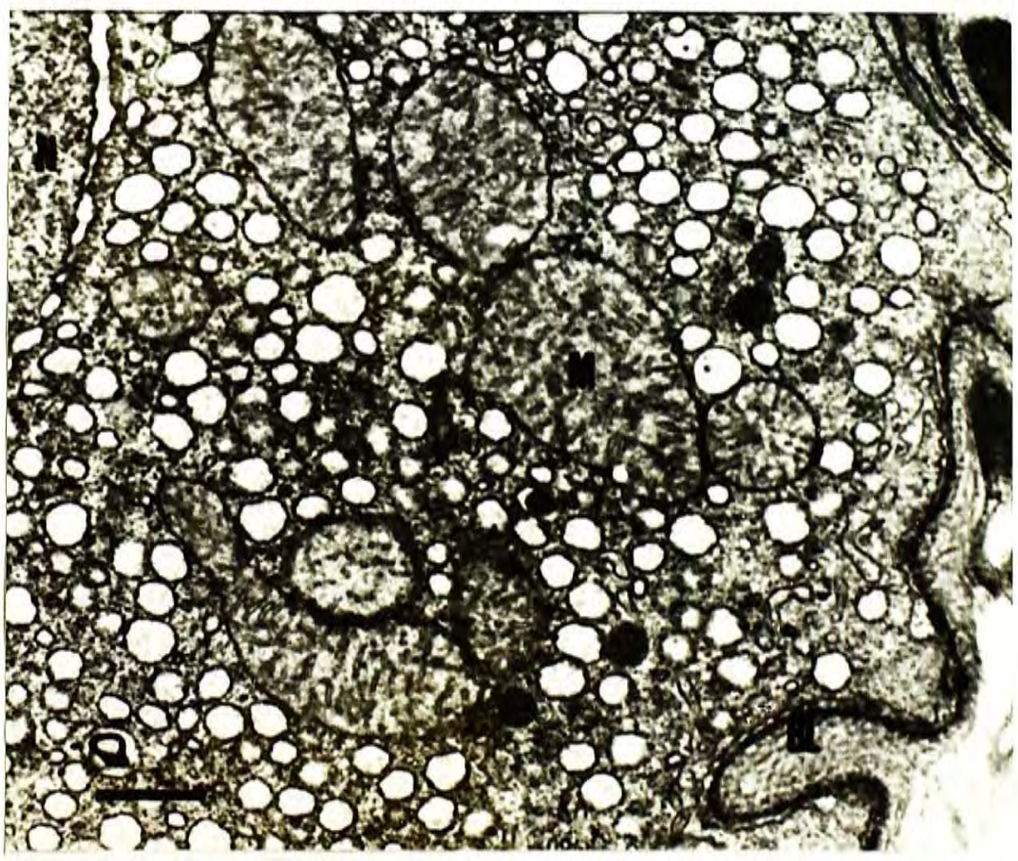

b

Fig.74. Transmission electron micrograph of the lamellated structure in the digestive vacuole of B-cell in the hepatopancreas of Metapenaeus ensis after 4 days of starvation. DV, digestive vacuole; arrow-head, lamellated structure. Scale bars represent 1 μm.


DV

Fig. 75. Transmission electron micrograph of B-cell in the hepatopancreas of Metapenaeus ensis refed for 2 days after 16 days of starvation. The ultrastructure is similar to those before starvation. The digestive vacuole (DV) is formed. M, mitochondrion; SA, sub–apical vacuole. Scale bar represent 2 μm.

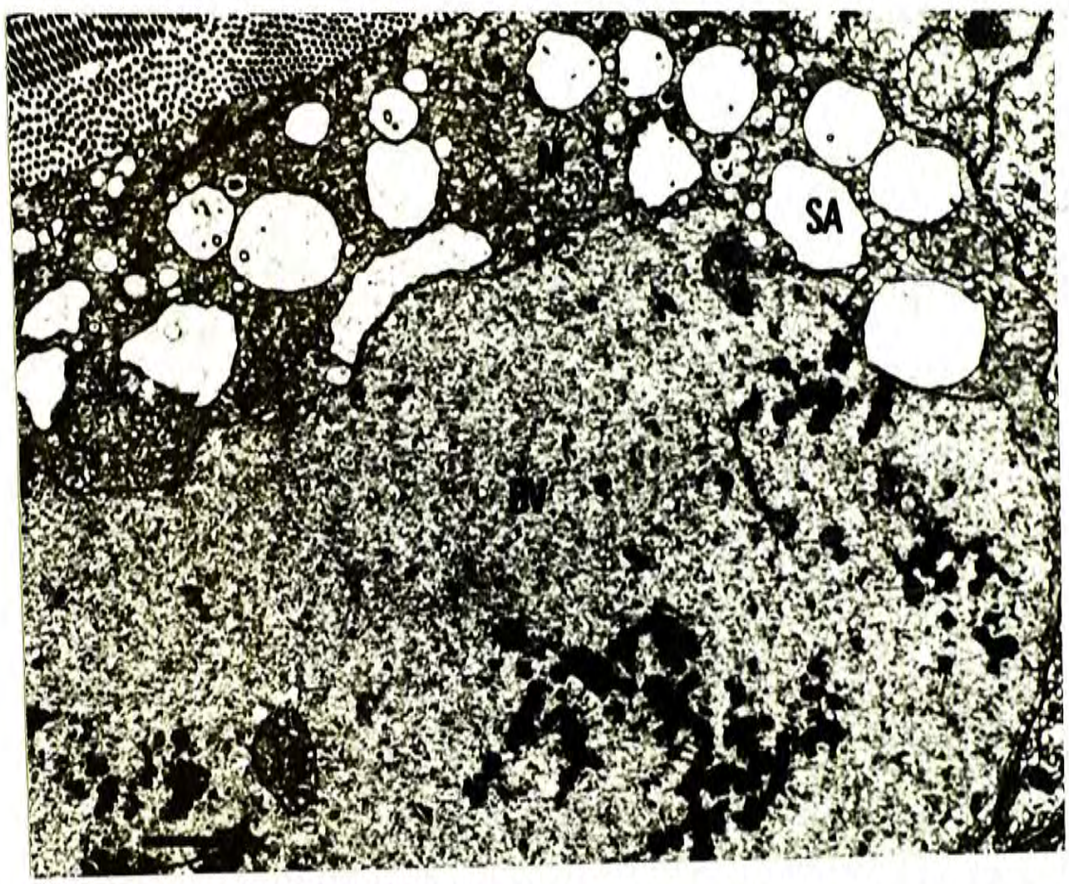
SA
M
DM

CHAPTER VIII

GENERAL CONCLUSION

Based on the experimental results reported, several conclusions on the present research can be drawn:

1. The morphology and ultrastructure of the hepatopancreas in Metapenaeus ensis are similar to those of other decapod crustaceans. Four types of cells, E-, F-, B-, and R-cells, can be identified on the tubular epithelium. There is a network of myoepithelial cells surrounding the tubules.

2. The development of the hepatopancreas in M. ensis through the larval stages is similar to that reported in other penaeid species. A pair of caeca arises from the gut in the non-feeding naupliar larva. In protozoeae, two pairs of gut caeca are formed. The complexity of the gut caeca increases as development proceeds. The four types of cells found in the adult hepatopancreas can be identified in the hepatopancreas of the larva.

3. In the study on the ultrastructural changes of the hepatopancreas

during the digestive cycle, intermediates between F- & B-cells are observed, supporting the transformation of F-cells to B-cells. The transformation process involves the uptake of luminal materials by pinocytosis and the enlargement and fusion of the pinocytotic vesicles forming the large digestive vacuole. Intracellular digestion and assimilation probably take place in the B-cells. B-cells extruded to the lumen at the end of the digestive cycle may carry the wastes left in the digestive vacuole. Lipid droplets in R-cells increased in size and number during the cycle possibly a result of nutrient uptake.

4. The hepatopancreas may act as an indicator of dietary status. It responds to prolonged absence of food in both cytological and biochemical aspects. The decrease in digestive enzyme activities during starvation reflects the decrease in synthesis and secretion of digestive enzymes. The decrease in digestive enzyme activities coincides with the decrease in the number of B-cells suggesting that B-cells are related to the secretion of digestive enzymes.

REFERENCES

Ahearn, G.A. 1974. Kinetic characteristics of glycine transport by the isolated midgut of the marine shrimp, Penaaeus marginatus. J. Exp. Biol., Vol. 61, pp. 677-696.

Ahearn, G.A. & L.A. Maginniss. 1977. Kinetics of glucose transport by the perfused midgut of the freshwater prawn Macrobrachium rosenbergii. J. Physiol. (London), Vol. 271, pp.319-336.

Al-Mohanna, S.Y. & J.A. Nott, 1986. B-cells and digestion in the hepatopancreas of Penaeus semisulcatus (Crustacea:Decapoda). J. Mar. Biol. Ass. U. K., Vol. 66, pp. 403-414.

Al-Mohanna, S.Y. & J.A. Nott, 1987a. R-cells and the digestrive cycle in Penaeus semisulcatus (Crustacea:Decapoda). Mar. Biol., Vol. 95, pp. 129-137.

Al-Mohanna, S.Y. & J.A. Nott, 1987b. M-'Midget" cells and moult cycle in Penaeus semisculcatus (Crustacea:Decapoda). J. Mar. Biol. Ass. U. K., Vol. 67, pp. 803-813.

Al-Mohanna, S.Y., J.A. Nott & D.J.W. Lane, 1985a. Mitotic E- and secretory F-cells in the hepatopancreas of the shrimp, Penaeus semisculcatus (Crustacea: Decapoda). J. Mar. Biol. Ass. U. K., Vol. 65, pp. 901-910.

Al-Mohanna, S.Y., J.A. Nott & D.J.W. Lane, 1985b. M- 'Midget' cells in the hepatopancreas of the shrimp, Penaeus semisculcatus De Haan, 1844 (Decapoda, Natantia). Crustaceana, Vol. 48, pp. 260-268.

Anderson, D.T. 1982. Embryology. In "The Biology of Crustacea, Vol. 2, Embryology, Morphology, and Genetics", edited by Abele, L.G. Academic Press, New York, pp. 1-49.

Anger, K., V. Storch, V. Anger & J.M. Capuzzo. 1985. Effects of starvation on moult cycle and hepatopancreas of stage I lobster (Homarus americanus) larvae. Helgolander Meeresunters, Vol. 39, pp. 107-116.

Barclay, M.C., W. Dall & D.M. Smith. 1983. Changes in lipid and protein during starvation and the moulting cycle in the tiger prawn, Penaeus esculentus Haswell. J. Exp. Mar. Biol. Ecol., Vol. 68, pp. 229-244.

Barker, P.L. & R. Gibson. 1977. Observations on the feeding mechanism, structure of the gut, and digestive physiology of the European lobster Homarus gammarus (L.) (Decapoda: Nephropidae). J. Exp. Mar. Biol. Ecol., Vol. 26, pp. 297-324.

Barker, P.L. & R. Gibson. 1978. Observations on the structure of the mouthparts, histology of the alimentary tract, and digestive physiology of the mud crab Scylla serrata (Forakal) (Decapoda: Portunidae). J. Exp. Mar. Biol. Ecol., Vol. 32, pp. 177-196.

Barnes, H. & J. Blackstock. 1973. Estimation of lipids in marine animals and tissues: detailed investigation of sulphophosphosvanillin method for "total" lipids. J. Exp. Mar. Biol. Ecol., Vol. 12, pp. 103-118.

Biesiot, P.M. 1986. Changes in midgut gland morphology and digestive enzyme activities associated with development in early stages of the American lobster (Homarus americanus). Ph.D. Thesis. MIT/WHOI, WHOI-86-20.

Biesiot, P.M. & J.M. Capuzzo. 1990. Changes in digestive enzyme activities during early development of the American lobster Homarus americanus. J. Exp. Mar. Biol. Ecol., ol. 135, pp. 107-122.

Brick, R.W. & G.A. Ahearn. 1978. Lysine transport across the mucosal border of the perfused midgut in the freshwater shrimp, Macrobrachium rosenbergii. J. Comp. Physiol., Vol. 124, pp. 169-179.

Bunt, A. H. 1968. An ultrastructural study of the hepatopancreas of Procambarus clarkii (Girard) (Decapoda, Astacidea). Crustaceana, Vol. 15, pp. 282-288.

Caceci, T., K.F. Neck, D.H. Lewis & R.F. Sis. 1988. Ultrastructure of the hepatopancreas of the Pacific white shrimp Penaeus vannamei (Crustacea: Decapoda). J. Mar. Biol. Ass. U. K., Vol. 68, pp. 323-337.

Chan, S.M. 1984. Effects of salinity, diets and chemincals on the development, growth and survival of sand shrimp (Metapenaeus ensis) during artificial propagation. M. Phil. Thesis. The Chinese University of Hong Kong.

Charney, J., & R.M. Tomarelli. 1947. A colormetric method for the determination of the proteolytic activity of duodenal juice. J. Biol. Chem., Vol.171, pp. 501-505.

Chu, K.H. 1986. Glucose transport by the in vitro perfused midgut of the blue crab, Callinectes sapidus J. Exp. Biol., Vol. 123, pp. 325-344.

Chu, K.H., W.W. Cheng, K.M. Cheng & K.M. Leung. 1989. Characterization of moult stages and changes in mineral levels in body tissues during the moult cycle of the shrimp Penaeus chinensis Asian Mar. Biol., Vol.15, pp. 699-714.

Cuzon, G., C. Cahu, J.F. Aldrin, J.L. Messager, G. Stephan & M. Mevel. 1980.

Starvation effect on metabolism of Penaeus japonicus. Proc. World Maricult. Soc., Vol. 11, pp. 410-423.

Dall, W. 1965. Studies on the physiology of a shrimp Metapenaeus sp. (Crustacea: Decapoda: Penaeidae). V. Calcium metabolism. Aust. J. Mar. Freshwater Res., Vol. 16, pp. 181-203.

Dall, W. 1967. The functional anatomy of the digestive tract of a shrimp Metapenaeus bennettae Racek & Dall (Crustacea: Decapoda: Penaeidae), Aust. J. Zool., Vol. 15, pp. 699-714.

Dall, W. 1981. Lipid absorption and utilization in the Norewegian lobster, Nyephrops norvegicus (L.). J. Exp. Mar. Biol. Ecol., Vol. 50, pp. 33-45.

Dall, W. & D.J.W. Moriarty. 1983. Functional aspects of nutrition and digestion. In The Biology of Crustacea, Vol. 5, Internal anatomy and physiology regulation, edited by Mantel, L.H. Academic Press, New York, pp. 251-262.

Davis, L.E. 1966. A study of growth and cell differentiation in the hepatopancreas of the crayfish. Diss. Abstr., Vol. 26. pp. 6316-6317.

Dendinger, J.E. 1987. Digestive proteases in the midgut gland of the Altantic blue crab Callinectes sapidus. Comp. Biochem. Physiol., Vol. 88B, pp. 503-506.

Dubois, M., K.A. Gilles, J.K. Hamilton, P.A. Rebbers & F. Smith. Colorimetic method for determination of sugars and related substances. Anal. Chem., Vol. 28, pp. 350-356.

Factor, J.R. 1981. Development and metamorphosis of the digestive system of larval lobsters, Homarus americanus (Decapoda:Nephropidae). J. Morph., Vol. 169, pp. 225-242.

Forster, G.R. 1953. Peritrophic membranes in the Caridea (Crustacea Decapoda). J. Mar. Biol. Ass. U. K., Vol. 32. pp. 315-318.

Galgani, F.G, Y. Benyamin, & H.J. Ceccaldi. 1984. Identification of digestive proteinases of Penaeus kerathurus (Forskal): a comparison with Penaeus japonicus Bate. Comp. Biochem. Physiol., Vol. 78B, pp. 335-361.

Galgani, F.G., Y. Benyamin, & A.V. Wormhoudt. 1985. Purification, properties and immunoassay of trypsin from the shrimp Penaeus japonicus. Comp. Biochem. Physiol., Vol. 81B, pp. 447-452.

Gao, J., Z. Yang, S. Ma & X. Jian. 1986. A preliminary study of the

development of the digestive system of Penaeus orientalis Kishinouye. Journal of Shandong College of Oceanology, Vol. 16, No. 4, pp. 18-23.

Gibson, R. & P.L. Barker. 1979. The decapod hepatopancreas. Oceanogr. Mar. Biol. Ann. Rev., Vol. 17, pp. 285-346.

Hartree, E.F. 1972. Determination of protein: a modification of the Lowry method that gives a linear photometric response. Anal. Biochem., Vol. 48, pp. 422-427.

Hinton, D.J. & S. Corey. 1979. The mouthparts and digestive tract in the larval stages of Homarus americanus. Can. J. Zool., Vol. 57, pp. 1413-1423.

Holliday, C.W., D.L. Mykles, R.C. Terwilliger & L.J. Dangott. 1980. Fluid secretion by the midgut caeca of the crab, Cancer magister. Comp. Biochem. Physiol., Vol. 67A, pp. 250-263.

Hopkin, S.P. & J.A. Nott. 1980. Studies on the digestive cycle of the shore crab Carcinus maenas (L.) with special reference to the B cells in the hepatopancreas. J. Mar. Biol. Ass. U. K., Vol. 60, pp. 891-907.

Humason, G.L. 1974. Animal tissue techniques. W.H. Freeman and Company, San Francisco.

Jacobs, W. 1928. Untersuchungen uber die cytologie der sekretbildung in der Mittedarmdruse von Astacus leptodactylus. Z. Zellforsch., Vol. 8, pp. 1-62.

Johnson, P.T. 1980. Histology of the blue crab, Callinectes sapidus: A model for the Decapoda. Praeger Scientific, New York.

Karunakaran, S.K., & K.P. Dphage. 1977. Amylase activities of the digestive tract of the prawns, Penaeus indicus and Metapenaeus monoceros. Bull. Inst. Zool., Academia Sinica., Vol. 16, pp. 85-90.

Leavitt, D.F. & R.C. Bayer. 1982. A description of the muscle net surrounding the digestive epithelium in the midgut gland of the lobster Homarus americanus. J. Crust. Biol., Vol. 2, pp. 40-42.

Leung, K.M., H.L. Chen & K.H. Chu. 1990. Effects of starvation on biochemical composition and digestive enzyme activities in the hepatopancreas of the shrimp Metapenaeus ensis. In "The Proceedings of the Second Asian Fisheries Forum", edited by Hirano, R. & I. Hanyu, pp. 445-448. Asian Fisheries Society, Manila, Philippines.

Loizzi, R.F. 1971. Interpretation of crayfish hepatopancreas function based on fine structural analysis of epithelial cell lines and muscle network. Z. Zellforsch., Vol. 113, pp. 420-440.

Lovett, D.L. & D.L. Felder. 1989. Onteogeny of gut morphology in the white shrimp Penaeus setiferus (Decapoda, Penaeidae). J. Morph. Vol. 201, 253-273.

Lovett, D.L. & D.L. Felder. 1990. Onteogeny of kinematics in the gut of the white shrimp Penaeus setiferus (Decapoda, Penaeidae). J. Crust. Biol., Vol. 10, 53-68.

Lowry, O.H., N.J. Rosebrough, A.L. Farr & R.J. Randall. 1951. Protein measurement with Folin phenol reagent. J. Biol. Chem., Vol. 193, pp. 265-275.

Maugle, P.D., O. Deshimaru, T. Katayama & K.L. Simpson. 1982. Characteristics of amylase and protease of the shrimp Penaeus japonicus. Bull. Japan Soc. Sci. Fish., Vol. 48, pp. 1753-1757.

Mykles, D.L. 1979. Ultrastructure of the alimentary epithelia of lobsters, Homarus americanus and H. gammarus, and crab, Cancer magister. Zoomorphologie, Vol. 92, pp. 201-215.

Ovsianico-Koulikowsky, N.N. 1987. Physiological and biochemical changes during growth and development in the shrimp Metapenaeus ensis. M.Phil. Thesis. The Chinese University of Hong Kong.

Papathanassiou, E. & P.E. King. 1984. Effects of starvation on the fine structure of the hepatopancreas in the common prawn Palaemon serratus (Pennant). Comp. Biochem. Physiol., Vol. 77, pp. 243-249.

Pillai, R.S. 1960. Studies on the shrimp Caridina laevis (Heller) 1. the digestive system. J. Mar. Biol. Ass. India, Vol. 2, pp. 57-74.

Powell, R.R. 1974. The functional morphology of the fore-guts of the thalassinid crustaceans, Calianassa californiensis and Upogebia pugettensis. Univ. Calif., Berkeley, Publ. Zool. Vol. 102, pp. 1-41.

Rigdon, R.H. & D.J. Mensik, 1976. Gastrointestinal tract of Penaeus aztecus Ives, 1891 (Decapoda, Natantia), a histological study. Crustaceana, Vol. 30, pp. 164-168.

Rosemark, R., P.R. Bowser & N. Baum. 1980. Histological observation of the hepatopancreas in juvenile lobsters subjected to dietary stress. Proc. World Maricul. Soc., Vol. 11, pp. 471-478.

Sasaki, G.C., & J.M. Capuzzo. 1984. Degradation of Artemia lipids under storage. Comp. Biochem. Physiol., Vol. 78B, pp. 525-531.

Smith, R.I. 1978. The midgut caeca and the limits of the hindgut of Brachyura: a clarification. Crustaceana, Vol. 35, pp. 195-199.

Tsai, I.H., K.L. Chuang & J.L. Chuang. 1986. Chymotrypsins in digestive tracts of crustacean decapods (shrimps). Comp. Biochem. Physiol., Vol. 85B, pp. 235-239.

Tseng, W.Y., G.T. Pan, W.W. Cheng & S.K. Ho. 1979. A preliminary study on the artificial propagation and cultivation of sand shrimp, Metapenaeus ensis (De Haan) in Hong Kong. Bull. Natl. Tai. Coll. Mar. Sci. Technol. Vol. 14, pp 429-450.

van Weel, P.B. 1970. Digestion in Crustacea. In "Chemical Zoology", Vol. 5, edited by Florkin, M. & B.T. Scheer, Academic Press, New York, pp. 97-115.

Vogt, V.G. 1985. Histology and cytology of the midgut gland of Penaeus monodon (Decapoda). Zool. Anz., Jena, Vol. 215, pp. 61-80.

Vogt, G., V. Storch, E.T. Quinitio & F.P. Pascual. 1985. Midgut gland as monitor organ for the nutritional value of diets in Penaeus monodon (Decapoda). Aquaculture, Vol. 48, pp. 1-12.

Vogt, G., E.T. Quinitio & F.P. Pascual. 1986. Leucaena leucocephala leaves in formulated feed for Penaeus monodon: a concrete example of the application of histology in nutrition research. Aquaculture, Vol. 59, pp. 209-234.

Wrint, R., & H.P. Stegbauer. 1974. Amylase. In Berymeyer, H.U. (ed.) Methods of Enzymatic Analysis. Vol. II. Academic Press, New York. pp. 885-889.

Yu, H.P. & T.Y. Chan. 1986. The illustrated penaeoid prawns of Taiwan. Southern Materials Center, Inc. Taiwan, pp. 139-142.